

Basin and Range Province Seismic Hazards Summit III

Utah Geological Survey and
Western States Seismic Policy Council

Short Course

Characterizing Hazardous Faults – Techniques, Data Needs, and Analysis: *Christopher DuRoss, U.S. Geological Survey*



BASIN AND RANGE PROVINCE SEISMIC HAZARDS SUMMIT III

SHORT COURSE

Characterizing Hazardous Faults – Techniques, Data Needs, and Analysis

by

Christopher B. DuRoss
U.S. Geological Survey
(formerly Utah Geological Survey)



January 12, 2015

SHORT COURSE: Characterizing Hazardous Faults – Techniques, Data Needs, and Analysis

Chris DuRoss

U.S. Geological Survey, Golden, Colorado
cduross@usgs.gov



Basin and Range Province Seismic Hazards Summit III – January 9, 2015

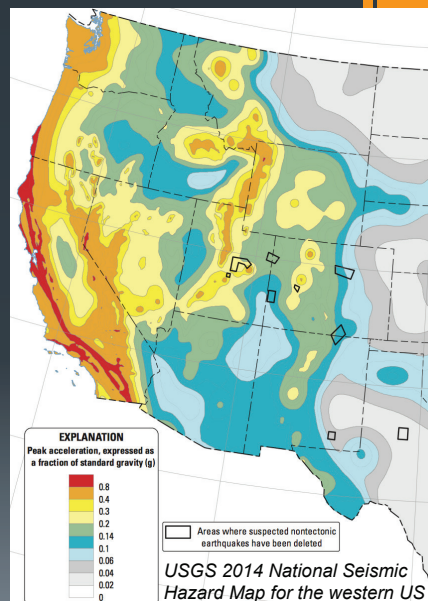
Agenda

BRPSHSIII Short Course agenda		
8:00	Introduction, outline, terminology	Chris DuRoss, USGS
8:20	Trench excavation	
8:40	Conducting the field investigation	
9:00	Working with paleoseismic data	
9:30	Discussion	
9:45 Break		
10:00	Luminescence dating	Shannon Mahan, USGS
10:45	Radiocarbon (¹⁴ C) dating and OxCal	Chris DuRoss
11:05	Lidar and other resources	Steve Bowman, UGS
11:20	Lidar mapping methods	Adam McKean, UGS
11:40	Photomosaic methods (Agisoft)	Adam Hiscock, UGS
12:00 Lunch		
1:30	Paleoseismic investigation of the West Valley fault zone	Mike Hylland, UGS
1:50	Geologic mapping and segmentation of the Washington fault	Tyler Knudsen, UGS
2:10 Break		
2:25	Exercise 1: Trench observation	
2:45	Exercise 2: Interpreting raw paleoseismic data and building an OxCal model	
3:45	Wrap up and additional resources	Chris DuRoss
4:00	Adjourn	

INTRODUCTION/ TERMINOLOGY

Why Characterize Hazardous Faults?

- *Define the hazard*
 - Investigate recent fault behavior
 - Reduce uncertainties in fault parameters (e.g., recurrence, slip rate)
 - Improve understanding of how faults generate large-**M** earthquakes
 - Update Q. fault & fold databases
- *Reduce earthquake vulnerability*
 - Pre-development fault studies
 - Fault mitigation
 - Improving building codes
- *Improve hazard & risk assessments*
 - Local seismic-hazard evaluations
 - USGS National Seismic Hazard maps
 - FEMA Hazus modeling
 - Regional earthquake forecasts (earthquake probability studies)



Characterizing Fault Activity

➤ Techniques

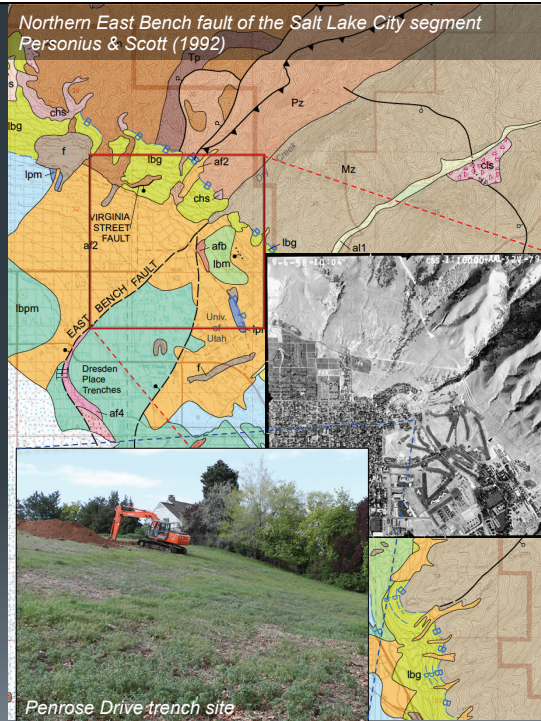
- Geologic mapping
- Geomorphic analysis
- Paleoseismic studies

➤ Purpose

- Define fault characteristics (fault geometry & rupture complexity)
- Define history of recent large **M** earthquakes

➤ 2nd order questions:

- Fault segmentation?
- Temporal clustering?
- Seismic moment, magnitude?



Active/Hazardous Fault

A fault likely to have another earthquake sometime in the future (USGS glossary)

➤ Fault recently active; define recent

- USGS, *Alquist-Priolo Act*: Holocene (<10 ka)
- WSSPC (BRP): Latest Pleistocene/Holocene (≤15 ka) to late Quaternary (≤130 ka) (draft policy 15-3)
- Utah: Holocene to Quaternary, depending on IBC risk category

➤ Other considerations:

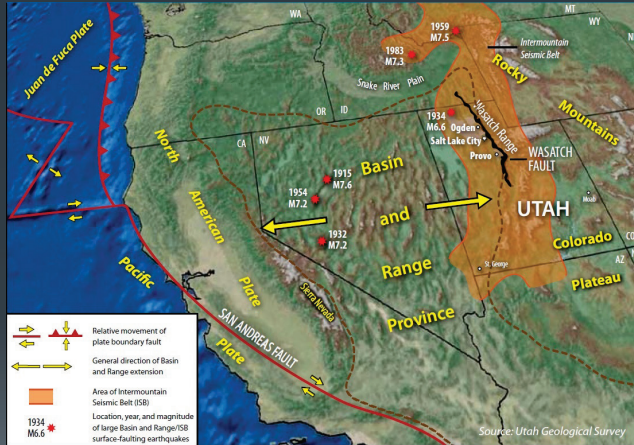
- Available data or lack of data (assume *active* unless data prove)
- Time since most recent earthquake and mean recurrence interval (or average slip rate)
- Risk: criticality of structure, exposure time



Quaternary faults of Utah; USGS

Defining an Active/Hazardous Fault

- Tectonic Province
- Range Front morphology
- Geologic mapping
- Scarp extent/morphology
- Age of youngest faulted surface/deposit
- Paleoseismic investigations
- Soil development



Source: Putting Down Roots (<http://ussc.utah.gov>)

Which Fault is More Hazardous?

Fairview fault zone: recurrence unknown, but 35,000 yr since last earthquake. Slip rate: <math><0.2 \text{ mm/yr}</math>

Nephi segment: ~1200 yr mean recurrence; 300 yr since most recent. Slip rate: ~1-2 mm/yr

Investigation Methods/Terminology

➤ *Physical Characteristics*

- Fault strike and dip
- Sense of slip/direction of movement (slip vector)
- Rupture complexity (width)
- Fault displacement
- Geologic slip rate

➤ *Tools – mostly noninvasive*

- Geologic mapping
- Scarp morphology
- Scarp profiling

➤ *Recent earthquake history*

- Timing of most recent earthquake
- Timing of older earthquakes
- Mean recurrence & periodicity
- Per-earthquake displacement
- Paleoseismic slip rate

➤ *Tools – mostly invasive*

- Fault trench investigation
- Geologic mapping
- Scarp morphology
- Scarp profiling

Focus of this short course

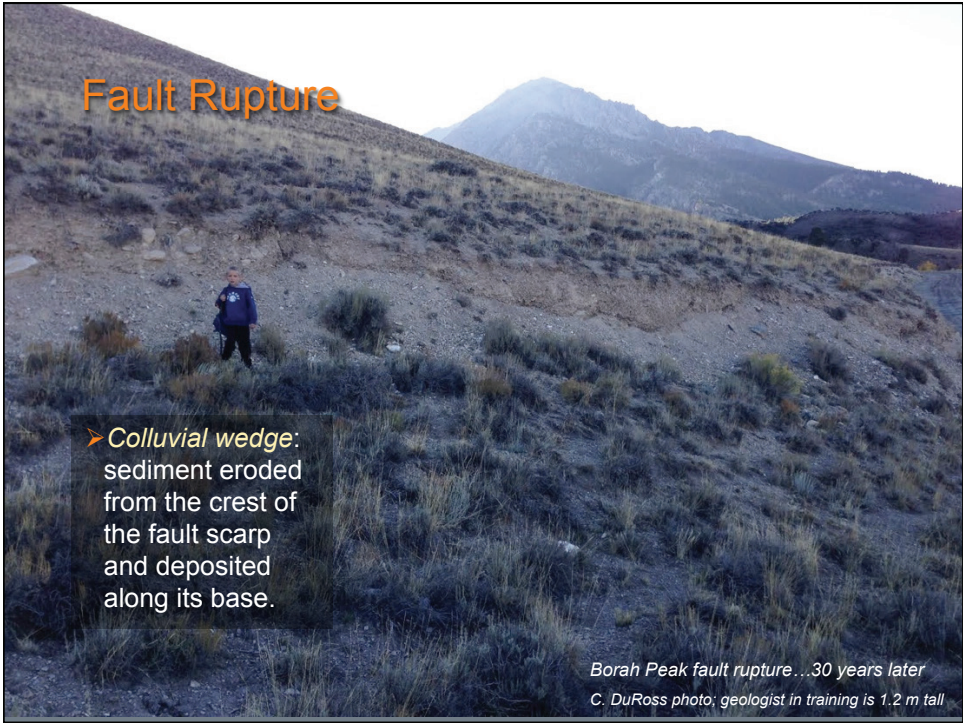
Fault Rupture

- *Fault Scarp*: Surface rupture formed during a moderate to large ($M \sim 6.5+$) earthquake; formed almost instantaneously as fault rupture propagates to the surface.



Surface rupture from 2010 M 7.2 Sierra El Mayor earthquake
(<http://eqclearinghouse.org/co/20100404-baja/general-information/sierra-el-mayor-earthquake-of-april-4-2010-baja-california>)

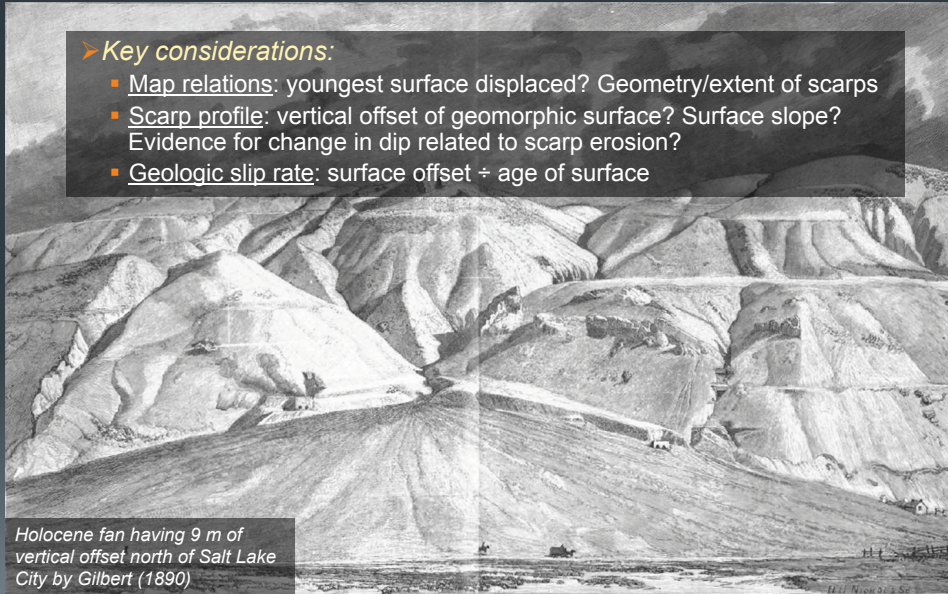




Tools: Scarp Mapping & Morphology

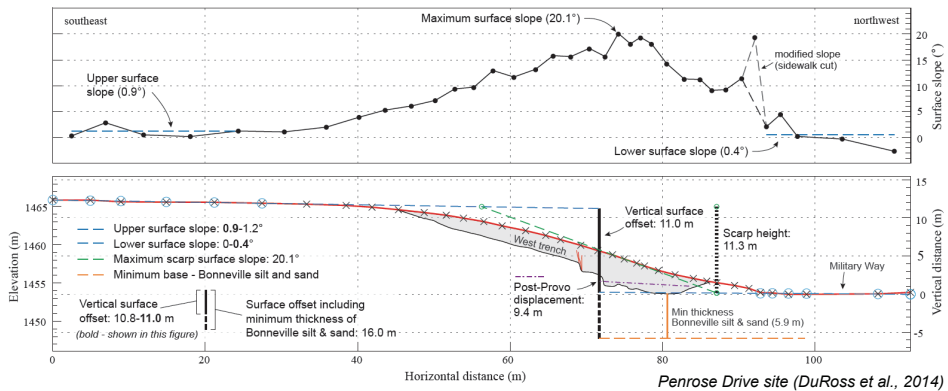
Key considerations:

- Map relations: youngest surface displaced? Geometry/extent of scarps
- Scarp profile: vertical offset of geomorphic surface? Surface slope? Evidence for change in dip related to scarp erosion?
- Geologic slip rate: surface offset ÷ age of surface



Holocene fan having 9 m of vertical offset north of Salt Lake City by Gilbert (1890)

Tools: Scarp Profiling



- Vertical surface offset and scarp height
- If present, graben dimensions and antithetic fault offset
- Pitfalls: noncorrelative surfaces, insufficient profile length to capture full deformation zone

Tools: Paleoseismic Trenching

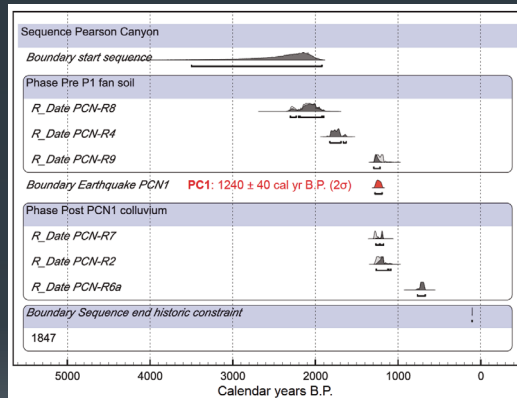
➤ *Purpose:* expose geologic evidence of recent surface-faulting earthquakes



Penrose Drive site (DuRoss et al., 2014)

Earthquake Timing

- *Earthquake time: time of fault rupture based on constraining ages*
- **Numerical:** radiocarbon, OSL, cosmogenic, etc.
 - **Relative:** soil formation, fan sedimentation, scarp morphology...
 - Typically reported as mean and 2σ uncertainty in calendar years B.P., BC/AD, or ka.
- **OxCal.** Powerful tool for determining earthquake times



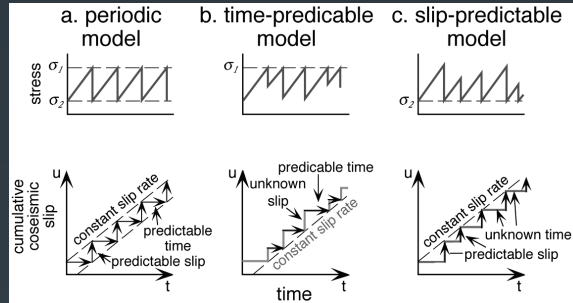
Earthquake PC1 time based on constraining numerical ages. From DuRoss et al. (2012)

Earthquake Recurrence

➤ **Recurrence time.** Elapsed time between earthquakes at a site or on a fault

➤ **Inter-event recurrence.** Elapsed time between two successive earthquakes

➤ **Closed mean recurrence.** Total elapsed time between the oldest and youngest earthquakes divided by the number of closed intervals between them



- Periodic earthquake model.** Constant recurrence and slip. Stress levels at time of earthquake and after are known.
- Time-predictable model.** Failure stress is known. Given previous slip, time until the next earthquake is predictable.
- Slip-predictable model.** Stress level following earthquake is known. Given time since the last rupture, slip is predictable.

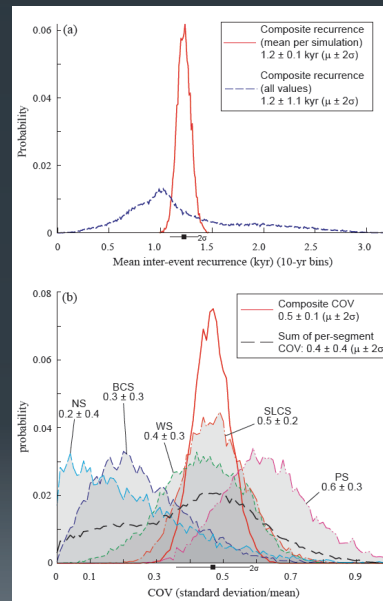
Source: Burbank and Anderson (2001)
<http://activetectonics.asu.edu/lipi/Schedule.html>

Earthquake Recurrence

➤ **Open mean recurrence.** Total elapsed time (to the present) from the maximum age constraint on the oldest event divided by the number of earthquakes that occurred in that period

➤ **Composite recurrence.** Mean recurrence based on grouped inter-event recurrence times for different fault segments

➤ **Periodicity.** Coefficient of variation (COV) on inter-event recurrence. Standard deviation of inter-event recurrence intervals divided by their mean.



Composite recurrence and COV for the Wasatch fault zone (DuRoss et al., in review)

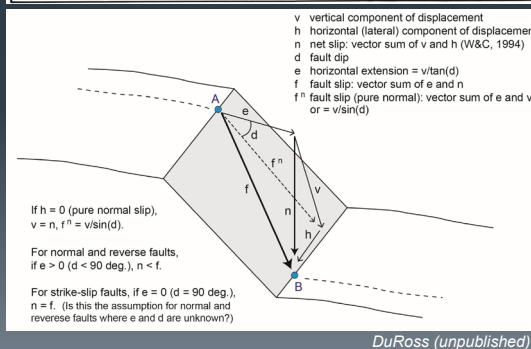
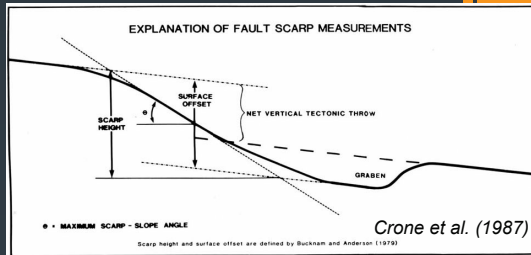
Displacement



Peter Haeussler preparing to measure a crevasse offset by the 2002 M 7.9 Denali earthquake fault rupture (USGS photo).

Fault Displacement

- **Scarp Height:** vertical separation of intersections of upper & lower surfaces with projection of maximum scarp slope
- **Surface offset (SO):** vertical or horizontal separation of geomorphic surfaces/features due to faulting. Total SO = NVTD.
- **Net displacement:** vector sum of vertical (V), horizontal (H) slip components
- **Fault displacement:** vector sum of net displacement & extensional (E) component
- **Other methods:**
 - Colluvial wedge height
 - Trench reconstruction
 - SO divided by number of earthquakes



Slip Rate

➤ Slip rate (SR)

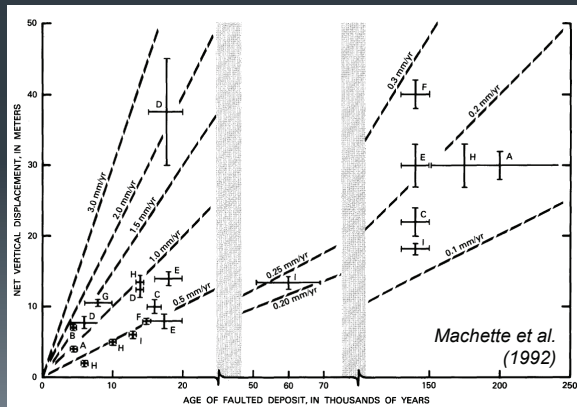
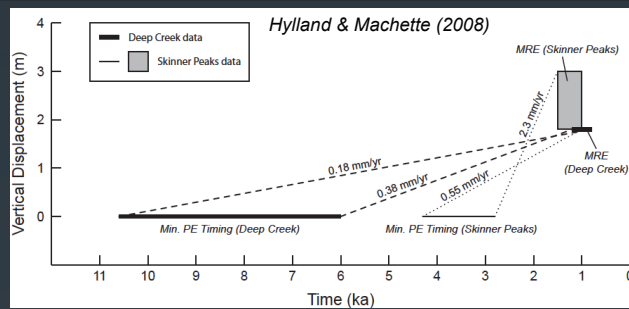
Vertical, horizontal, or net rate of fault movement (mm/yr)

➤ Paleoseismic SR

Displacement divided by preceding interseismic period

➤ Geologic SR

Total displacement divided by age of displaced surface



Seismic Moment (M_0) & Magnitude

➤ Seismic moment (M_0) = $\mu \cdot A \cdot AD$

- μ = crustal rigidity/shear modulus ($\sim 3 \times 10^{11}$ dyne-cm)
- Area (A) = surface-rupture length (SRL) * down-dip width (W)
- AD = Average slip on fault (average dislocation over area of fault surface)

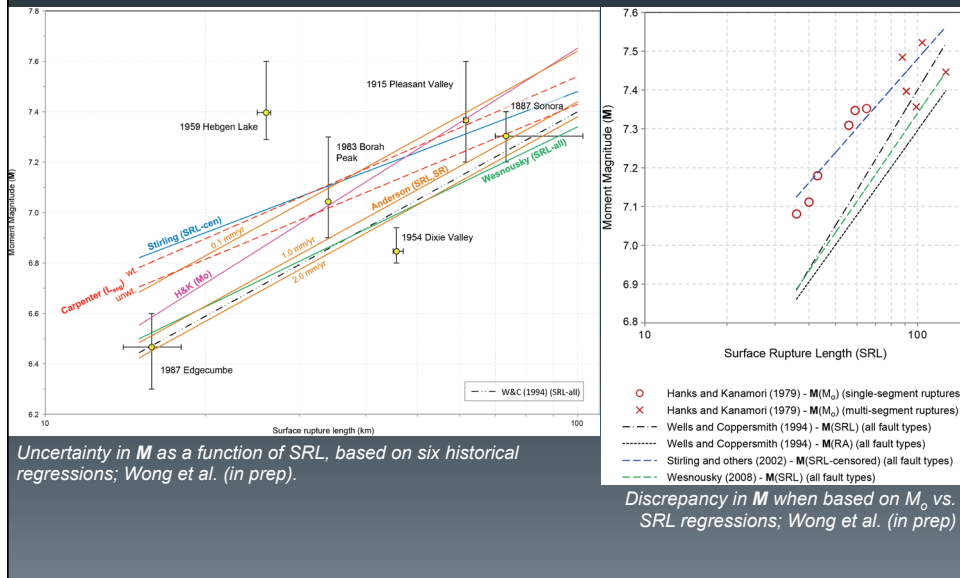
➤ Moment magnitude (M) (Hanks and Kanamori, 1979)

- $M = 2/3 \log M_0 - 10.7$

➤ Empirical linear regressions (e.g., Wells & Coppersmith, 1994)

- $M = a \log X + b$
- X = fault parameter, e.g., SRL, W, A, D, SRL*D, A*D...
- a, b = constants

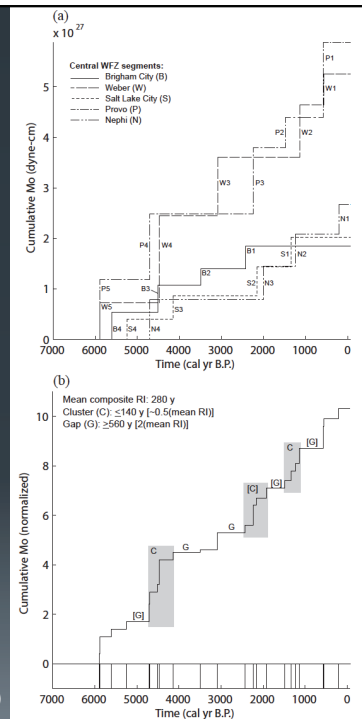
Magnitude Regressions



M_0 Release

- Is strain completely released in each large earthquake?
- Pattern of strain release over time (compare Nephi and Brigham City segments)
- Evidence for clustering?
- What recurrence model is most applicable (*periodic, slip predictable, time predictable*)?

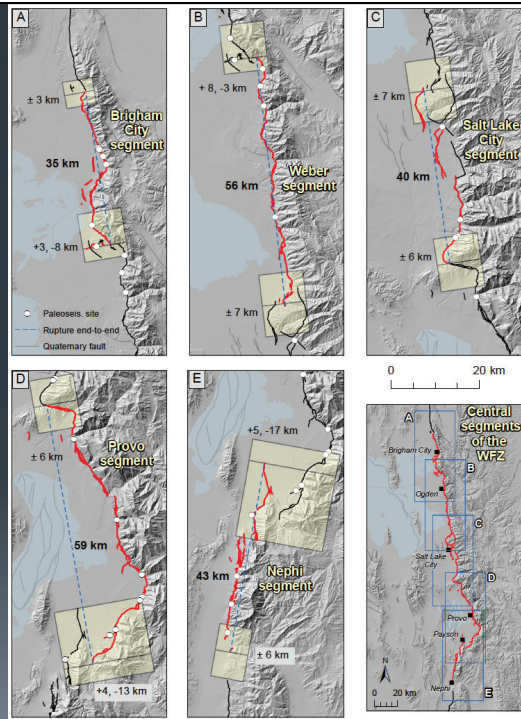
DuRoss et al., in review (BSSA)



Rupture Length

- *Rupture lengths* depend on segmentation model and affect estimates of M_0 and M .
- *Segment boundaries* arrest ruptures over many earthquake cycles, but also fail depending on local stresses, earthquake propagation, displacement, etc.
- *Defining uncertainties* consider segment boundaries as areas rather than points

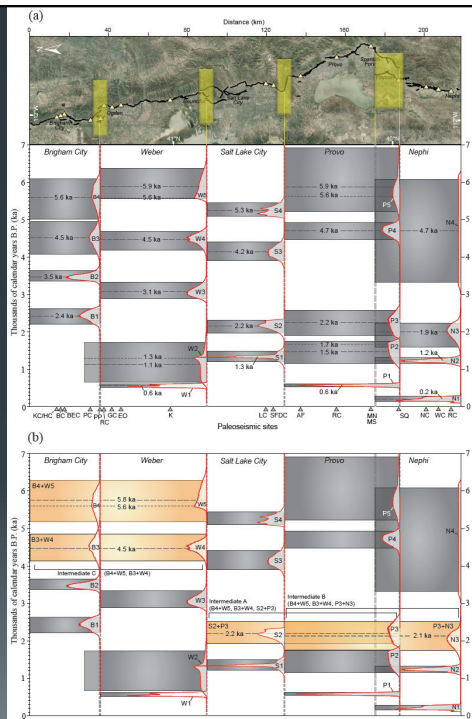
DuRoss et al., in review (BSSA)



Segmentation

- *Rupture models* help address uncertainties in rupture length
- *Can multi-segment ruptures be ruled out considering uncertainty in earthquake-timing data?*
- Displacements can help selecting possible multi-segment ruptures (e.g., large displacements at segment boundaries?)

DuRoss et al., in review (BSSA)



TRENCH EXCAVATION

Trench Site Selection

➤ *Depends on purpose of study*

- Locate fault?
- Most recent earthquake timing and displacement?
- Long record and/or earthquake recurrence?

➤ *Other factors:*

- Scarp height
- Surface slope
- Sediment type/character (thickness of units vs. amount of displacement)
- Location along fault
- Recent modification (human or otherwise)

➤ *Ideal site characteristics:*

- Moderate scarp height (~4-10 m)
- Moderate surface slope
- Simple fault geometry
- Fine grained sediments
- Limited hanging-wall deposition



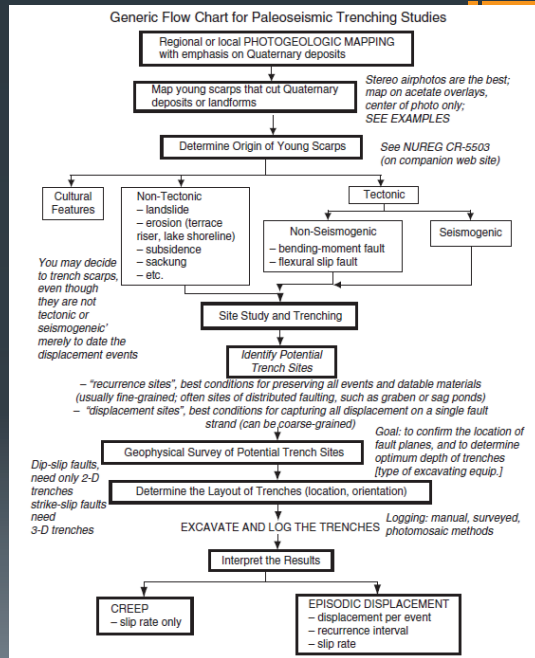
Tyler Knudsen (UGS) evaluating a possible trench site on the Washington fault

Site Selection

➤ Key steps:

1. Literature/data review
2. Map the fault and surficial deposits (air photos, LiDAR, drone, etc.)
3. Determine origin of scarps? (complex deformation, landslides?)
4. Evaluate fault geometry (is this the best place to trench?)
5. Remember focus of study (MRE vs. long history?)
6. Lay out trenches at site

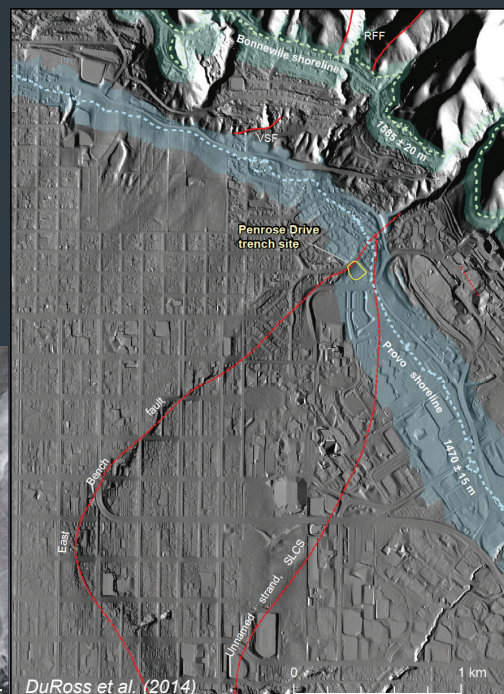
<http://activetectonics.asu.edu/lipi/Schedule.html>



Example: Penrose Drive Site

➤ Positives:

- Simple, well located fault
- Moderately large scarp, but moderate surface slope
- Limited development
- Bonneville shoreline nearby



Example: Penrose Drive Site

➤ Potential negatives:

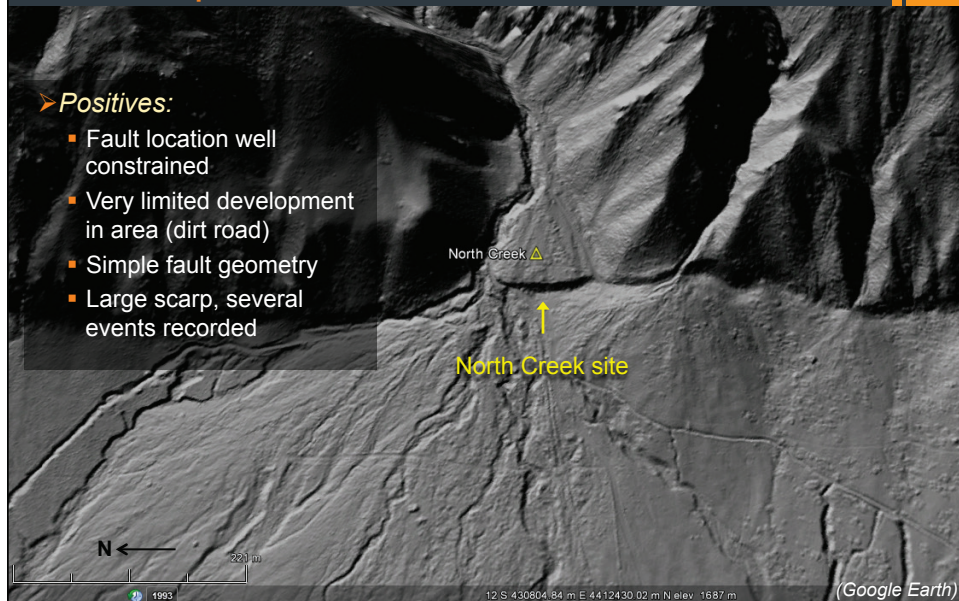
- Fault trace to the east – earthquakes on that strand, not recorded at this site?
- Close to the northern end of the fault strand – did all ruptures make it to the end?
- Origin or scarp – possible lateral stream terrace?
- Development at the site – limited room for trenching



Example: North Creek Site

➤ Positives:

- Fault location well constrained
- Very limited development in area (dirt road)
- Simple fault geometry
- Large scarp, several events recorded

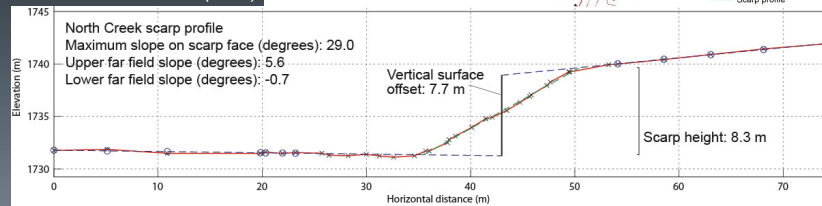
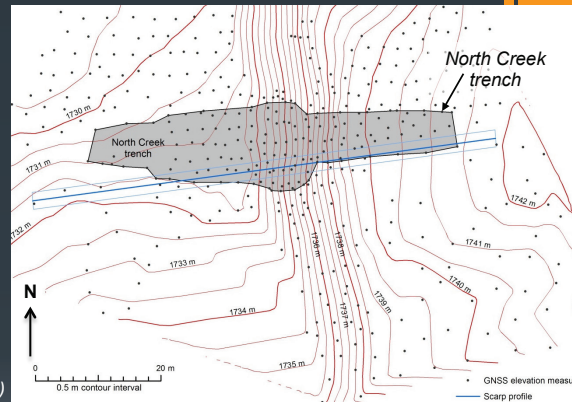


Example: North Creek Site

➤ Potential negatives...

- Large scarp (a lot of sediment to move) – may not get correlative units across fault
- Coarse stream and debris flow sediments
- Deposition of young alluvial fan on hanging wall

DuRoss (2014)



Example: Warm Springs Site



➤ Positives:

- Close to left step between the Warm Spring and East Bench faults
- Only option on the Warm Springs fault
- Moderately large "scarp"

Trench Design (*moderate scarp*)

- Dig at least as deep as $\sim\frac{1}{2}$ the scarp height or vertical surface offset (deeper if there are hanging wall deposits or a large graben)
- Keep benches wide, straight, and continuous along the trench

Corner Canyon trench
Scarp height: ~ 9 m
Trench depth: ~ 4.5 m



Trench Design (*large scarp*)

- Dig as deep as possible in the fault zone
- Avoid large headwall by keeping walls planar and benches continuous
- Time consuming (often have to move excavated sediment twice)

North Creek trench
Scarp height: ~ 9 m (~ 8 m offset)
Trench depth: ~ 5 m



DuRoss (2014)

Trench Design (megatrench)

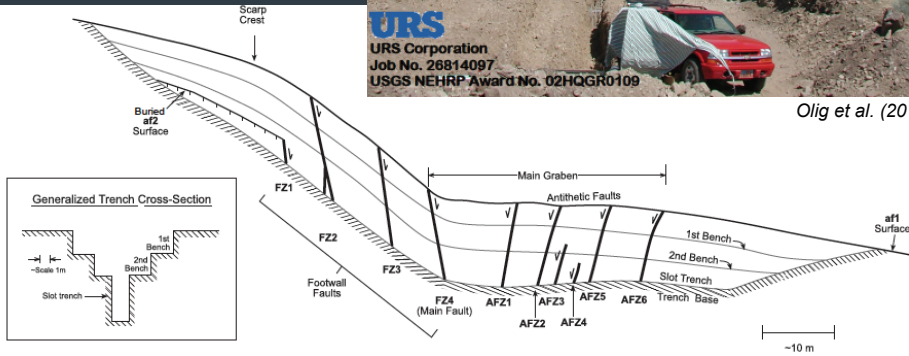
- Correlative units across fault zone unlikely
- Footwall & antithetic faults are important
- Concerns: equipment size, spoils placement, budget...

Mapleton megatrench
Scarp height: 19-23 m
Trench depth: ~12 m



URS Corporation
Job No. 26814097
USGS NEHRP Award No. 02HQGR0109

Olig et al. (2011)

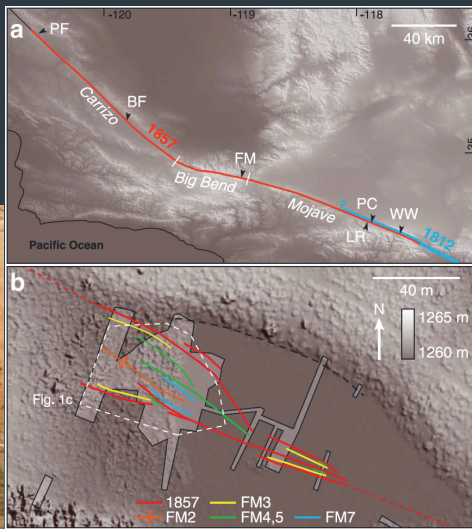


Trench Design (other)

- Other trenching methods:
 - Slot trenching
 - Fault parallel trenching
 - Sloped/complex trenches
 - See Burbank and Anderson (2011)



Streams offset by the San Andreas fault along the Carrizo plain; Wallace (1990)



Frazier Mountain site, San Andreas fault (Scharer et al., 2014)

Trench Excavation Equipment

Table 2A.2: Excavating capabilities of various types of machines

Type of machine	Photographs of typical machines made by Caterpillar company	Digging depth	Width of digging bucket	Capacity of digging bucket	Advantages or disadvantages for paleoseismology
Rubber-tired backhoe loader	 Cat 420	Typically 4-5 m	0.3-0.9 m	Up to 0.6 m ³	Inexpensive; widely available; good for single-slot trenches up to ca. 4 m; can backfill trenches as well as dig them
Tracked hydraulic excavator ("trackhoe")	 Cat 325	Up to 11 m	Up to 2.4 m	Up to 5.8 m ³	Widely available; digs over twice as deep as a backhoe, and moves material much faster; more maneuverable on steep terrain; can dig single-slots deeper than 4 m, OR move larger volumes of material needed in 1- or 2-bench trenches; can dig deep slots within in wider trenches by walking onto their floors (if wide enough)
Rubber-tired (wheel) loader	 Cat 994	unlimited	Typically 3.2 m	Up to 36 m ³ , but typically 3-5 m ³	Good for multibenched trenches, if material is unconsolidated and soft, such as eolian deposits; has the most flexibility in placing the spoil dirt

<http://activetectonics.asu.edu/lipi/Schedule.html>

Trench Excavation Equipment

Table 2A.2: Excavating capabilities of various types of machines—Cont'd

Type of machine	Photographs of typical machines made by Caterpillar company	Digging depth	Width of digging bucket	Capacity of digging bucket	Advantages or disadvantages for paleoseismology
Scraper (Cat 621)		unlimited	Up to 3.7 m	Up to 34 m ³	Expensive; not widely available; best for very large benched trenches, due to its large capacity (see Figure 2A.28)
Track-type tractor ("bulldozer") Cat D8		unlimited	Up to 3 m	Not applicable	Widely available, but expensive in larger sizes; can rip hard rocks, unlike scrapers and loaders; best for deep trenches in semi-consolidated deposits or bedrock; to distribute soil dirt from trench, may need to work in combination with a loader

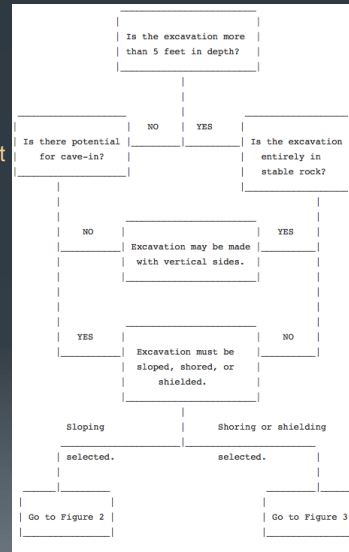
The largest machines of each type are generally made for the mining industry, rather than for the construction industry.

<http://activetectonics.asu.edu/lipi/Schedule.html>

Trench Safety

➤ OSHA general trench & excavation rules:

- Keep heavy equipment away from trench edges.
- Identify other sources that might affect trench stability.
- Keep excavated soil (spoils) and other materials at least 2 feet (0.6 meters) from trench edges.
- Know where underground utilities are located before digging.
- Test for atmospheric hazards such as low oxygen, hazardous fumes and toxic gases when > 4 feet deep.
- Inspect trenches at the start of each shift.
- Inspect trenches following a rainstorm or other water intrusion.
- Do not work under suspended or raised loads and materials.
- Inspect trenches after any occurrence that could have changed conditions in the trench.

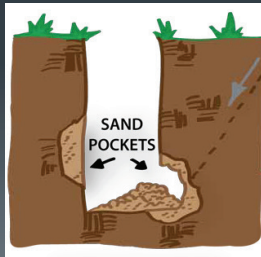
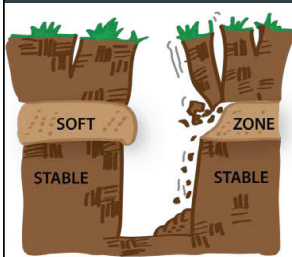
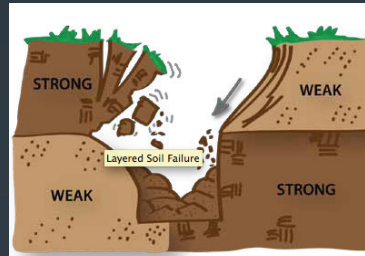


<https://www.osha.gov/SLTC/trenchingexcavation/>

Trench Safety

➤ Other guidelines:

- Recognize hazards associated with alternating weak (e.g., sand) and strong (e.g., clay) layers
- Be wary of very young or modern deposits
- Walk the perimeter of the trench to look for incipient cracks



<http://underspace.com/how-trenches-collapse/>



CONDUCTING THE FIELD INVESTIGATION

Field Investigation

1. Inspect trench walls (in and above trench); fence
2. Coarse cleaning
3. Grid trench walls
4. Fine cleaning
5. Photograph (office: build mosaics)
6. Interpret and mark walls (sketch)
7. Determine sampling strategy
8. Log on grid paper or photomosaics
9. Sample for radiocarbon/OSL
10. Photograph samples, final interpretation
11. Misc: fault measurements, soil descriptions, GPS trench extent
12. Field review
13. Backfill & site reclamation



*What's missing from this picture?
Cleaning a trench at the Dutchman Draw site on the Washington Fault*

Trench Prep

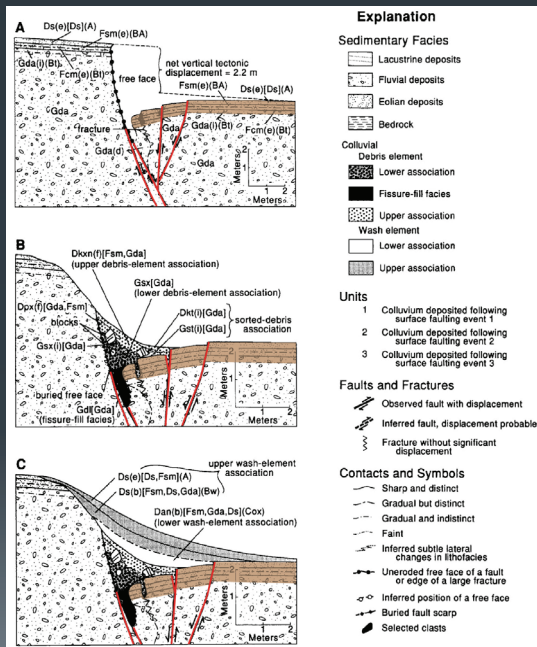
- Rough cleaning – make wall as planar as possible
- Grid walls using string line or spikes/flagging
- Fine cleaning – brush wall, clean up fault zones
- Photograph for mosaics (early morning or overcast)



Corner Canyon trench, cleaned, gridded and ready to photograph

Evidence for Earthquakes

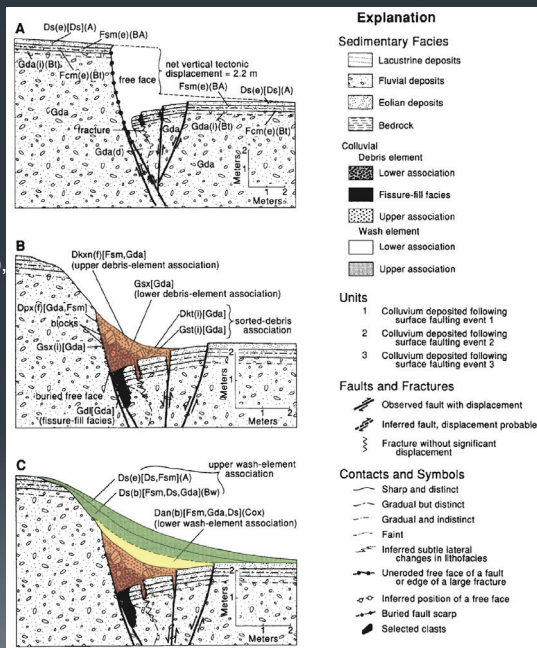
- **Scarp derived colluvium**
 - Debris and wash facies
 - Stone lines (slope fabric)
 - Fissure fill
 - Buried free face (?)
 - Footwall blocks
- **Evidence for a paleosurface**
 - Faulted/buried soil
 - Fault/fracture terminations
- **Other evidence**
 - Back rotation (steepening toward fault)
 - Fault drag
 - Sag pond deposits
 - Sedimentation between events
 - Unconformities



Modified from Nelson et al., 1992

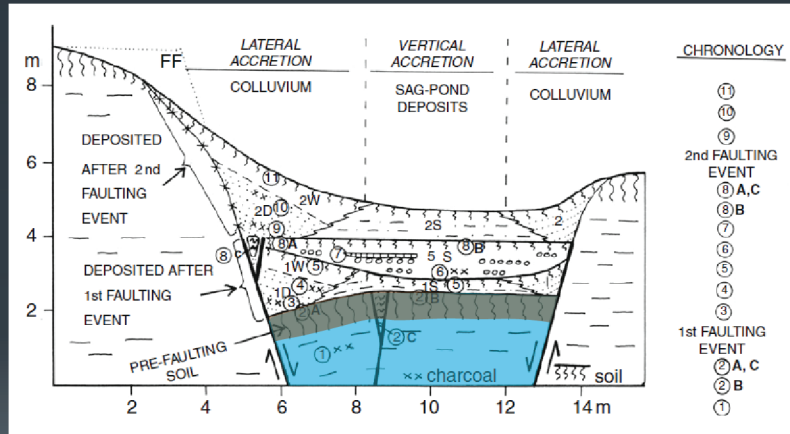
Scarp-Derived Colluvium

- **Debris Facies**
 - Wedge shaped
 - Abuts scarp
 - Sharp lower contact
 - **Deposition:** mostly gravity-controlled (e.g., block failure), some surface wash and eolian input
 - Generally coarse
- **Wash facies**
 - Less wedge shaped
 - Overlaps eroded free face
 - Extends beyond debris facies;
 - **Deposition:** mostly surface wash, eolian
 - Gradational lower contact
 - Mostly fine grained



Modified from Nelson et al., 1992

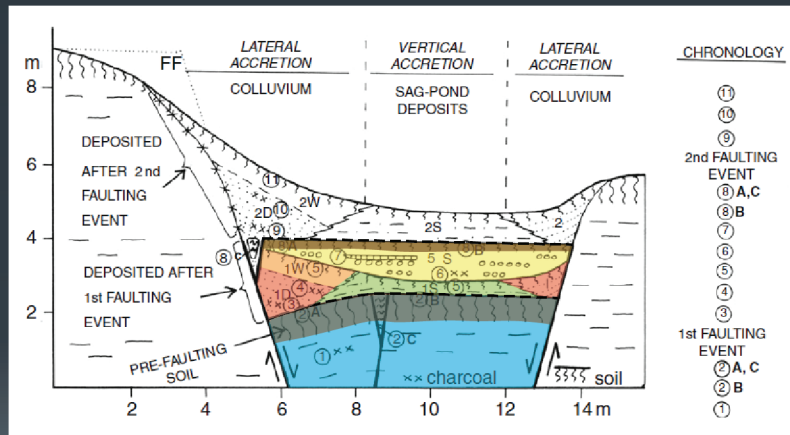
Evidence for Earthquakes



Pre-earthquake 1 deposits and soil

Modified from McCalpin & Nishenko (1996)

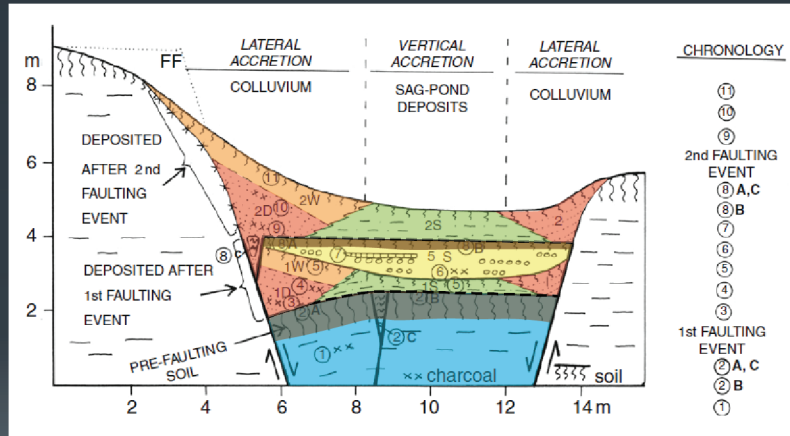
Evidence for Earthquakes



Post-earthquake 1 deposits and soil

Modified from McCalpin & Nishenko (1996)

Evidence for Earthquakes



Post-earthquake 2 deposits and soil

Modified from McCalpin & Nishenko (1996)

Stratigraphic Evidence for Earthquakes

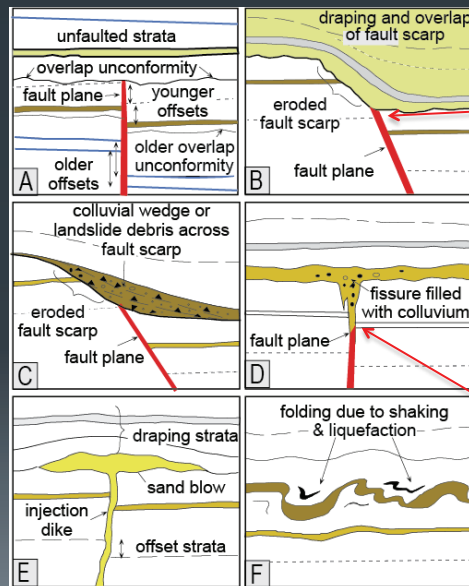
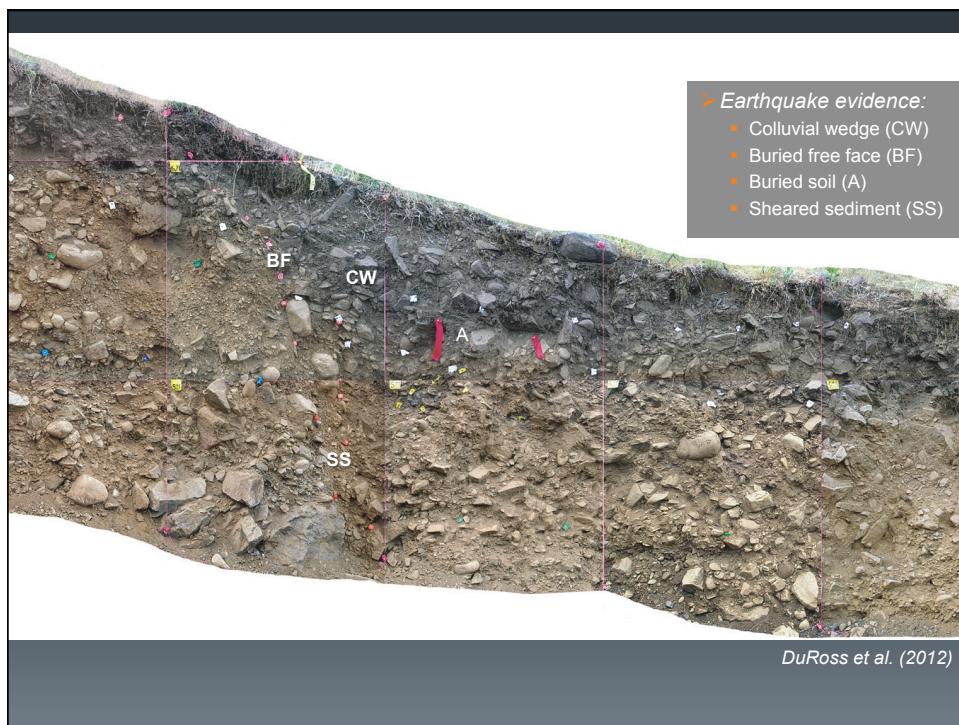
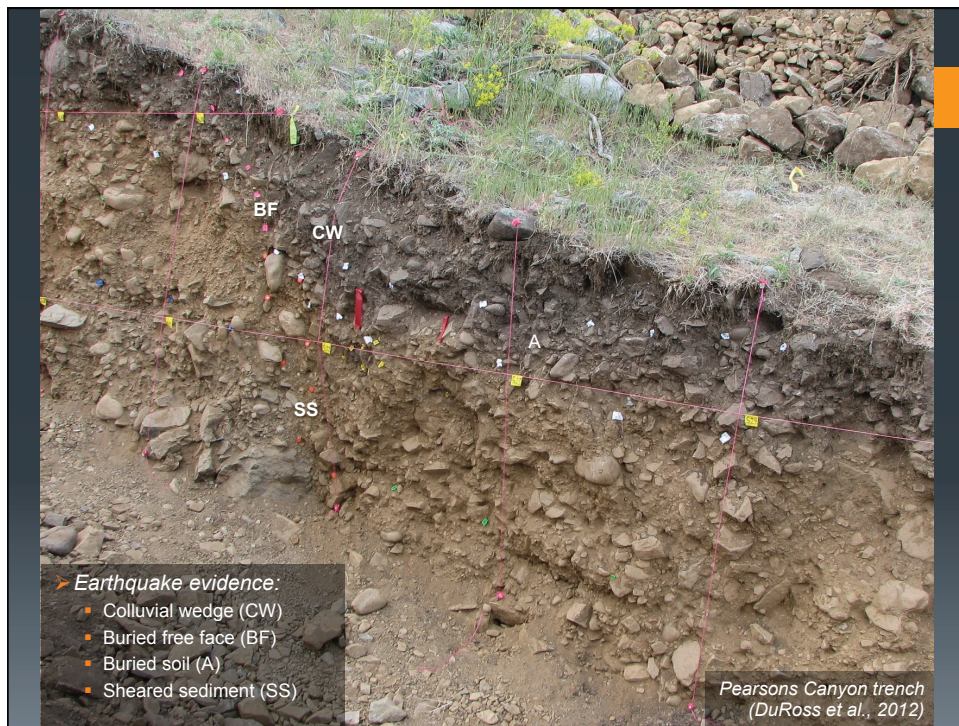
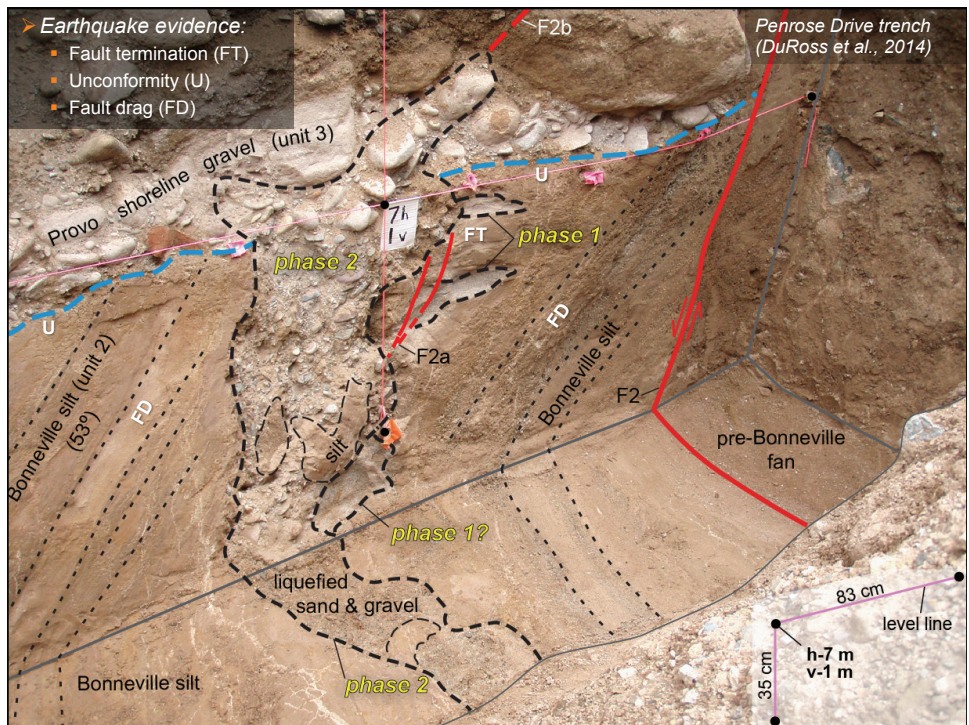
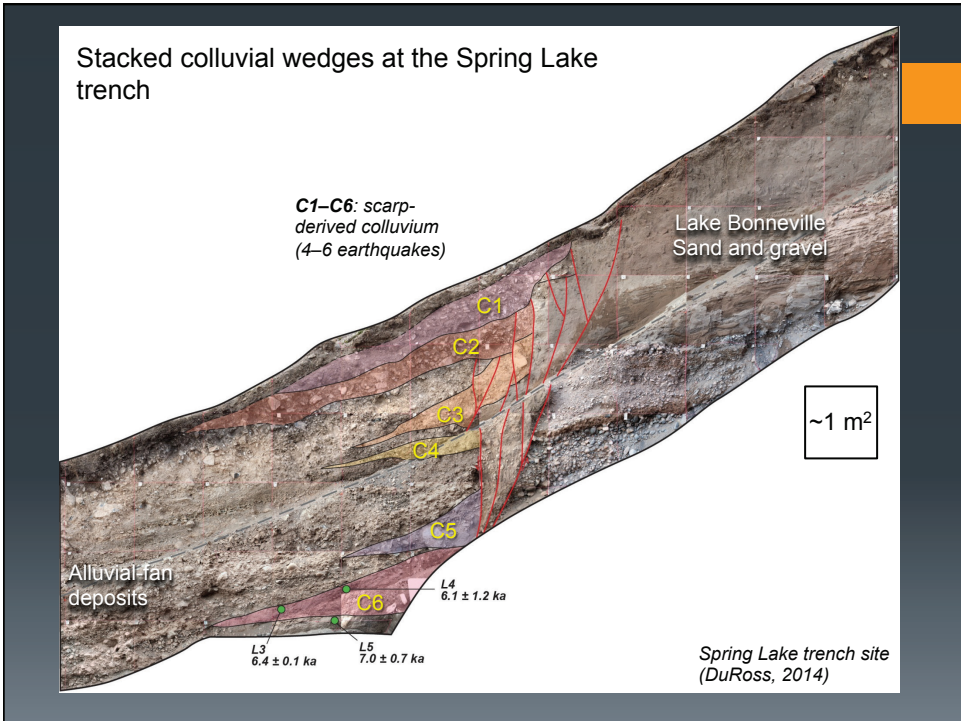


Figure and photos from Burbank and Anderson (2011)
http://www.geol.ucsb.edu/faculty/burbank/Site/Tect_Geom_2nd_Ed_Figs.html





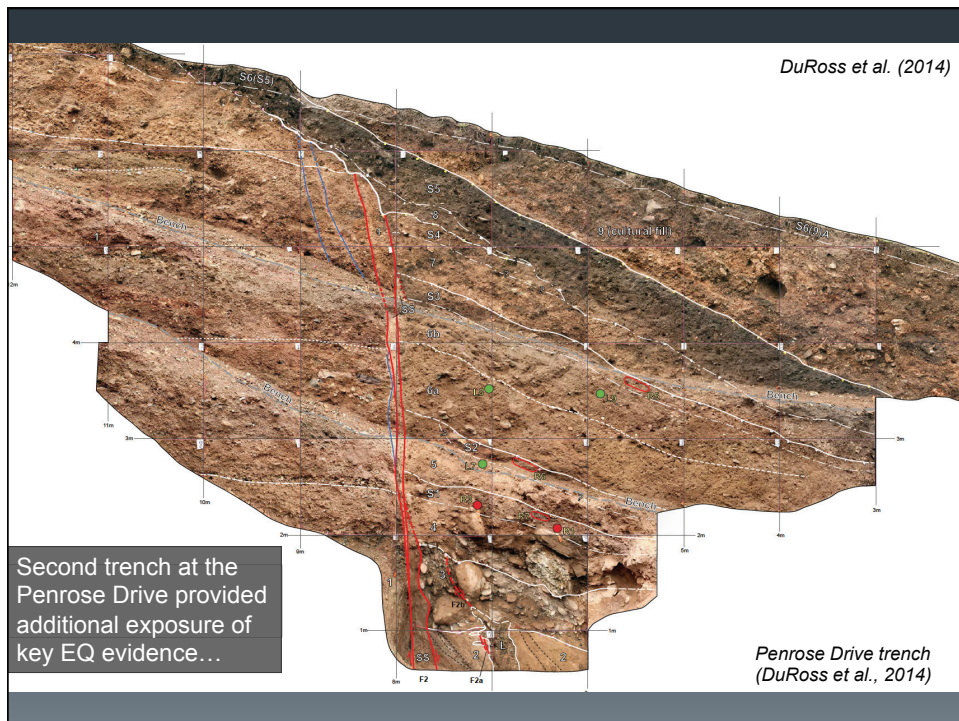


Evidence...?

- But sometimes things don't go quite as planned...
- Alternate approaches:
 - Clean both walls
 - Interpret easy/obvious contacts first
 - Dig back a few centimeters
 - Hand dig in fault zone
 - Excavate an additional trench?
 - Additional site?

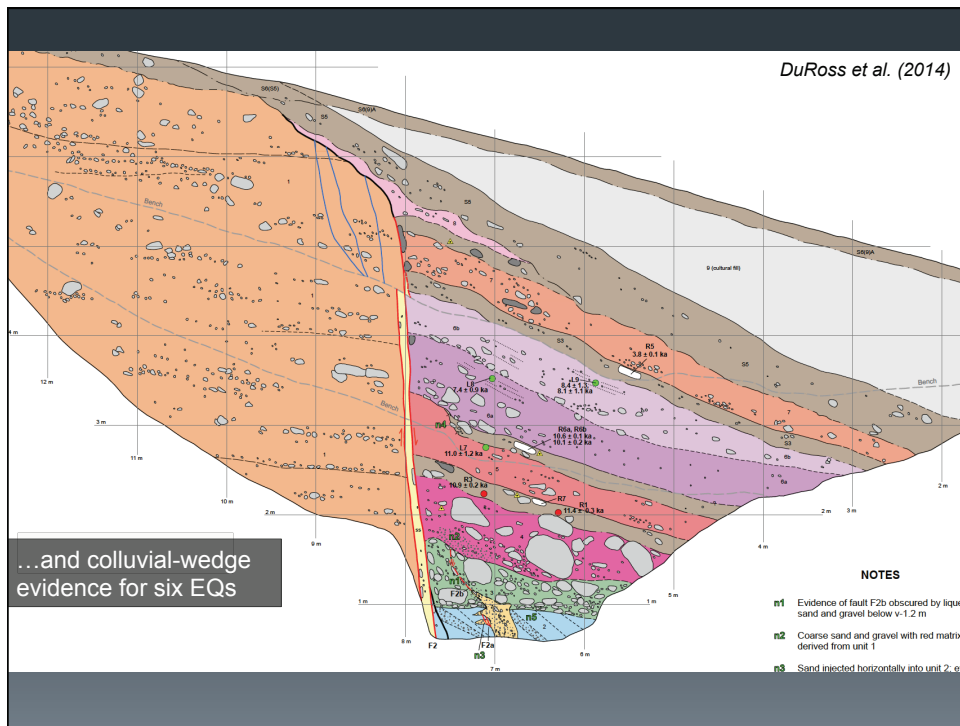


Tony Crone (USGS-retired) adjacent to massive colluvial wedges exposed at the Penrose Drive trench site (DuRoss et al., 2014)



Second trench at the Penrose Drive provided additional exposure of key EQ evidence...

Penrose Drive trench (DuRoss et al., 2014)



Sampling Strategy

- **Colluvial wedges**
 - 2-4 samples per colluvial wedge
 - ¹⁴C samples from buried soil and wedge sediment
 - OSL from distal wedge sediment
 - Duplicate samples
- **Footwall, hanging wall units**
 - 2-4 samples (ideally)
 - Less critical than wedge samples
- **Considerations:**
 - Avoid heavily burrowed areas
 - Stack samples vertically
 - Sample from same wall
 - For youngest units, sample as deep as possible
 - Record as many details as possible (context, importance...)



Sampling Strategy

➤ Soil excavation:

- As close to, but confidently above/below contact or soil
- Larger excavations within wedge or other sedimentary unit
- *Where is the contact?* Long, shallow excavation better than short, deep
- Collect more than you need.



Sample locations at the Corner Canyon trench

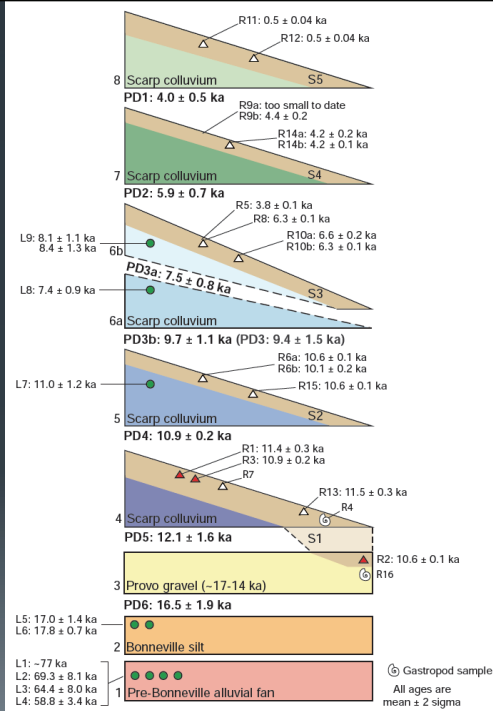
Dating Strategy

➤ Colluvial wedges

- At least 2 ages per colluvial wedge
- Additional ages reduce earthquake timing uncertainty
- Ages from top/bottom of wedges
- OSL ages from wedge

➤ Additional considerations:

- Ages for footwall/hanging wall sediments
- Able to correlate units & wedges from parallel faults?
- Constrain slip rate?



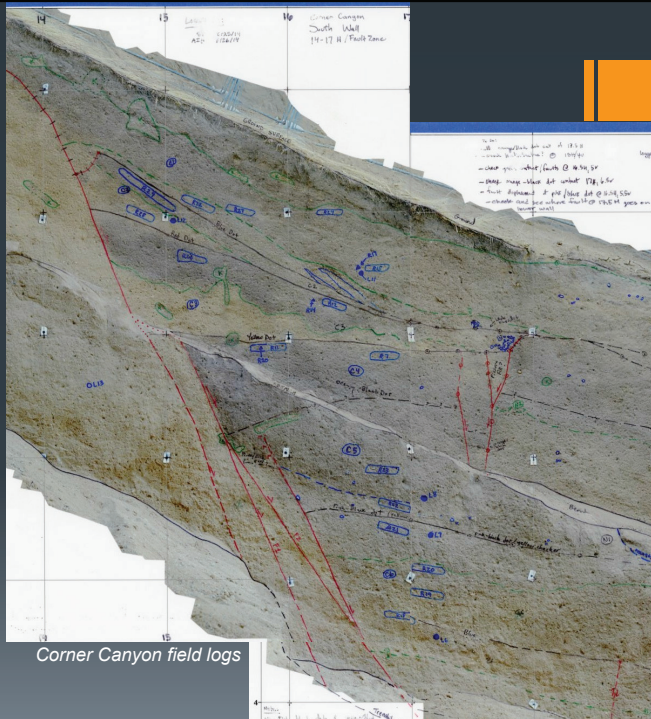
Logging

➤ *Field logs should include:*

- Unit origin/interpretation
- To Do list
- Notes
- Sample locations

➤ *Other considerations:*

- Evidence for earthquakes
- Consistent labels/line types
- Edge matching
- Burrows



WORKING WITH PALEOSEISMIC DATA

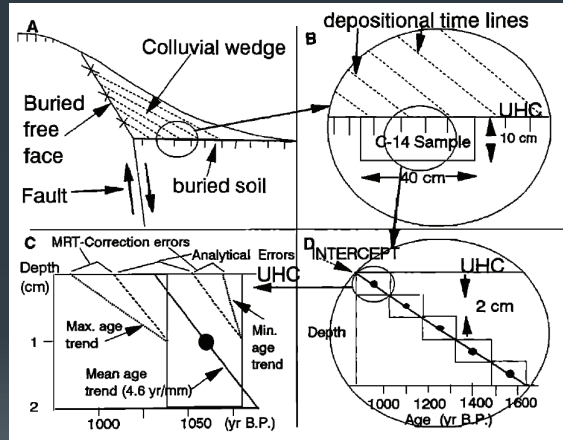
Earthquake Timing

➤ Minimum limiting ages

- Organics or sediment from colluvial wedge or other post-earthquake deposits (e.g., debris flow, loess)

➤ Maximum limiting ages

- Organics or sediment from buried soil or deposits predating earthquake



McCalpin and Nishenko (1996)

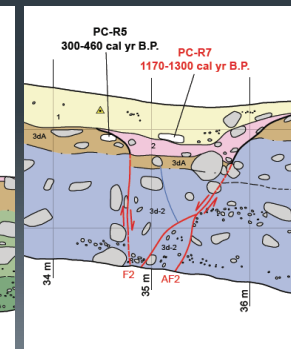
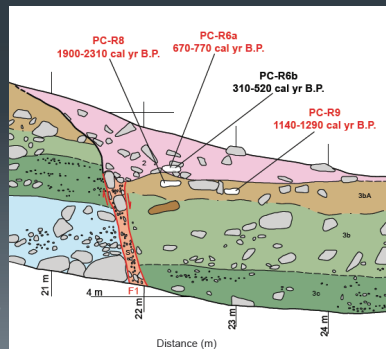
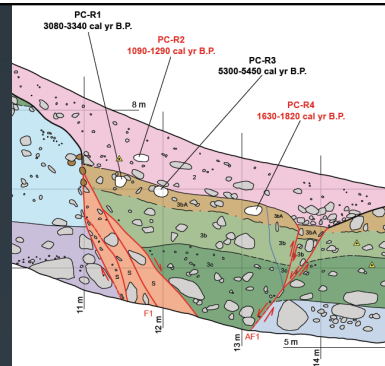
Earthquake Timing

➤ Maximum ¹⁴C ages:

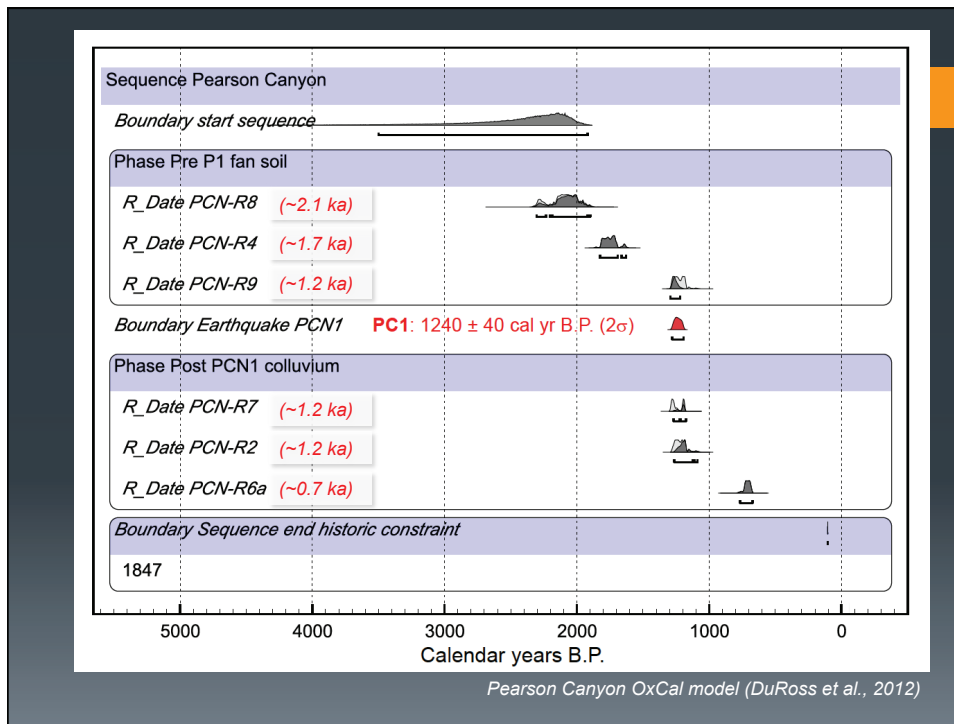
- R5: ~0.4 ka
- R9: ~1.2
- R4: ~1.7
- R8: ~2.1
- R1: ~3.2 ka
- R3: ~5.3 ka

➤ Minimum ¹⁴C ages:

- R6b: ~0.4 ka
- R6a: ~0.7 ka
- R2: ~1.2 ka
- R7: ~1.2 ka



Pearson Canyon trench logs (DuRoss et al., 2012)



Displacement per Earthquake

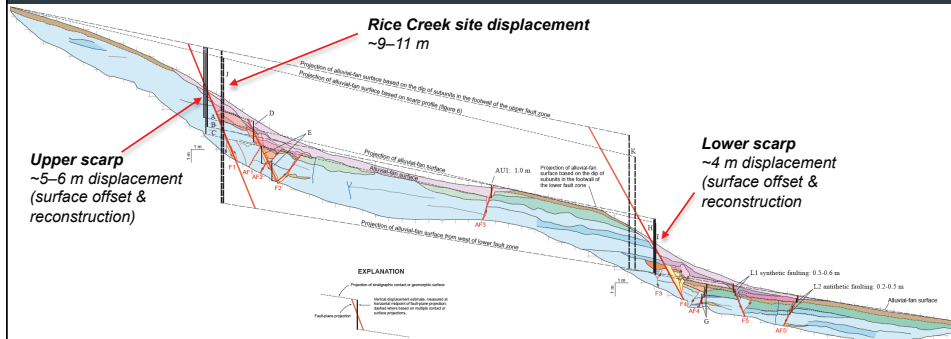
➤ Measurement types

- Surface offset
- Stratigraphic displacement
- Offset or displacement divided by # of events
- Colluvial wedge height (minimum)
- Colluvial wedge area
- Trench reconstruction



Santaquin trench
(DuRoss et al., 2008)

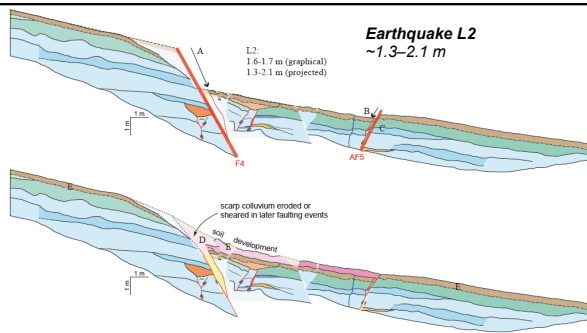
Displacement per Earthquake



DuRoss et al. (2009)

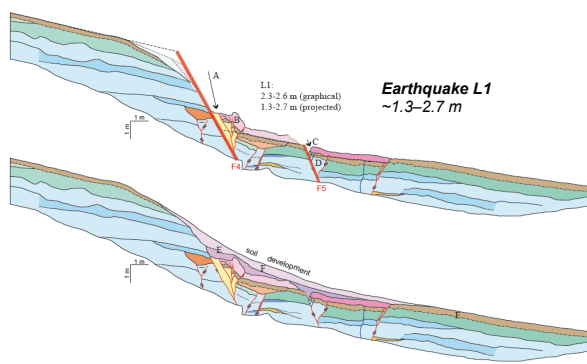
Earthquake L2

- A: 2 m of vertical displacement on fault F4
- B: 0.5 m antithetic-fault displacement on fault AF5
- C: Near-fault drag (6.5 degrees counterclockwise) in footwall of antithetic fault AF5
- D: Deposition of earthquake L2 scarp colluvium
- E: A-horizon development on alluvial-fan surface and L2 colluvium (not mapped)

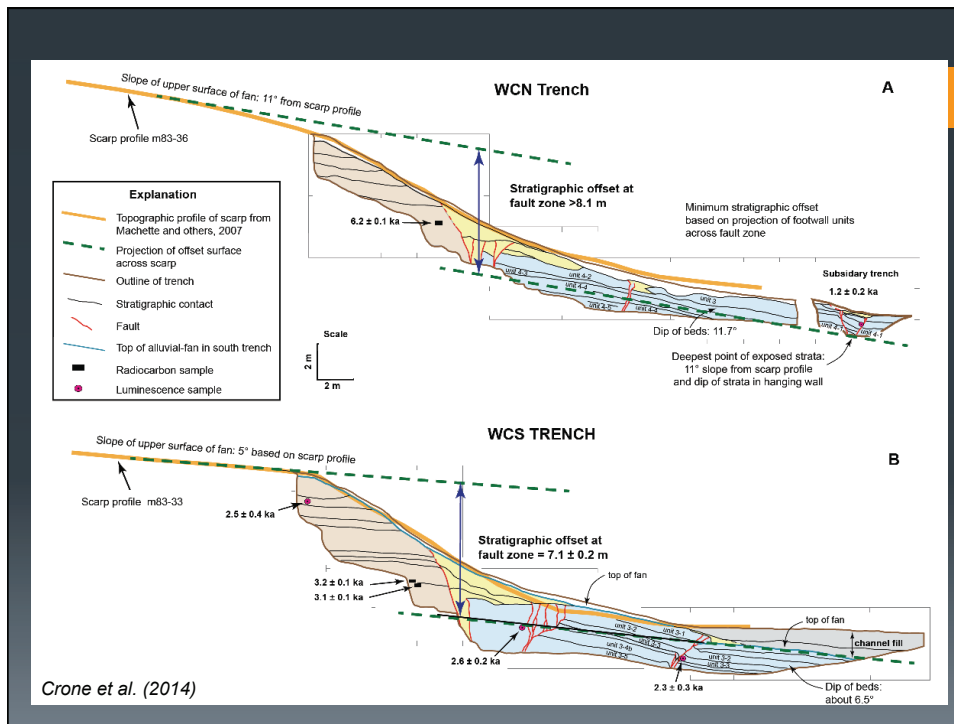


Earthquake L1

- A: 2 m vertical displacement on fault F4
- B: Blocks of alluvial-fan deposits and L2 colluvium compressed along fault F4
- C: 0.6 m synthetic displacement on fault F5 (about one-half accommodated by 3 degrees of counterclockwise hanging-wall rotation)
- D: 1-m-wide block bounded by minor fault antithetic to fault F5 rotates 7 degrees clockwise
- E: Deposition of earthquake L1 scarp colluvium
- F: A-horizon development on alluvial-fan surface and L1 colluvium (not mapped)

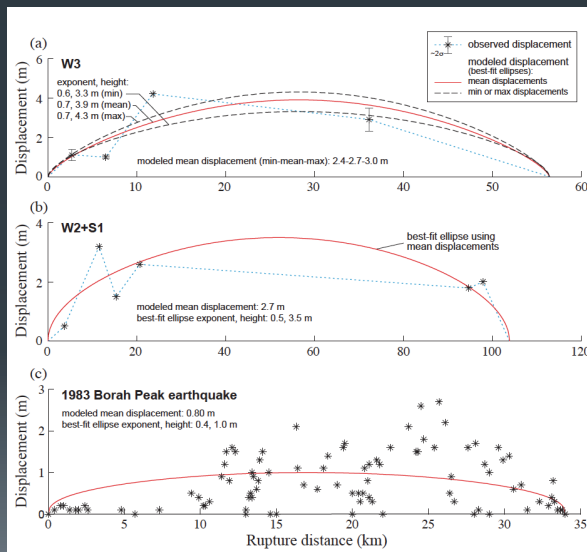


DuRoss et al. (2009)



Displacement per Rupture

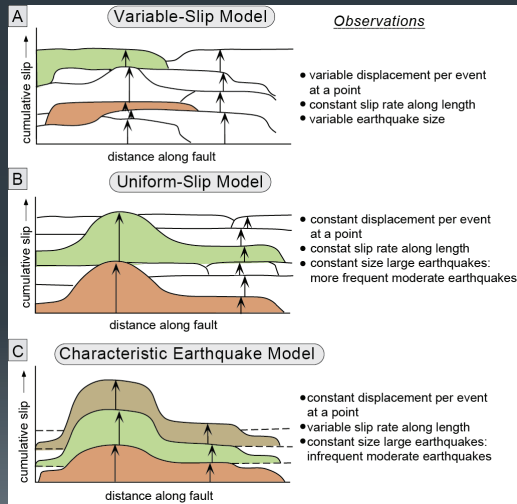
- *Distribution of displacement*
- Position along rupture is important – assuming than slip increases toward the center of the fault.
- References:
 - Chang & Smith (2002)
 - Biasi and Weldon (2009)
 - DuRoss and Hylland (2014)



Displacement along Strike

➤ Characteristic earthquake model

- Faults/segments tend to produce similar-sized earthquakes at the upper end of their possible magnitude ranges
- Thus, these faults/segments have relatively large and similar displacements at a point during individual earthquakes.
- Source: Schwartz and Coppersmith (1984)



Source: Burbank and Anderson (2011)
http://www.geol.ucsb.edu/faculty/burbank/Site/Tect_Geom_2nd_Ed_Figs.html

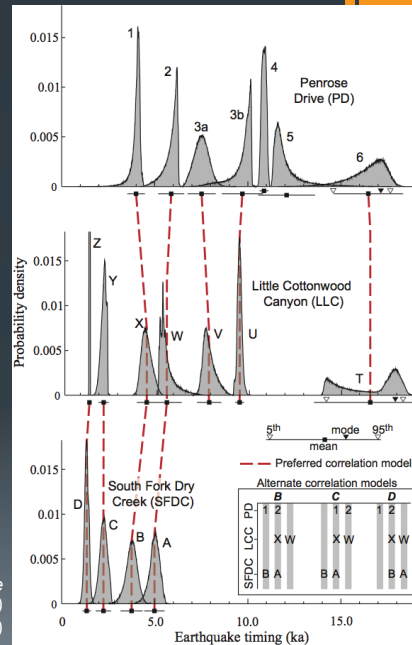
Synthesizing Data

➤ Correlation of earthquake-timing PDFs

- Qualitative: eye-ball correlation
- Quantitative: compare overlap in PDFs (Biasi & Weldon, 2009)

➤ Other issues?

- Methods for combining?
- Implications for rupture extent, segmentation?
- Consider multiple models



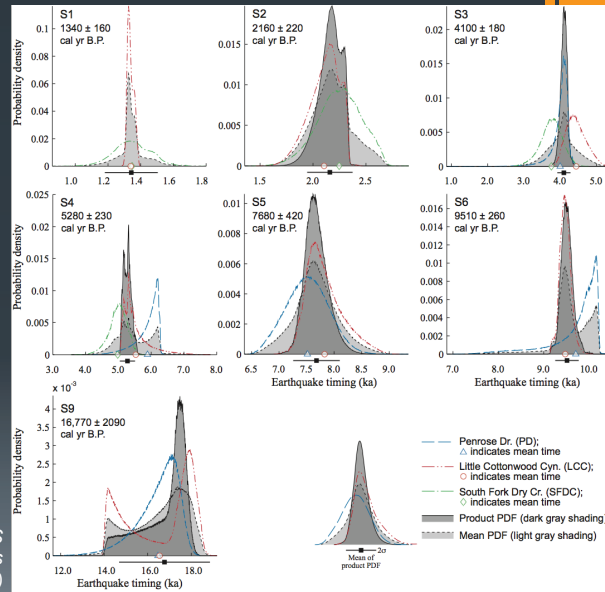
Correlation of earthquakes on the Salt Lake City segment (SLCS) (DuRoss & Hylland, 2014)

Synthesizing Data

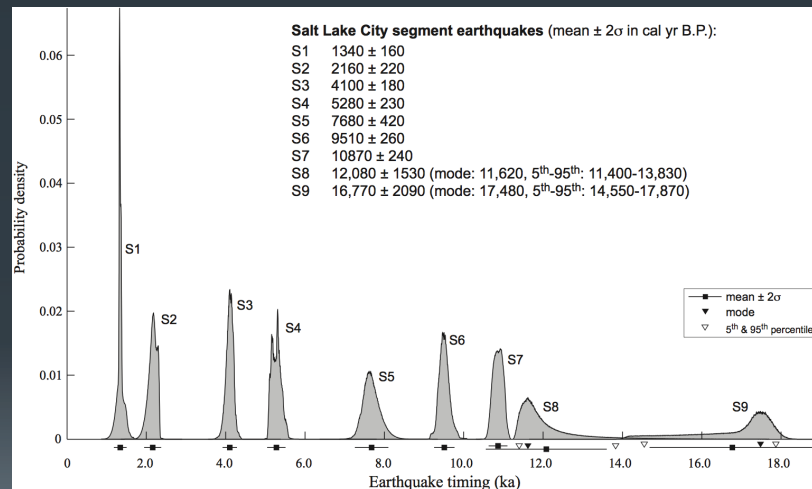
Combining earthquake-timing PDFs

- Qualitative: use mean times and 2σ ranges
- Quantitative: bin-by-bin mean or product of probabilities
- (Biasi & Weldon, 2009; DuRoss et al., 2011)

Integration of SLCS earthquake-timing PDFs (DuRoss & Hylland, 2014)



Synthesizing Data



Resulting SLCS earthquake chronology (DuRoss & Hylland, 2014)

Earthquake Recurrence

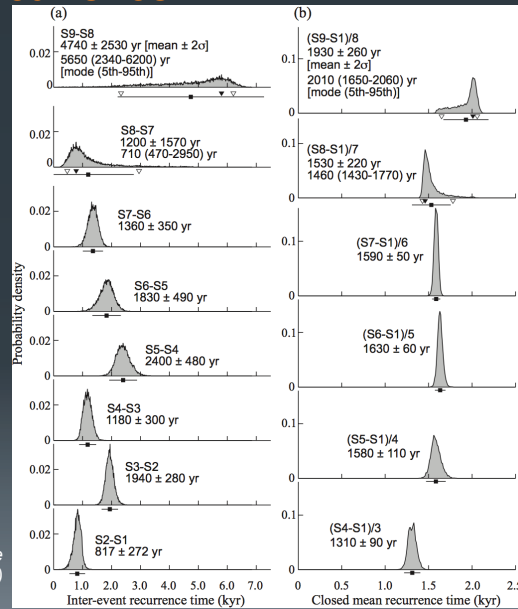
➤ Earthquake recurrence

- Per site
- Per segment/fault (preferred)

➤ Recurrence types:

- Inter-event recurrence (a)
- Closed mean recurrence (b)
- Open mean recurrence

SLCS earthquake recurrence
(DuRoss & Hylland, 2014)



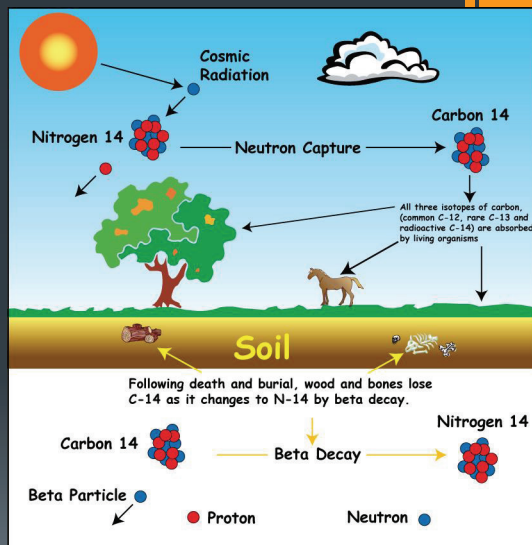
DISCUSSION

- What are the current limitations in paleoseismology?
- Which fault/earthquake parameters have uncertainties that are model driven vs. just variability in earthquake processes? (epistemic vs. aleatory uncertainty)
- Which parameters need further refinement/study?
- Which issues/parameters need to be addressed in site specific vs. regional seismic hazard analyses?

RADIOCARBON (^{14}C) DATING AND OXCAL

^{14}C Dating

- ^{14}C decays at a constant rate
 - Given any set of ^{14}C atoms, half of them will decay in 5730 yr
 - Because of this slow rate, all carbon in biomass at earth's surface contains atmospheric levels of ^{14}C .
- As soon as any carbon drops out of the cycle of biological processes (e.g., through burial), the abundance of ^{14}C begins to decline.
 - After 5730 yr only half remains; after another 5730 yr only $\frac{1}{4}$ remains.
 - This process continues until no ^{14}C remains (~10 half lives or ~50k yr).



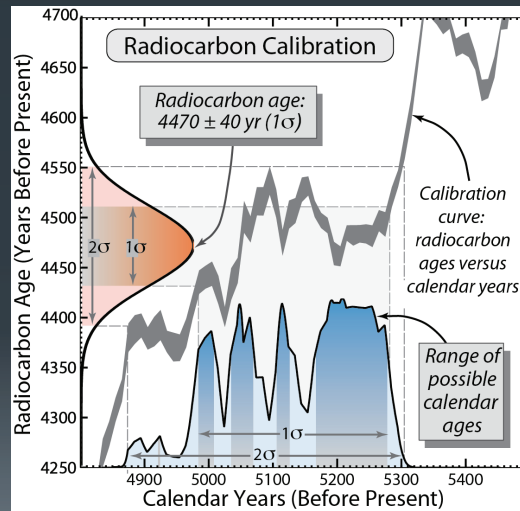
Text modified from the Woods Hole Oceanographic Institute (WHOI); <http://www.whoi.edu/nosams/page.do?pid=40138>

Figure from: <http://rse.s.anu.edu.au/research/groups/radiocarbon-dating-laboratory/radiocarbon-dating-background>

Radiocarbon Calibration

➤ Calibration Curve

- Used to convert laboratory ^{14}C years to “calendar years before present (1950)” (cal yr B.P.)
- Calendar age depends on the calibration curve (*radiocarbon age vs. calendar age*), which shows how atmospheric radiocarbon has changed over time



Source: Burbank and Anderson (2011)
http://www.geol.ucsb.edu/faculty/burbank/Site/Tect_Geom_2nd_Ed_Figs.html

^{14}C Dating

➤ Material for ^{14}C dating:

- Charcoal fragments
- Soil organic matter concentrate (bulk A horizon sediment), which yields *apparent mean residence time (AMRT)* ages
- Other: seeds, pollen, shells...

➤ Key Questions:

- What are you dating?
- What are the contextual uncertainties?
- What are the soil properties
- What part of the soil was sampled?



3.7 mg fragments of *Rosaceae* charcoal: ~10.6 ka; DuRoss et al. (2014)

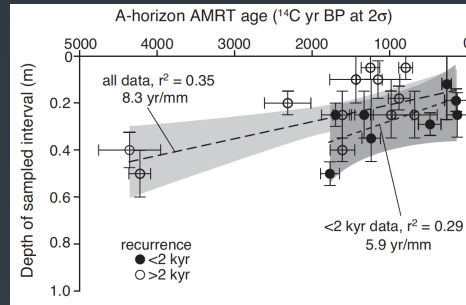
Sources of Uncertainty

➤ Charcoal ages:

- Context of sample
- Detrital charcoal (~100s to 1000s of years older than host sediment)
- Burrowing (~100s of years younger than host sediment)

➤ AMRT ages:

- Context of sample
- Detrital and burrowed sediment/organics
- Age range of carbon in the soil (1000s of years)
- Position of the sample in the soil (top, base, etc.)
- Pretreatment (what part of soil was isolated?)
- Nelson et al., 2005: *On average, AMRT ages are 100 to 700 yr older than TL or AMS ^{14}C ages on charcoal from the same units (but some as much as 1200 yr older).* **Correction: 100-500 yr**



AMRT age vs. sample depth; Nelson et al. (2006)

Reducing Uncertainty

➤ While sampling:

- Know what/where you are sampling
- Buried soils – sample close (within 5-10 cm) of contact,
- Avoid burrowed/disturbed sediment.
- Sample for both ^{14}C and OSL

➤ After sampling:

- Have bulk soil samples sorted to yield charcoal fragments
- Identify charcoal fragments if possible

➤ While dating:

- Preferentially date charcoal having a short age span (e.g., grass, flowers) rather than a long age span (e.g., conifer).
- *What charcoal type is likely to be local to your site?*
- Date footwall/hanging soils/sediments that help with general age control
- Date multiple samples from each soil/unit.



^{14}C and OSL samples at the Corner Canyon trench site

Soil Analysis

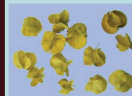
- **Soil sorting:** extraction of charcoal (or other datable macrofossils) for identification and dating
- **Laboratory: Paleo Research Institute (PRI)**
 - Sort and identify charcoal, plant parts, seeds, roots, insect parts...
 - Rate ~\$150/hr; typical ~1-2 Liter sample takes 2-3 hours.
 - Yield: dateable (~0.5+ mg) remains

Macrofloral

Macrofloral remains can be charred or uncharred and include remains such as seeds, charcoal, wood, corn cobs, kernels, and other plant parts. These remains are usually recovered from sediment samples by water flotation or directly from their cultural contexts during excavation. Macrofloral remains can provide evidence for the utilization, processing, or domestication of plant resources by the occupants of an archaeological site, which can help answer questions regarding diet, subsistence, season of occupation, trade, and site function. Macrofloral remains also can provide environmental information. In addition to archaeology, macrofloral analysis is being used in other areas of research including paleofood studies, paleoecology, and paleoclimatology to separate and identify charred organic material to submit for radiocarbon analysis, rather than trying to date bulk soil samples (See POSTED PAPERS for "Being Bulk Soil vs. Identified Organic at Archaeological Sites").



In archaeological sites, macrofloral remains most often are recovered in cultural features such as hearths, fire pits, thermal features, middens, structure floors, structure fill, roof/floor storage pits, basins, vessels, ash/charcoal lens, extramural activity areas, and others, as well as from cultural strata in stratified deposits. Paleofeces (coprolites) contain macrofloral remains that indicate directly what people (or animals) ate. Some large macrofloral remains such as corn, charcoal, large seeds, and other plant material do not require flotation to remove them from sediment and can be submitted as single specimens for identification. Artifacts such as basketry, textiles, sandals, digging sticks, and roof beams also should be submitted for macrofloral analysis to identify the plant resources used in making these objects.



When collecting flotation samples from archaeological features, a standard sample size is 2 to 4 liters of fill. For large features such as structure floors or deep, stratified roasting pits, multiple samples should be collected. For stratified features, it is important to sample and process each layer separately. Often, this can provide a more detailed record of how the feature was used, rather than mixing the deposits in a single sample.



We process flotation samples using a "bucket" method. One to two liters of each sample is added to approximately 3 gallons of water, then stirred until a strong vortex formed. The floating material (light fraction) is poured through a 100 micron mesh sieve. Additional water is added and the process repeated until all floating material is removed from the sample (a minimum of 5 times). The material which remains in the bottom (heavy fraction) is poured through a 0.5 mm mesh screen. The floated portions are allowed to dry, then examined under a binocular microscope at magnifications of 10-70x. This process is repeated for each one to two liters of sample until the entire sample is floated.



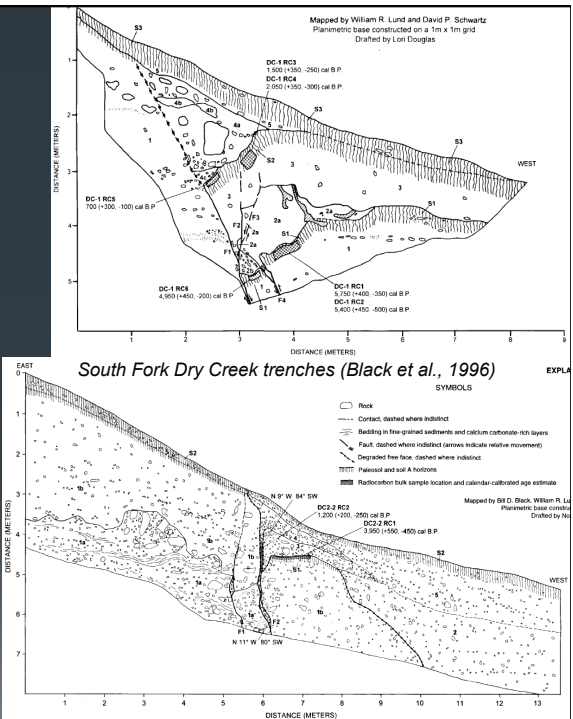
Flotation samples commonly contain both charred and uncharred macrofloral remains. At most sites, only charred macrofloral remains are considered prehistoric. This is because few seeds live longer than a century, and most live for a much shorter period of time. Most uncharred seeds will not survive through common archaeological time spans. It is presumed that once seeds have died, decomposing organisms act to decay the seeds. Sites in caves, waterlogged areas, and in very acid soils, however, can contain uncharred prehistoric remains. Interpretation of uncharred macrofloral remains to represent presence in the prehistoric record is considered on a sample-by-sample basis. Extraordinary conditions for preservation are required.



*<http://paleoresearch.com/services.html>; see Puseman & Cummings (2005)

Geochronological and Stratigraphic Data

- **Stratigraphic info**
 - Depositional order
 - Soil development (time)
- **Geochronological data**
 - Numerical (e.g., radiocarbon and luminescence) ages
 - Historical constraints
- **Other**
 - Depositional ordering unknown
 - An event happened... significant change in depositional system



OxCal Basics

- **Bayesian modeling** (Bronk Ramsey 1995, 2001, 2008)
 - Prior: “what is known about any system before we start some et of measurements” (stratigraphic ordering)
 - Likelihood: “Information...from the set of measurements” (age constraints)
 - Posterior: Possible solutions based on *Prior* and *Likelihood* data
 - Agreement index: overlap between likelihood and posterior distributions (“acceptable” = 60%)

➤ Model terms

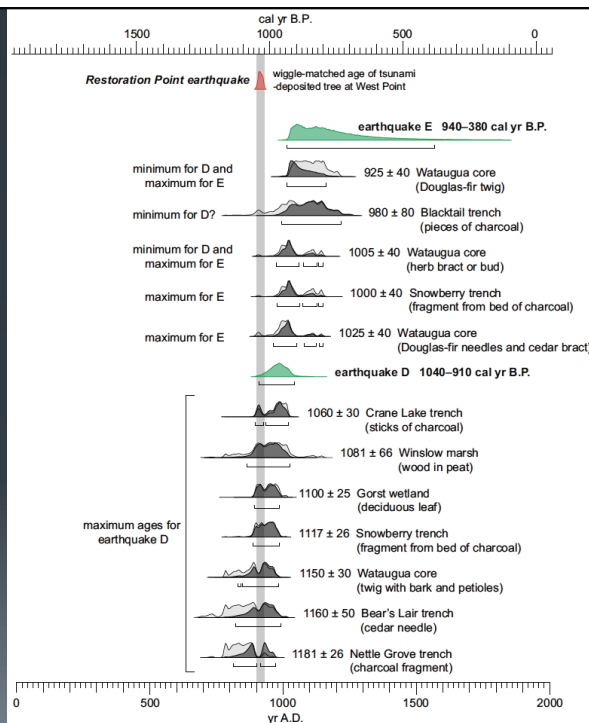
- Boundary: significant changes in deposition
- Sequence: stratigraphic ordering known (but deposition rate unknown)
- Phase: stratigraphic ordering unknown
- Date: (R_date, C_date): numerical constraint
- Event: undated event (e.g., an earthquake) in the model
- Calibration curve: used to convert ¹⁴C yr to calendar years (before 1950) (Reimer et al. (2009)
- Delta_R: shift age

OxCal: <https://c14.arch.ox.ac.uk/oxcal/OxCal.html>

OxCal help: https://c14.arch.ox.ac.uk/oxcalhelp/hlp_contents.html

Example Model

- Nelson et al. (2014) figure 12.
 - Probability distributions for the times of earthquakes (green)
 - Light-gray distributions show original probability distribution for each calibrated age.
 - Dark-gray distributions show how distributions shift as a result of the OxCal analysis.



Nelson et al. (2014)

OxCal Code

```

Plot()
{
  Sequence("SLCS SFDC ver 6f")
  {
    Boundary("Sequence start");
    Phase("Soil on fan deposits; DC-1, DC-2")
    {
      Delta_R("MRT-200yr1", 200, 200);
      R_Date("DC-1-R1", 5230, 160);
      R_Date("DC-1-R2", 4910, 200);
      R_Date("DC-2-R1", 4710, 180);
      Delta_R("MRT-0yr", 0, 100);
      R_Date("DC-1-R6", 4520, 120);
    };
    Boundary("EW");
    Zero_Boundary("W");
    Delta_R("MRT-150yr1", 150, 75);
    R_Date("DC2-2-R1", 3810, 180);
    Boundary("EX");
    Phase("post EX deposits; DC2-4")
    {
      Delta_R("MRT-300yr1", 300, 300);
      R_Date("DC2-4-R3", 3910, 140);
      R_Date("DC2-4-R4", 3760, 160);
    };
    Phase("Soil on fan - pre EY; DC2-5, DG")
    {
      Delta_R("MRT-200yr2", 200, 200);
      R_Date("DC2-5-R3", 3090, 120);
      Delta_R("MRT-100yr2", 100, 50);
      R_Date("APST-BS2", 2370, 140);
      R_Date("APST-BS3", 2410, 120);
    };
    Boundary("EY");
    Zero_Boundary("Y");
    Phase("soil on fan/colluvium pre EZ");
    {
      Delta_R("MRT-200yr3", 200, 200);
      R_Date("DC-1-R4", 2310, 140);
      R_Date("DC-1-R3", 1830, 160);
      Delta_R("MRT-150yr2", 150, 150);
      R_Date("DC2-1-R2", 1850, 120);
      Delta_R("MRT-200yr4", 200, 200);
      R_Date("DC-2-R3", 1640, 100);
      Delta_R("MRT-100yr3", 100, 50);
      R_Date("APST-BS1", 1770, 120);
      R_Date("DC2-3-R2", 1420, 160);
    };
    Boundary("EZ");
    Phase("Post EZ deposits");
    {
      Delta_R("MRT-300yr2", 300, 300);
      R_Date("DC2-4-R2", 1620, 100);
      R_Date("DC2-2-R2", 1570, 120);
      Delta_R("MRT-100yr5", 100, 50);
      R_Date("DC2-3-R1", 1240, 140);
      Delta_R("MRT-200yr5", 200, 200);
      R_Date("DC2-3-R3", 1160, 160);
    };
    C_Date("Historic constraint AD 1850", 1850, 5);
    Boundary("Sequence end");
  };
};
  
```

OxCal code modified from DuRoss et al. (2014)

OxCal Results

- **Model terms:**
 - Unmodeled: pre-Bayesian analysis (existing ages)
 - Modeled: results of Bayesian analysis (posterior ranges for ages; event ages)
- **Example ages:**
 - DC-1-R6: 5170 ± 210 cal yr B.P. (1σ); 95% range: 4830–5590 cal yr B.P.
 - Earthquake W: 4980 ± 280 cal yr B.P. (1σ); 95% range: 4410–5510 cal yr B.P.
- **Indices:**
 - Agreement: prior vs. posterior ranges
 - A_{model}: overall agreement for model

Name	Unmodelled (BP)	Modelled (BP)	Indices
Show all	from to % p	from to % p	A _{posterior} 127.5
Show structure	or from to % p	or from to % p	A _{prior} 187.8
			A _{model} A L P C
Sequence SLCS SFDC ver 6f - Zero Boundaries, Events as Boundaries, no Claps			
Boundary Sequence start		6270 4930 95.4 5960 300	
Phase Soil on fan deposits; DC-1, DC-2			
Delta_R MRT-200yr1	200 0 647 95.4 333 386 162 56	94.7	99.4
R_Date DC-1-R1	4400 5090 95.4 3790 300 9910 4870 95.4 5410 270	85.6	99.7
R_Date DC-1-R2	5190 4800 95.4 5370 360 5780 4830 95.4 5270 260	105.4	99.8
R_Date DC-2-R1	3890 4420 95.4 5140 340 5520 4900 95.4 5190 240	115.3	99.9
Delta_R MRT-0yr	200 200 95.4 -1.82276e-7 100 -108 174 95.4 -8.88798 82 0309 104	104	99.8
R_Date DC-1-R6	5990 4830 95.4 5170 210 5580 4870 95.4 5220 190	102	99.9
Boundary EW		5510 4410 95.4 4980 280	99.5
Zero_Boundary W		5130 3720 95.4 4410 360	99.5
Delta_R MRT-150yr1	0 300 95.4 150 75 4 299 95.4 151 586 73.6144	100.9	99.9
R_Date DC2-2-R1	4530 3480 95.4 4020 270 4440 3500 95.4 3960 230	106.2	99.8
Boundary EX		4360 3120 95.4 3760 300	99.8
Phase post EX deposits; DC2-4			
Delta_R MRT-300yr1	300 900 95.4 300 300 145.5 1012 95.4 580 837 222 109	96	99.2
R_Date DC2-4-R3	4840 3080 95.4 3970 430 4070 2980 95.4 3510 290	81.1	99.7
R_Date DC2-4-R4	4790 2870 95.4 3780 440 3960 2820 95.4 3400 290	91.6	99.8
Phase Soil on fan - pre EY; DC2-5, DG			
Delta_R MRT-200yr2	200 800 95.4 200 200 87 627 95.4 250 872 178 804	104.5	99.4
R_Date DC2-5-R3	3590 2380 95.4 3050 280 3440 2450 95.4 2960 240	102.8	99.7
Delta_R MRT-100yr2	0 200 95.4 100 50 22.5 178 95.4 75 4281 49 7092	93.9	99.9
R_Date APST-BS2	2720 1960 95.4 2310 200 2760 2120 95.4 2470 180	86	99.8
R_Date APST-BS3	2730 2030 95.4 2360 190 2720 2160 95.4 2480 170	92.8	99.8
Boundary EY		2660 1850 95.4 2230 210	99.8
Zero_Boundary Y		2430 1520 95.4 1980 230	99.8
Phase soil on fan/colluvium pre EZ			
Delta_R MRT-200yr3	200 800 95.4 200 200 80 647 95.4 333 386 162 56	94.7	99.4
R_Date DC-1-R4	2730 1860 95.4 2110 270 1830 1560 95.4 1920 240	81.1	99.7
R_Date DC-1-R3	2190 1000 95.4 1980 210 1000 95.4 1980 230	91.6	99.8
Delta_R MRT-150yr2	0 150 95.4 75 75 4 299 95.4 151 586 73.6144	100.9	99.9
R_Date DC2-1-R2	1850 1850 95.4 1850 1850 1850 1850 95.4 1850 1850	1850	1850
Delta_R MRT-200yr4	200 100 95.4 200 200 100 100 95.4 200 200	100	99.8
R_Date DC2-2-R2	1870 90 95.4 1300 1870 90 95.4 1300	1870	90
Delta_R MRT-100yr3	0 200 95.4 100 200 200 200 95.4 100 200	100	99.8
R_Date APST-BS1	1770 1770 95.4 1770 1770 1770 1770 95.4 1770 1770	1770	1770
R_Date DC2-3-R2	1420 1420 95.4 1420 1420 1420 1420 95.4 1420 1420	1420	1420
Boundary EZ			
Phase Post EZ deposits			
Delta_R MRT-300yr2	300 900 95.4 300 300 145.5 1012 95.4 580 837 222 109	96	99.2
R_Date DC2-4-R2	1620 1620 95.4 1620 1620 1620 1620 95.4 1620 1620	1620	1620
R_Date DC2-2-R2	1570 1570 95.4 1570 1570 1570 1570 95.4 1570 1570	1570	1570
R_Date DC2-3-R1	1240 1240 95.4 1240 1240 1240 1240 95.4 1240 1240	1240	1240
Delta_R MRT-200yr5	200 200 95.4 200 200 200 200 95.4 200 200	200	99.8
R_Date DC2-3-R3	1160 1160 95.4 1160 1160 1160 1160 95.4 1160 1160	1160	1160
C_Date Historic constraint AD 1850	1850 1850 95.4 1850 1850 1850 1850 95.4 1850 1850	1850	1850
Boundary Sequence end			

Raw data (always BC/AD)

Boundary EZ

Unmodelled Data Modelled Data

44.24 probability

1493AD (49.24) 112AD

92.14 probability

373AD (92.14) 833AD

Save

185.5 0.000026158

195.5 0.000021446

195.5 0.00003187

205.5 0.00002791

205.5 0.00003775

215.5 0.00003112

215.5 0.00004196

225.5 0.00004609

225.5 0.00005236

235.5 0.00005694

245.5 0.00006178

245.5 0.00006692

255.5 0.00007255

265.5 0.00007854

275.5 0.00008485

285.5 0.00009147

285.5 0.00009838

295.5 0.00010558

305.5 0.00011296

315.5 0.00012061

325.5 0.00012852

335.5 0.00013668

345.5 0.00014508

355.5 0.00015372

365.5 0.00016261

375.5 0.00017174

385.5 0.00018111

395.5 0.00019072

405.5 0.00020056

415.5 0.00021063

425.5 0.00022093

435.5 0.00023145

445.5 0.00024218

455.5 0.00025312

465.5 0.00026426

475.5 0.00027560

485.5 0.00028713

495.5 0.00029885

505.5 0.00031076

515.5 0.00032295

525.5 0.00033532

535.5 0.00034787

545.5 0.00036059

555.5 0.00037348

565.5 0.00038654

575.5 0.00039976

585.5 0.00041314

595.5 0.00042667

605.5 0.00044035

615.5 0.00045417

625.5 0.00046813

635.5 0.00048223

645.5 0.00049646

655.5 0.00051082

665.5 0.00052531

675.5 0.00053992

685.5 0.00055464

695.5 0.00056947

705.5 0.00058441

715.5 0.00059946

725.5 0.00061461

735.5 0.00062987

745.5 0.00064523

755.5 0.00066070

765.5 0.00067627

775.5 0.00069194

785.5 0.00070771

795.5 0.00072358

805.5 0.00073954

815.5 0.00075560

825.5 0.00077176

835.5 0.00078801

845.5 0.00080436

855.5 0.00082080

865.5 0.00083734

875.5 0.00085397

885.5 0.00087069

895.5 0.00088750

905.5 0.00090440

915.5 0.00092139

925.5 0.00093847

935.5 0.00095564

945.5 0.00097290

955.5 0.00099025

965.5 0.00100769

975.5 0.00102521

985.5 0.00104282

995.5 0.00106042

1005.5 0.00107810

1015.5 0.00109586

1025.5 0.00111370

1035.5 0.00113162

1045.5 0.00114961

1055.5 0.00116768

1065.5 0.00118582

1075.5 0.00120403

1085.5 0.00122231

1095.5 0.00124066

1105.5 0.00125908

1115.5 0.00127756

1125.5 0.00129610

1135.5 0.00131470

1145.5 0.00133336

1155.5 0.00135208

1165.5 0.00137086

1175.5 0.00138969

1185.5 0.00140857

1195.5 0.00142750

1205.5 0.00144648

1215.5 0.00146551

1225.5 0.00148459

1235.5 0.00150371

1245.5 0.00152288

1255.5 0.00154209

1265.5 0.00156134

1275.5 0.00158063

1285.5 0.00160006

1295.5 0.00161953

1305.5 0.00163904

1315.5 0.00165859

1325.5 0.00167817

1335.5 0.00169779

1345.5 0.00171744

1355.5 0.00173712

1365.5 0.00175683

1375.5 0.00177657

1385.5 0.00179634

1395.5 0.00181614

1405.5 0.00183597

1415.5 0.00185582

1425.5 0.00187570

1435.5 0.00189560

1445.5 0.00191552

1455.5 0.00193546

1465.5 0.00195542

1475.5 0.00197540

1485.5 0.00199540

1495.5 0.00201542

1505.5 0.00203546

1515.5 0.00205551

1525.5 0.00207558

1535.5 0.00209566

1545.5 0.00211576

1555.5 0.00213587

1565.5 0.00215599

1575.5 0.00217612

1585.5 0.00219626

1595.5 0.00221641

1605.5 0.00223657

1615.5 0.00225674

1625.5 0.00227692

1635.5 0.00229711

1645.5 0.00231731

1655.5 0.00233752

1665.5 0.00235774

1675.5 0.00237796

1685.5 0.00239819

1695.5 0.00241843

1705.5 0.00243868

1715.5 0.00245893

1725.5 0.00247919

1735.5 0.00249945

1745.5 0.00251972

1755.5 0.00253999

1765.5 0.00256026

1775.5 0.00258054

1785.5 0.00260082

1795.5 0.00262110

1805.5 0.00264139

1815.5 0.00266168

1825.5 0.00268197

1835.5 0.00270227

1845.5 0.00272257

1855.5 0.00274287

1865.5 0.00276317

1875.5 0.00278347

1885.5 0.00280377

1895.5 0.00282407

1905.5 0.00284437

1915.5 0.00286467

1925.5 0.00288497

1935.5 0.00290527

1945.5 0.00292557

1955.5 0.00294587

1965.5 0.00296617

1975.5 0.00298647

1985.5 0.00300677

1995.5 0.00302707

2005.5 0.00304737

2015.5 0.00306767

2025.5 0.00308797

2035.5 0.00310827

2045.5 0.00312857

2055.5 0.00314887

2065.5 0.00316917

2075.5 0.00318947

2085.5 0.00320977

2095.5 0.00322997

2105.5 0.00325027

2115.5 0.00327057

2125.5 0.00329087

2135.5 0.00331117

2145.5 0.00333147

2155.5 0.00335177

2165.5 0.00337207

2175.5 0.00339237

2185.5 0.00341267

2195.5 0.00343297

2205.5 0.00345327

2215.5 0.00347357

2225.5 0.00349387

2235.5 0.00351417

2245.5 0.00353447

2255.5 0.00355477

2265.5 0.00357507

2275.5 0.00359537

2285.5 0.00361567

2295.5 0.00363597

2305.5 0.00365627

2315.5 0.00367657

2325.5 0.00369687

2335.5 0.00371717

2345.5 0.00373747

2355.5 0.00375777

2365.5 0.00377807

2375.5 0.00379837

2385.5 0.00381867

2395.5 0.00383897

2405.5 0.00385927

2415.5 0.00387957

2425.5 0.00389987

2435.5 0.00392017

2445.5 0.00394047

2455.5 0.00396077

2465.5 0.00398107

2475.5 0.00400137

2485.5 0.00402167

2495.5 0.00404197

2505.5 0.00406227

2515.5 0.00408257

2525.5 0.00410287

2535.5 0.00412317

2545.5 0.00414347

2555.5 0.00416377

2565.5 0.00418407

2575.5 0.00420437

2585.5 0.00422467

2595.5 0.00424497

2605.5 0.00426527

2615.5 0.00428557

2625.5 0.00430587

2635.5 0.00432617

2645.5 0.00434647

2655.5 0.00436677

2665.5 0.00438707

2675.5 0.00440737

2685.5 0.00442767

2695.5 0.00444797

2705.5 0.00446827

2715.5 0.00448857

2725.5 0.00450887

2735.5 0.00452917

2745.5 0.00454947

2755.5 0.00456977

2765.5 0.00459007

2775.5 0.00461037

2785.5 0.00463067

2795.5 0.00465097

2805.5 0.00467127

2815.5 0.00469157

2825.5 0.00471187

2835.5 0.00473217

2845.5 0.00475247

2855.5 0.00477277

2865.5 0.00479307

2875.5 0.00481337

2885.5 0.00483367

2895.5 0.00485397

2905.5 0.00487427

2915.5 0.00489457

2925.5 0.00491487

2935.5 0.00493517

2945.5 0.00495547

2955.5 0.00497577

2965.5 0.00499607

2975.5 0.00501637

2985.5 0.00503667

2995.5 0.00505697

3005.5 0.00507727

3015.5 0.00509757

3025.5 0.00511787

3035.5 0.00513817

3045.5 0.00515847

3055.5 0.00517877

3065.5 0.00519907

3075.5 0.00521937

3085.5 0.00523967

3095.5 0.00525997

3105.5 0.00528027

3115.5 0.00530057

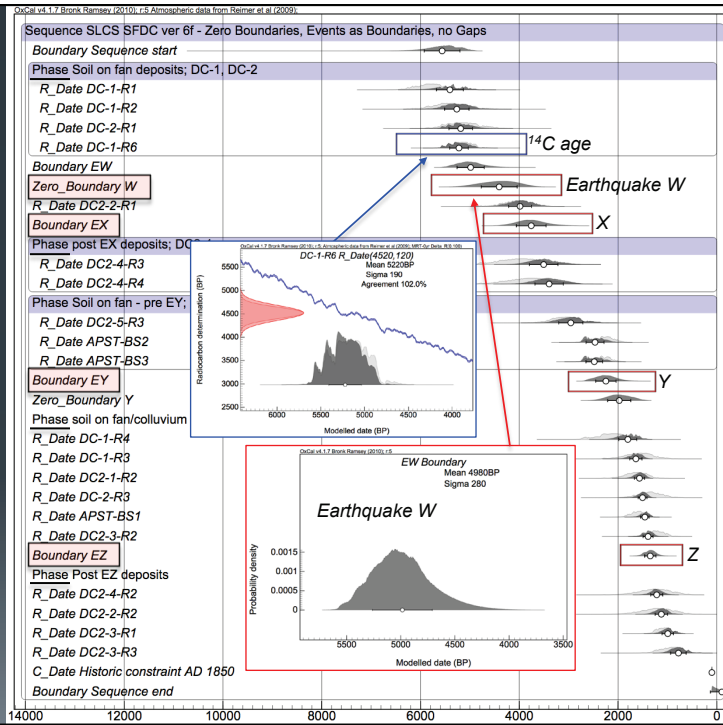
3125.5 0.00532087

3135.5 0.00534117

Example Model

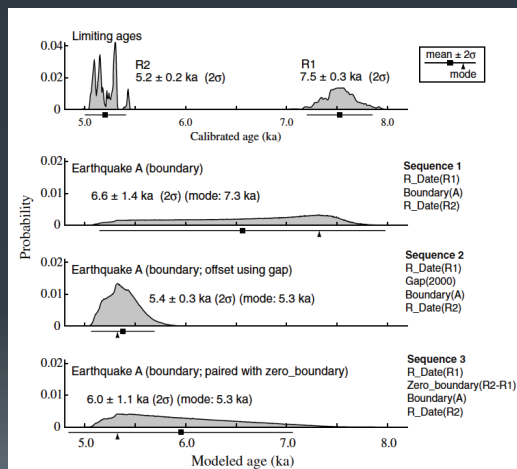
- Four EQs post ~6 ka at the South Fork Dry Creek site on the Salt Lake City segment (DuRoss et al., 2014)

Modified from DuRoss et al. (2014)



Advanced OxCal Techniques

- *Date or Boundary?*
- **Earthquake A** – constrained by close maximum limiting age (R2) and a loose minimum age (R1)
 1. Boundary – treats ages equally
 2. Gap – preference given to one age
 3. Boundary paired with Zero Boundary – symmetrically skews earthquake time toward one age
- *Difference command:* recurrence time between events

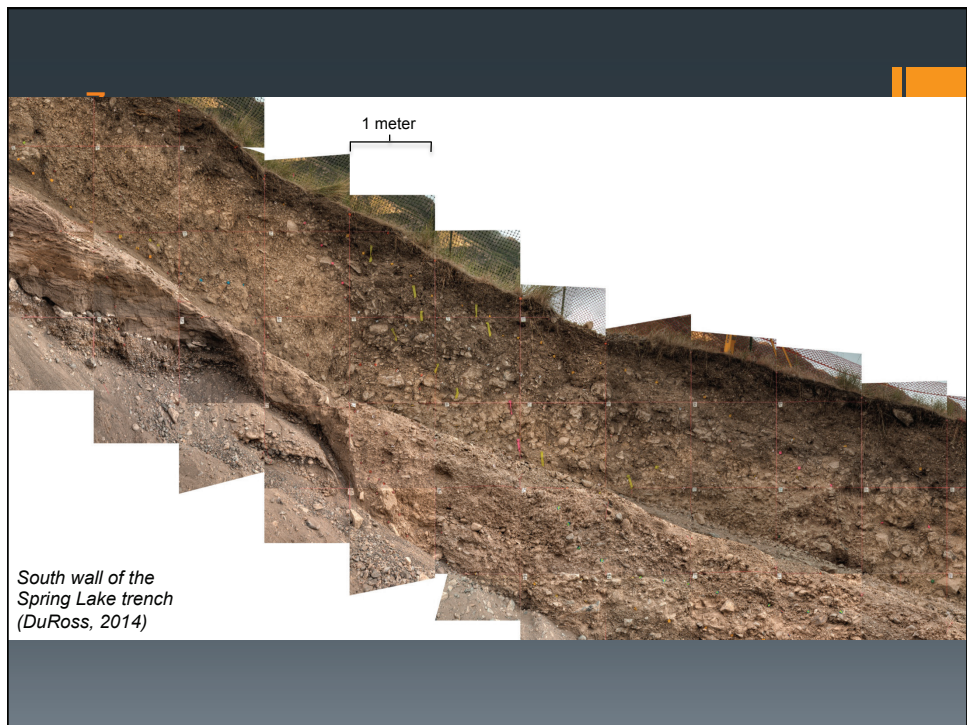
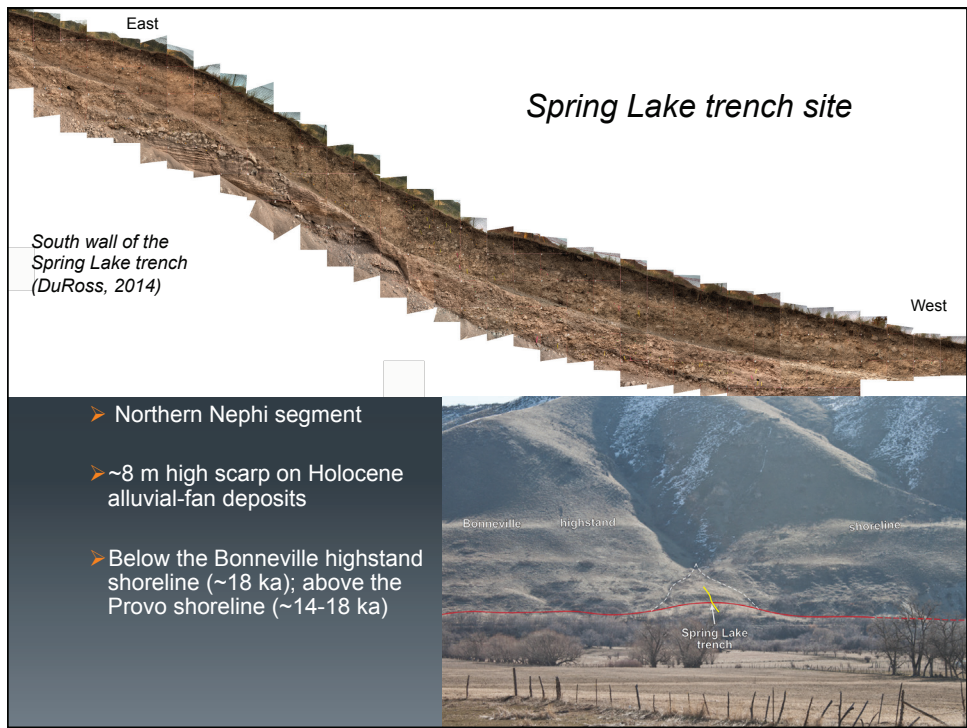


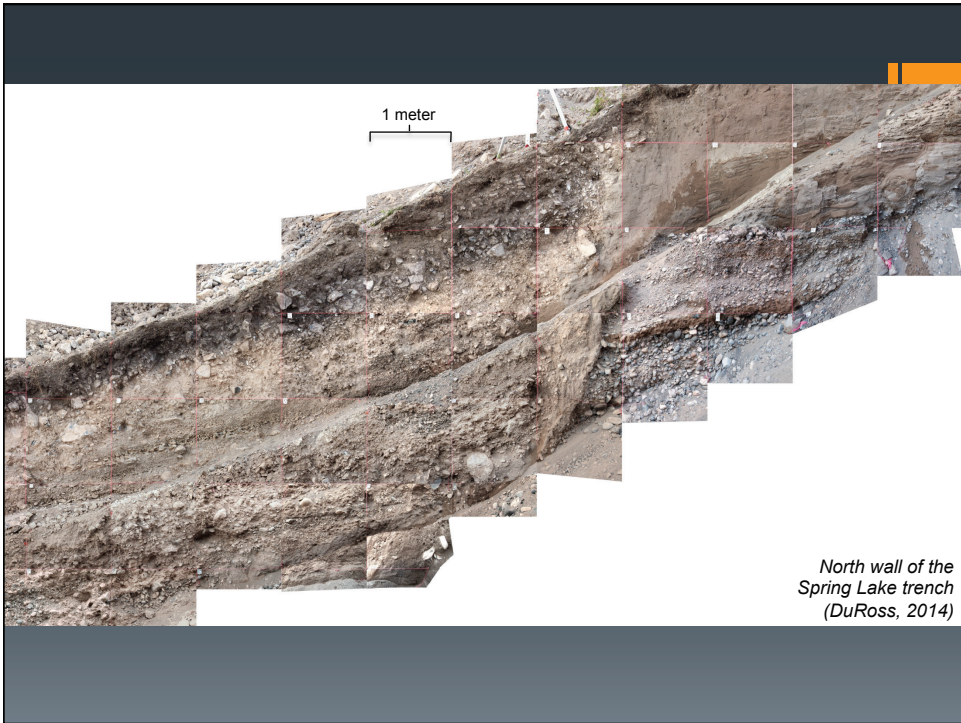
DuRoss et al. (2011)

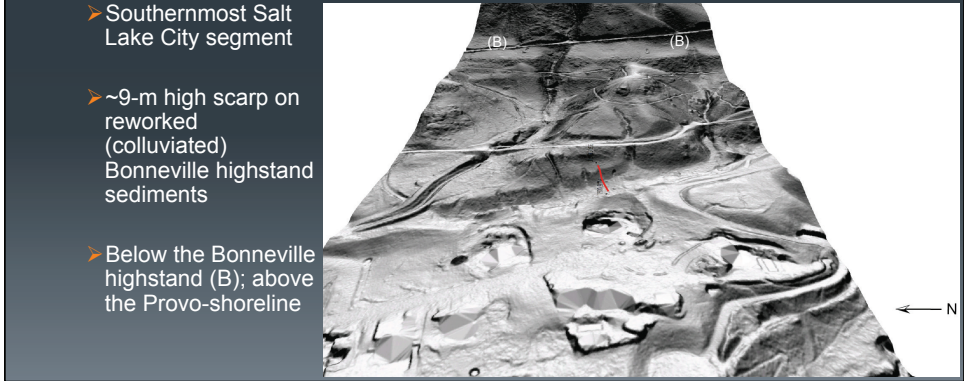
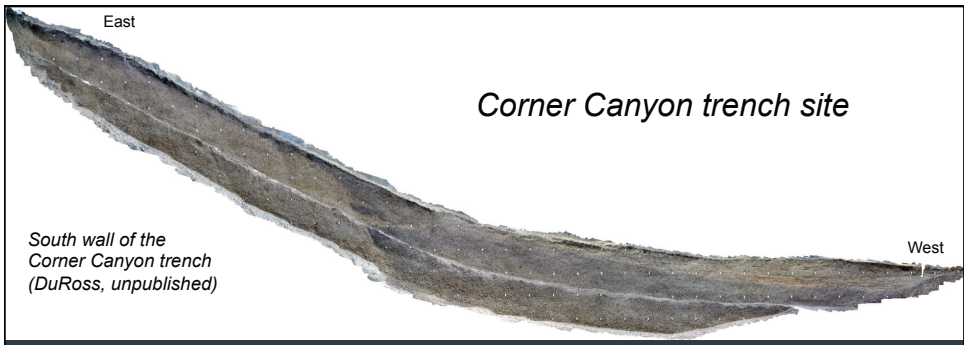
Additional Resources

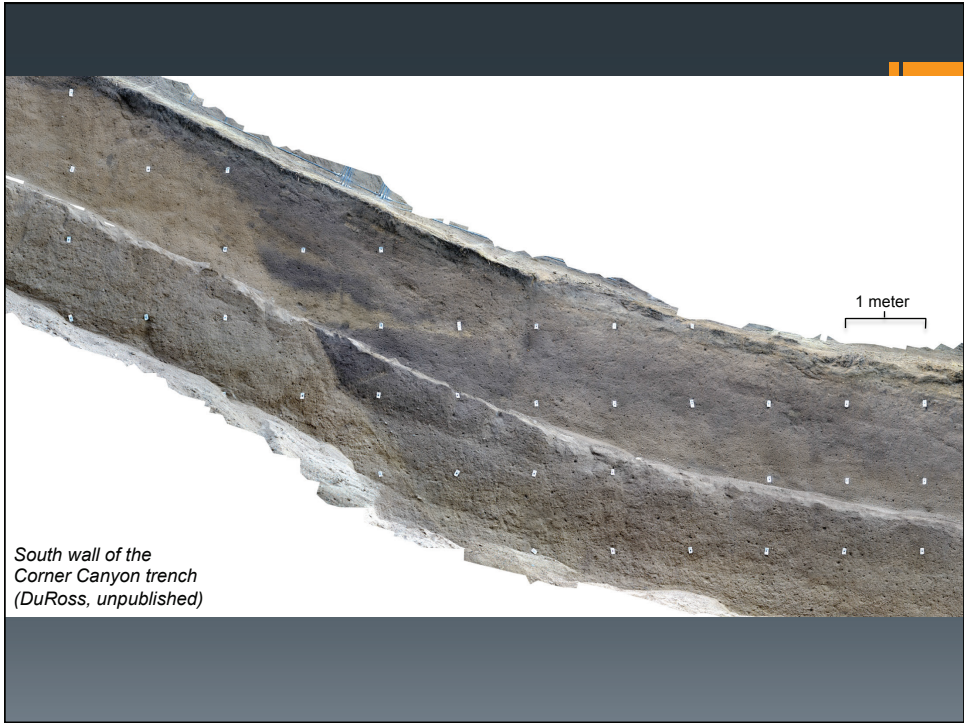
- Quaternary faults & folds
 - **US:** <http://earthquake.usgs.gov/hazards/qfaults/>
 - **Utah:** http://geology.utah.gov/emp/geothermal/quaternary_faults.htmOxCal
- USGS NEHRP External Research grants
 - <http://earthquake.usgs.gov/research/external/>
- USGS National Seismic Hazard Maps
 - <http://earthquake.usgs.gov/hazards/?source=sitenav>
- UGS Paleoseismology of Utah series
 - http://geology.utah.gov/ghp/consultants/paleoseismic_series.htm
- UGS Earthquake Working Groups
 - <http://geology.utah.gov/ghp/workgroups/index.htm>
 - Lund (2013)
 - Working Group on Utah Earthquake Probabilities (in prep)
- LiDAR data and tutorials
 - Data: <http://www.opentopography.org>
 - Working with Lidar in ArcMap: http://coast.noaa.gov/digitalcoast/_pdf/Lidar-data-handler-ArcGISy10-tutorial.pdf
 - Lidar coverage & sample density: http://blogs.esri.com/esri/arcgis/2008/11/06/lidar-solutions-in-arcgis_part-1-assessing-lidar-coverage-and-sample-density/
 - Raster DEMs: http://blogs.esri.com/esri/arcgis/2008/12/15/lidar-solutions-in-arcgis_part2-creating-raster-dems-and-dsms-from-large-lidar-point-collections/
- OxCal
 - Lienkaemper and Bronk Ramsey (2009)
 - Help: https://c14.arch.ox.ac.uk/oxcalhelp/hlp_contents.html
 - **Google Group:** <https://groups.google.com/forum/#forum/oxcal>
- Wasatch fault paleoseismic data
 - Swan et al. (1980)
 - Schwartz andoppersmith (1984)
 - Machette et al. (1992)
 - McCalpin & Nishenko (1996)
 - Friedrich et al. (2006)
 - Chang and Smith (2002)
 - Lund (2005)
 - DuRoss (2008)
 - DuRoss et al. (in review)
- Data synthesis
 - Weenousky (2008)
 - Biasi and Weldon (2009)
 - DuRoss et al. (2011)
 - Personius et al. (2012)
- OSL
 - Duller (2008)
 - **USGS Luminescence Dating Lab:** http://crustal.usgs.gov/laboratories/luminescence_dating/
 - **USU Luminescence Lab:** <http://www.usu.edu/geo/luminlab/>
- ¹⁴C dating
 - **WHOI NOSAMS:** <http://www.whoi.edu/nosams/>
 - <http://www.c14dating.com/int.html>
- Miscellaneous
 - **UGS:** <http://geology.utah.gov/utahgeo/hazards/index.htm>
 - **USGS:** <http://earthquake.usgs.gov>
 - **ASU Active Faults Short Course:** <http://activetectonics.asu.edu/lipi/Schedule.html>
 - Burbank and Anderson (2012)

EXERCISE 1: Trench Observation





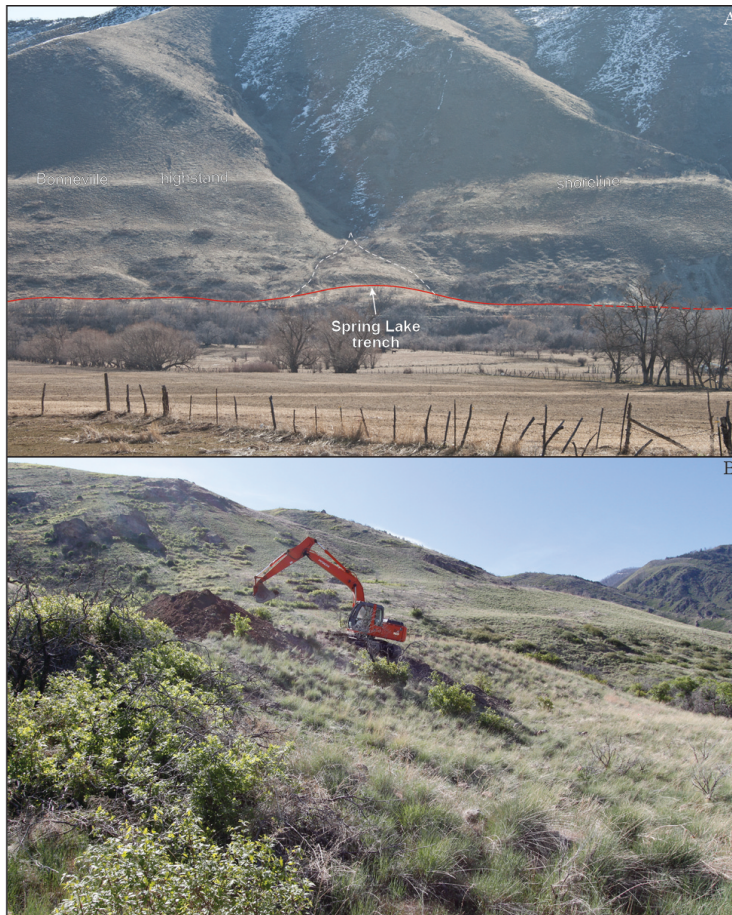






EXERCISE 2: Interpreting Raw Paleoseismic Data

Exercise 2: Interpretation of Paleoseismic Data from the Spring Lake Trench site



The Spring Lake (SL) site is on the northern strand of the Nephi segment, where a west-facing scarp offsets a small post-Bonneville alluvial-fan surface. The site is at ~1470–1510 m elevation, below the elevation of the Bonneville highstand shoreline (~1500 m) and above the elevation of the Provo shoreline (~1440–1450 m). We chose the site because of the simple geometry and moderately large height of the fault scarp, and because the site had minimal evidence of cultural disturbance based on aerial photographs.

Surficial deposits at the SL site include lacustrine sediments deposited

during the highstand of Lake Bonneville (~18 ka) and stream and debris flows that are part of a post-Bonneville (Holocene) alluvial fan. The Lake Bonneville highstand sediments include sand to coarse gravel forming wave-built terraces. The stream and debris flows, which have incised into the Lake Bonneville sediments, form a west-sloping alluvial fan surface. The Wasatch fault has displaced both of these units down to the west, forming an 8-m high scarp on the alluvial-fan surface (larger scarps are present on the lacustrine surfaces). Locally, the uplifted fan surface has been incised by more recent (late Holocene) stream and debris flows as the locus of fan deposition has shifted west of the fault scarp. We estimate 5.0-m of vertical surface offset across the scarp based on a 130-m long profile; however, based on the trench stratigraphy, it is unlikely that the fan surfaces above and below the scarp are contemporaneous.

We excavated a 36-m long trench at the SL site and cleaned, photographed, sampled, and logged both the north and south facing walls of the exposure. Note that all data for the SL trench used in this exercise are derived from DuRoss, C. B. (2014).

Paleoseismic investigation to determine the mid-Holocene chronology of surface-faulting earthquakes on the Nephi segment of the Wasatch fault zone, Utah and Juab Counties, Utah, *Final Tech. Rept. to the U.S. Geol. Surv.*, award no. G12AP20076, 48 pp.

SL trench data:

1. Interpreted trench logs and photomosaics. Excerpts of the trench logs and photomosaics for the north and south walls are included. Full versions (plates) will be provided. Bulk soil samples for radiocarbon dating and fine-grained sediment samples for OSL are shown. The resulting ages are mean and 2σ ranges. Note that each square is 1 m^2 .
2. Unit descriptions. Brief descriptions of the stratigraphic units are included below. Note the discussion of (1) evidence for surface faulting, (2) soil development, and (3) radiocarbon and OSL ages. Descriptive field data are included in a separate table.
3. Colluvial wedge thicknesses & displacement data. A table showing the maximum thicknesses of the individual colluvial wedges is included. A discussion includes estimates of the total displacement at the site.
4. Macrofloral analysis. Results from Paleoresearch Institute for bulk soil samples are included. These results are also shown in the radiocarbon dating results table.
5. Radiocarbon dating results. Sample locations, material dated, and final calendar calibrated ages are shown.
6. OSL dating results. Laboratory data (dosimetry) and final OSL ages are shown.

Using the SL trench data, determine:

1. Number of events at the site. How many earthquakes have colluvial-wedge evidence in support of them? What other lines of evidence are there? Which earthquakes do you have the most confidence in?
1. Ideal sample locations to constrain event timing. Since sample locations have already been determined, do you agree with the locations selected? Would you have sampled differently?
2. Earthquake timing. Which ages constrain the earthquakes? Which ages should be discarded? Any other considerations?
3. Earthquake recurrence. Determine inter-event and mean earthquake recurrence intervals using your earthquake-timing estimates above. Which earthquake combinations should you use? Which recurrence values do you have the most confidence in?
4. Displacement. How would you estimate per-event and total displacement for the site? Are you confident enough in your estimates to calculate fault slip rates?

**U.S. Geological Survey External Grant Award Number
G12AP20076**

**PALEOSEISMIC INVESTIGATION TO DETERMINE THE MID-HOLOCENE
CHRONOLOGY OF SURFACE-FAULTING EARTHQUAKES ON THE NEPHI
SEGMENT OF THE WASATCH FAULT ZONE, UTAH AND JUAB COUNTIES, UTAH**

Submitted by
Christopher B. DuRoss¹
christopherduross@utah.gov

With assistance from Michael D. Hylland¹, Adam Hiscock¹, Gregg Beukelman¹, Greg N. McDonald¹, Ben Erickson¹, Adam McKean¹, Stephen F. Personius², Rich Briggs², Ryan Gold², Steve Angster³, Roselyn King⁴, Anthony J. Crone⁵, and Shannon A. Mahan⁶

¹Utah Geological Survey, Salt Lake City, Utah

²U.S. Geological Survey, Golden, Colorado

³Formerly U.S. Geological Survey, currently University of Nevada, Reno

⁴Formerly U.S. Geological Survey, currently Colorado School of Mines

⁵U.S. Geological Survey—retired

⁶U.S. Geological Survey, Denver, Colorado

February 7, 2014

Research supported by the U.S. Geological Survey (USGS), Department of the Interior, under USGS award number G12AP200076. The views and conclusions contained in this document are those of the authors and should not be interpreted as necessarily representing the official policies, either expressed or implied, of the U.S. Government.

Although this product represents the work of professional scientists, the Utah Department of Natural Resources, Utah Geological Survey, makes no warranty, expressed or implied, regarding its suitability for a particular use. The Utah Department of Natural Resources, Utah Geological Survey, shall not be liable under any circumstances for any direct, indirect, special, incidental, or consequential damages with respect to claims by users of this product.

of Reimer and others, 2009). OxCal probabilistically models the timing of undated events (e.g., earthquakes) by weighting the time distributions of chronological constraints (e.g., radiocarbon and OSL ages and historical constraints) included in a stratigraphic model (Bronk Ramsey, 2008, 2009). The program uses a Markov Chain Monte Carlo sampling method (Bronk Ramsey, 1995, 2001) to generate a probability density function (PDF) for each undated event in the model, or the likelihood that an earthquake occurred at a particular time, using the chronologic and stratigraphic constraints. For more detailed discussions of the application of OxCal modeling to paleoseismic data, see Lienkaemper and Bronk Ramsey (2009) and DuRoss and others (2011).

OxCal depositional models for the Spring Lake and North Creek sites (appendix H) use stratigraphic ordering information, radiocarbon and OSL ages, and a historical constraint that no large surface-faulting earthquakes ($M \sim 6.5+$) have occurred since about 1847 to define the time distributions of earthquakes identified at the site. Where necessary, we removed numerical-age outliers using geologic judgment (knowledge of sediments, soils, and sample contexts), the degree of inconsistency with other ages in the model for comparable deposits (e.g., stratigraphically inverted ages), and agreement indices for the original (unmodeled) and modeled numerical ages and the OxCal model as a whole (Bronk Ramsey, 1995, 2008). We report earthquake times for each site as the mean and $\sim 2\sigma$ uncertainty in thousands of calendar years B.P. (ka) rounded to the nearest century. For earthquakes having skewed (highly asymmetric) time distributions, we also report the mode (peak of the probability distribution) and 95% confidence interval. For skewed distributions, the mode better characterizes the earthquake time than the mean or median values, which are influenced by the tail of the time distribution.

SPRING LAKE TRENCH SITE

Surface Faulting and Geology

The Spring Lake site is on the north-central part of the northern strand, where a moderately large, north trending scarp offsets a small ($\sim 0.02 \text{ km}^2$) post-Bonneville alluvial-fan surface that is inset below Lake Bonneville transgressive and highstand sediments (Machette, 1992) (figures 3 and 4). The Spring Lake scarp, as well as discontinuous scarps immediately to the north and the Benjamin fault, make up the northern part of the northern strand that forms an en-echelon right step with the Provo segment (figure 2). The Spring Lake site is at ~ 1470 – 1510 m (~ 4800 – 5000 ft) elevation, below the elevation of the Bonneville highstand shoreline (~ 1500 m; ~ 5100 ft) and above the elevation of the Provo shoreline (~ 1440 – 1450 m; 4740 – 4760 ft) (based on mapping by Solomon and others, 2007).

Surficial geology near the Spring Lake site is dominated by Lake Bonneville lacustrine sediments and geomorphic features, and post-Bonneville alluvial-fan deposits. Deposits associated with the Lake Bonneville highstand include sand to coarse gravel that form wave-built terraces. The Provo-phase shoreline is less well expressed than the Bonneville shoreline, and below the elevation of the trench site. The post-Bonneville alluvial fan slopes gently west and is incised into the Lake Bonneville highstand sediments. The fan surface is underlain by stream and debris-flow sediments derived from a $\sim 0.8 \text{ km}^2$ drainage basin cut in the Mississippian limestone bedrock of the Wasatch Range to the east (Solomon and others, 2007).

The Nephi segment is expressed at the Spring Lake site as a single, prominent, ~100-m long by 8-m high, west-facing scarp (figure 5). Locally, both the fault scarp and the uplifted fan surface have been incised by recent (late Holocene?) stream and debris flows as the locus of fan deposition has shifted west of the WFZ. We estimate 5.0-m of vertical surface offset across the scarp based on a 130-m long profile (figure 6); however, based on the trench stratigraphy (discussed below), it is unlikely that the fan surfaces above and below the scarp are contemporaneous.

Trench Stratigraphy and Structure

The Spring Lake trench exposed the northern strand of the Nephi segment as well as three distinct sedimentary packages: Lake Bonneville lacustrine sediments, post-Bonneville alluvial-fan deposits, and scarp-derived colluvium (colluvial wedges). In the footwall of the fault, Lake Bonneville transgressive and highstand lacustrine sediments are overlain by post-Bonneville stream and debris-flow deposits. In the hanging wall, presumably younger alluvial-fan sediments are interfingered with scarp-derived colluvial wedges deposited adjacent to the WFZ (figure 7; plate 1). Although we found similar stratigraphic units in both the north and south walls of the trench, we discuss sedimentary units (with the exception of colluvial wedges) as either those on the north wall (e.g., N1c), south wall (e.g., S1c), or for the trench as a whole (e.g., N1c/S1c). Colluvial wedges have a single unit designation for both walls (e.g., C1).

Lake Bonneville Sediments

The oldest units exposed at the Spring Lake site are in the footwall of the Nephi segment and consist of lacustrine sediments deposited during the transgression and highstand of Lake Bonneville. The lacustrine package comprises a distinct fining-upward sequence of interbedded gravel and sand (units N1a and S1a) overlain by thinly bedded medium to fine sand (units N1b1 and S1b1). The sand and gravel units are overlain by sand-rich units N1b2 and S1b2, which have remnants of preserved bedding, but are locally massive, and units N1c and S1c, which do not have preserved bedding. These units are overlain by a poorly sorted, boulder-rich deposit (units N1d and S1d). Although units N1b2/S1b2, N1c/S1c, and N1d/S1d were likely deposited in a subaerial environment, they occurred shortly after Lake Bonneville occupied the site, and thus we discuss them as part of the Lake Bonneville sedimentary package.

Units N1a/S1a and N1b1/S1b1 are likely sediments deposited during the transgression of Lake Bonneville across the site. The units slope gently west, are each about 2 m thick, and mostly consist of well-rounded gravel clasts and interbedded sand (units N1a/S1a) conformably overlain by continuous well-bedded sand (units N1b1/S1b1). These units are extensively faulted by west-dipping normal faults, which we could not trace into the overlying post-Bonneville sediments. Unit N1b1/S1b1 included a laterally continuous, 1–2-cm thick clay interbed that we used to measure fault displacement. In the north wall, an OSL sample for the well-bedded fine sand (unit N1b1; sample SL-L9) yielded an age of 17.3 ± 1.9 ka (2σ). This age corresponds well with the age of the latest highstand occupation (Bonneville flood) of 14,500 ^{14}C yr B.P. (Oviatt, 1997), which DuRoss and Hylland (in press) calendar calibrated to 17.6 ± 0.3 ka (2σ) using OxCal.

Units N1b1/S1b1 are overlain by well-sorted sand that locally has poorly preserved bedding (units N1b2/S1b2) but is mostly massive (units N1c/S1c). We interpret the mostly massive sand of units N1b2/S1b2 and N1c/S1c as Bonneville lacustrine sand (of an origin similar to S1b1/S1b1) that has been remobilized by eolian or slope-wash processes, or disturbed by bioturbation and weathering (e.g., soil creep and freeze-thaw processes). We do not consider remobilization by water (e.g., sheet flooding) likely on account of the limited stratification. An OSL age of 10.0 ± 1.2 ka (sample SL-L8) for unit N1c indicates deposition in a subaerial (post-Bonneville) environment. A wind-blown origin for units N1b2/S1b2 and N1c/S1c is most likely considering the well-sorted and unstratified character of the unit and the OSL age, which does not show evidence of sediment mixing (e.g., grains having inherited ages). Furthermore, the massive sand appears to have draped the local topography based on the slope-parallel nature of the unit N1b1–N1b2 and N1b2–N1c contacts, in contrast to the gentle, west-sloping, undisturbed Bonneville unit contacts. Units N1b2/S1b2 and N1c/S1c each have maximum thicknesses of about 1 m.

We exposed massive sand—units “N1c?” and “S1c?”—in the hanging wall of the Wasatch fault that possibly corresponds with footwall units N1c and S1c, respectively (plate 1). Units N1c?/S1c? consist of medium to coarse sand below colluvial-wedge unit C6 that is mostly massive, but locally has minor well-sorted sand lenses. Unit N1c? is possibly ~1.5 m thick, based on a discontinuous 1–2-cm-thick, sub-horizontal clay bed that we exposed at the base of a temporary exposure below the unit N1c?/S1c?–C6 contact (figure 8). However, because of the short (~1-hour) duration of the exposure (excavated prior to backfilling the trench), there is considerable uncertainty in the thickness and origin of N1c?/S1c?. OSL ages for the top of units N1c? and S1c? are 7.0 ± 0.7 ka (SL-L5) and 7.8 ± 1.0 ka (SL-L3), respectively, and indicate subaerial (post-Bonneville) deposition. On the basis of their thickness (>1 m), texture (massive well-sorted sand), and age (>7–8 ka), we tentatively correlate units N1c?/S1c? with footwall units N1c/S1c, which likely consist of Lake Bonneville sand reworked by eolian (and possibly slope-wash) processes. Although units N1c?/S1c? could have a colluvial origin—on the basis of scarp-parallel sand lenses thickening toward the Wasatch fault—we have low confidence in this interpretation because of the limited extent and duration of the exposure. Furthermore, the slope-parallel lenses could simply represent eolian deposition on a preexisting fault scarp near the fault zone, similar to that on well-bedded lacustrine sand (e.g., unit N1b) outside of the fault zone. About 5 m west of the Wasatch fault, units N1c?/S1c? are interfingered with and overlain by alluvial-fan units N3/S3 and soils S3aA/S3bA. The ~10-ka OSL age for unit N1c provides a possible maximum time of deposition of units N1c?/S1c?, whereas the ~7.0–7.8-ka OSL ages for N1c?/S1c? (samples SL-L3 and -L5) (which are similar to ~7.6–8.0-ka ages for soil S3bA; discussed below) indicate a possible younger depositional time.

Unit N1d/S1d is possibly a shoreline-related boulder deposit, or an early post-Bonneville debris flow sourced from near-shore (beach?) deposits above the site. Because units N1d/S1d clearly postdates the massive (disturbed?) sand of unit N1c in the north wall (h-19 m, v-11 m; plate 1), for which we have an OSL age of ~10 ka, we have greater confidence in the latter interpretation. Furthermore, the dramatic change in thickness from the south wall (~0.5-m; h-16-m, v-10.5 m, plate 1) to the north wall (~2.0 m; h-16 m, v-12 m, plate 1) supports a debris-flow origin. Thus, unit N1d/S1d postdates the Lake Bonneville transgressive sand (and period of

bioturbation and erosion in the north wall possibly at about 10 ka) and predates the post-Bonneville alluvial fan sediments exposed in the footwall of the fault (units N2 and S2).

Post-Bonneville Alluvial-Fan Deposits

Alluvial-fan deposits exposed in the footwall and hanging wall of the Wasatch fault consist of laterally discontinuous stream and debris-flow deposits. Footwall units include N2 and S2 and subunits (e.g., N2a, S2a); hanging-wall units include units N3 and S3 and subunits (e.g., N3a, S3a, N3b1). Alluvial-fan units in the footwall likely predate those in the hanging wall based on the interbedded nature of the hanging-wall alluvial-fan units with the colluvial wedges, indicating that hanging-wall fan deposition occurred in between surface-faulting earthquakes.

Footwall alluvial-fan deposits: Footwall alluvial-fan units N2 and S3 include gently west-dipping coarse gravel interbeds (subunits N2a-c and S2a-c). The units reach a maximum thickness of about 3.2 m in the south wall and are laterally continuous for at least 5 m in the north wall and 15 m in the south wall, where they are fully exposed in the footwall of the fault. In the north wall, units N2a and N2b are locally incised into debris-flow unit N1d (h-14.7 m, v-12 m, plate 1). Individual subunits are about 0.4 to 1.5 m thick. Units N2 and S3 are faulted by the easternmost trace of the Wasatch fault (fault F1) in both walls, and in the south wall, extensively faulted along the main trace of the Wasatch fault zone (fault F1).

We mapped three soil A horizons within the footwall alluvial-fan units. Soil N2bA/S2bA is about 1 m below the ground surface and laterally discontinuous. Charcoal from soil S2bA (SL-R28) yielded an age of 13.7 ± 0.2 ka. However, charcoal from soil S2bA is older than the ~ 10 -ka OSL age for unit N1c stratigraphically below it and may be detrital in origin. Soils S2cA1 and S2cA2 are formed on unit S2c about 0.5–1.0 m above soil N2bA. We differentiated these soils in the south wall, where soil S2cA1 has been faulted down along fault F1 and buried by scarp colluvium (unit CF3). Soil S2cA2 is formed on the scarp colluvium and merges with soil S2cA1 outside of the area of colluvial-wedge deposition (h-13 m, v-14 m, south wall, plate 1). A soil A horizon below unit CF3 was not present in the north wall. Charcoal from soil S2cA1 yielded an age of 6.1 ± 0.1 ka (SL-R24). Although we did not extract charcoal from soil S2cA2, the soil must be younger than 3.6 ± 0.1 ka based on the charcoal sample from scarp colluvium unit CF3 (SL-R25).

Hanging wall alluvial-fan deposits: The hanging-wall alluvial-fan units consist mostly of gently west-dipping coarse gravel interbeds and sub-horizontal channel cuts and fills (subunits N3a-g and S3a-j). The deposits reach a thickness of at least 4 m in the south wall, and individual subunits are <0.1 m to about 1.5 m thick. The deposits are mostly laterally discontinuous: although some subunits (e.g., S3h and N3d) can be traced horizontally for as much as about 18 m, most subunits (especially those lower in the fan sequence) are laterally continuous for only ~ 3 –10 m. For this reason, there is significant uncertainty in the correlation of units along, and especially between, the north and south trench walls. Several of the hanging-wall fan units are faulted along fault F1, where they indicate fan deposition interspersed with surface-faulting earthquakes and colluvial-wedge deposition.

Soil horizons in units N3 and S3 include two buried soil A horizons and a modern soil A horizon. Soils N3aA and S3bA, which likely correlate, mark the oldest buried soil—an A horizon developed in the oldest alluvial-fan sediments exposed on the fault hanging wall (e.g., h-32 m, v-2.5 m, south wall, plate 1). These soils are laterally continuous for about 6–7 m, and extend to within about 6–7 m of fault F1, where they have been locally removed by cross-cutting alluvial-fan channels. Concordant OSL and ^{14}C ages indicate a soil burial time of about 7.6 ± 0.1 ka (SL-R2) to 8.0 ± 1.5 ka (SL-L2). About 2–3 m above S3bA, soil S3iA developed on unit S3i and overlain by units S3j and soil S3jA. In the north wall, a single soil N3A is developed on fan units N3g1, N3f, and N3g2, and likely correlates with both soils S3iA and S3jA in the south wall. Because the relation of soil S3iA to surface faulting is unclear, and because S3jA and N3A are modern soils, we did not sample these soils for ^{14}C dating.

Alluvial-fan units S3d, S3g, and S3h, all of which postdate soil S3bA, had detrital charcoal fragments dispersed throughout them. Charcoal samples SL-R1 and SL-R3 indicate ages of 7.2 ± 0.2 ka (SL-R3) and 7.5 ± 0.2 ka (SL-R1) for unit S3d. In contrast, an OSL sample (SL-L1) of unit S3d yielded an age of 5.2 ± 0.3 ka. We have low confidence in these detrital-charcoal ages as they conflict with several soil-charcoal and OSL ages from above and below unit S3d. Below unit S3d, ^{14}C and OSL ages for soil S3bA and units C6 and N1c?/S1c? are between $\sim 6.1 \pm 1.2$ ka (SL-L4) and 8.0 ± 1.5 ka (SL-L2); above unit S3d, we have the most confidence in an OSL age of 5.7 ± 0.8 ka (SL-L6) for unit S3h. A charcoal fragment from unit S3h yielded an age of 7.1 ± 0.1 ka (SL-R11); however, we have low confidence in this age, as well as the 7.2–7.5-ka ages for unit S3d, because of the detrital nature of the charcoal dated (possibly having an inherited age component).

Scarp-Derived Colluvium

Scarp-derived colluvial wedges (units C1–C6 and CF1–3) at the Spring Lake site consist of lacustrine to alluvial-fan sediment eroded from scarps formed during individual surface-faulting earthquakes on the Nephi segment. The wedges have similar wedge-shaped geometries, horizontal extents (~ 2 –5 m), and maximum thicknesses of about 0.3–0.7 m where unaffected by synthetic or antithetic faulting (table 2). Using units C1–C6, the mean of the maximum wedge thicknesses is 0.6 m. Although the youngest colluvial wedges (C1, CF1, and CF3) are not faulted, units C2–C6 and CF2 have been faulted down to the west along the Nephi segment. We group and discuss the colluvial wedges according to whether they 1) are interbedded with alluvial-fan deposits (units C6–C4), 2) post-date the majority of the alluvial-fan units (units C3–C1), or 3) formed as a result of rupture in the footwall of the fault (units CF1–3).

Units C4–C6 are the oldest colluvial wedges exposed at Spring Lake. These colluvial wedges are interbedded with alluvial-fan deposits, which indicate active fan deposition in between surface-faulting earthquakes. In addition, units C4–C6 mostly lack organic sediment (in contrast to abundant organic sediment in units C1–C3), likely reflecting active depositional processes (rather than soil development) during scarp formation and erosion. For the youngest colluvial wedges (C1–C3 and CF1–3), organic A-horizon soil matter is locally dispersed throughout the wedges, indicating cumulic A horizon development during wedge deposition.

Table 2. Colluvial-wedge thickness at the Spring Lake site.

Unit	North wall (m)	South wall (m)	Preferred (m)
C1	0.7	0.7	0.7
C2	0.5	0.5	0.5
C3	0.5	0.5	0.5
C4	0.3	~0.4 [†]	0.4
C5	0.5	0.6	0.6
C6	0.7	>0.4 [†]	0.7
CF1	0.6	NE	0.6
CF2	NE	0.6	0.6
CF3	0.3	0.3	0.3

[†] poor measurement because of bench (C4) or uncertainty in lower contact (C6).

NE – not exposed.

CF3 based on height of buried free face, rather than maximum wedge thickness.

Unit C6 is the oldest completely exposed colluvial wedge. The wedge consists mostly of sand that is massive to weakly bedded, and locally has slope-parallel fabric that unconformably overlies the sub-horizontal top of unit N1c? (h-28 m, v-3.2 m, north wall, plate 1) (figure 8). Unit C6 is a maximum of 0.7 m thick based on the north wall exposure and is overlain by several extensive alluvial-fan deposits (units S3c and N3d) that taper to the east, reflecting deposition on preexisting topography (the toe of the scarp). Unit C6 postdates the ages for unit N1c? (~7.0–7.8 ka) and soil S3bA (~7.6–8.0 ka). In the north wall, OSL and ¹⁴C samples from the uppermost part of unit C6 provide minimum ages of 6.1 ± 1.2 ka (SL-L4) and 16.9 ± 0.3 ka (SL-R10). The anomalously old age for SL-R10 likely reflects detrital charcoal eroded from unit N1.

Scarp colluvium (unit C5), which overlies unit C6 and alluvial-fan units N3d and S3c, is likely evidence of a separate surface-faulting earthquake. Unit C5 is a maximum of about 0.5–0.6 m thick and has a limited horizontal extent of ~2.2–2.6 m. We were unable to sample unit C5 because of the lack of organic sediment for ¹⁴C dating, or well-sorted sand for OSL dating. However, unit C5 must postdate the ~6.1-ka OSL age for C6, and may also postdate charcoal ages ~7.2–7.5 ka for unit S3d based on the correlation of alluvial-fan unit S3c across a prominent channel fill (unit S3g). However, it is possible that these detrital charcoal fragments sampled from unit S3d have an inherited age component as they are stratigraphically inverted with OSL ages L4 (~6.1 ka) and L5 (~7.0 ka). Unit C5 predates an OSL age of ~5.7 ka and a ¹⁴C age on charcoal of 7.1 ka (SL-R11) for unit S3h1. Considering the similarity of the detrital-charcoal age for S3h1 (~7.1 ka) to those from unit S3d, we have low confidence in the 7.1-ka age.

Because unit C5 directly overlies part of unit C6 (north wall, h-27.5 m, v-4.2 m) and has a very limited area, C5 could be a younger pulse of unit C6 sedimentation. In this scenario, fan deposition (units S3c, S3e, and S3g) between units C6 and C5 would be contemporaneous with deposition of units C6 and C5. However, because the fan deposits between units C6 and C5 are extensive (laterally continuous for several meters and including several subunits), they likely indicate a period of scarp stabilization and fan deposition. In addition, OSL ages show that a significant amount of time (~1 kyr) elapsed between deposition of uppermost unit N1c? (~7 ka) and uppermost unit C6 (~6 ka). Considering this elapsed time, scarp erosion and colluvial-wedge

(unit C6) deposition were likely complete by the time alluvial-fan units S3c and N3e were deposited, making unit C5 (similar in geometry to unit C6) a separate colluvial wedge related to a younger surface rupture. However, deposition of units C5 and C6 occurred in a relatively short time (~1.3 kyr between the 7.0-ka for uppermost unit N1c? and the 5.7-ka age for unit S3h1) and thus we cannot rule out the possibility that units C5 and C6 were deposited following a single earthquake.

Unit C4 postdates a period of alluvial-fan channel formation (erosion) and deposition (units S3g and N3e-f). Similar to C5, unit C4 has a limited lateral extent of ~2.5–4.3 m and a maximum thickness of ~0.3–0.4 m. In the south wall, unit C4 overlies alluvial-fan units S3g and S3h, as well as a weak carbonate soil horizon developed on these units (h-26 m, v-5.3 m, south wall, plate 1). OSL and ^{14}C ages for units S3g and S3h indicate that unit C4 deposition occurred after ~5.7 ka (OSL sample SL-L6), and possibly ~7.1 ka using the age for ^{14}C sample SL-R11. A ^{14}C sample of uppermost C4 colluvium yielded an age of 4.4 ± 0.1 ka (SL-R20). An additional sample of unit C4 colluvium consisted of sand likely eroded from the footwall (unit N1) and yielded an OSL age of 4.5 ± 0.5 ka (SL-L10). Unit C4 is overlain by a debris flow that is ~0.3 m thick in the south wall (S3h2) and ~0.2 m thick in the north wall (unit N3g1).

Considering the limited thickness and extent of unit C4 (particularly in the north wall), we cannot rule out the possibility that C4 is an earlier phase of the unit C3 colluvial wedge. However, the limited (~0.3-m) thickness for unit C4 in the north wall may be related to a limited exposure as the unit crosses a ~1.5-m-wide horizontal bench. In the south wall, C4 also has a limited thickness (again, possibly related to the limited exposure across a horizontal bench), but the unit has a geometry that is more consistent with younger colluvial wedges C1–C3. Alternatively, the limited thickness for C4 may stem from alluvial-fan deposition (unit S2h2) which occurred between C4 and C3, and may have taken up part of the accommodation space created by the C4 earthquake. Finally, ^{14}C ages for units C4 and C3 indicate that at least 1.1-kyr elapsed between deposition of these colluvial-wedge units. Thus, we consider it unlikely, that C3 and C4, which were deposited at least 1.1 kyr apart and are separated by a distinct alluvial-fan unit, formed in response to the same surface-faulting earthquake.

Scarp colluvium in unit C3 is the youngest wedge formed during the period of alternating alluvial-fan and colluvial-wedge deposition. Unit C3 has a horizontal extent of 2.6–4.5 m and a maximum thickness of ~0.5 m. Unit C3 is overlain by a debris flow (north wall unit N3g1); however, the likely corresponding debris flow in the south wall (unit S3i) is only exposed west of unit C3. Unit C3 postdates the 4.4–4.5-ka ages for unit C4, and predates an age of 3.5 ± 0.1 ka (SL-R19) for charcoal extracted from the upper part of the unit. Charcoal extracted from unit N3g1 (postdating unit C3) yielded an age of 5.7 ± 0.1 ka (SL-R27); however, this age is stratigraphically inverted with several ages (e.g., SL-L10 and SL-R20) and thus, we consider it a maximum age (likely for detrital charcoal) for unit N3g1. Unit C3 is extensively faulted by subsidiary fault traces.

Unit C2, which overlies unit C3 in the south wall and units C3 and N3g1 in the north wall, is the youngest faulted colluvial wedge along the main fault zone (fault F1). The colluvial wedge extends horizontally for 5.1–5.4 m and has a maximum thickness of ~0.5 m. Fault-related evidence for C2 includes subsidiary faults that displace the C3 wedge, but do not extend into unit

C2 (h-26 m, v-6.5 m, north wall, plate 1). Unit C2 post-dates the 3.5-ka age for unit C3 as well as the erroneously old 5.7-ka age for alluvial-fan unit N3g1 (SL-R27). Minimum ages for C3 deposition are derived from charcoal extracted from the uppermost part of the C2 colluvial wedge. In the south wall, two charcoal samples (SL-R17 and -R18) yielded ages of 2.3 ± 0.08 ka (SL-17) and 4.1 ± 0.1 ka (SL-R18). However, we dismiss the 4.1-ka age for SL-R18 as it is stratigraphically inverted with the 3.5-ka age (SL-R19) for the soil sediment (within unit C3) buried by unit C2. Sample SL-R18 likely contained charcoal eroded from the faulted soil sediment within unit C3. In the north wall, charcoal from unit C2 yields a minimum age of 1.1 ± 0.04 ka (SL-R22) for unit C2.

Unit C1 consists of unfaulted scarp colluvium that overlies unit C2 in the north and south walls. Unit C1 extends horizontally for about 4.7–5.6 m and has a maximum thickness of 0.7 m. Evidence for C1 includes silt, sand, and gravel that locally forms slope-parallel fabric and has buried a shear zone and eroded scarp free face. The timing of unit C1 deposition is complicated by poor agreement between the north- and south-wall ^{14}C ages. In the north wall, charcoal derived from C1 soil sediment provides a minimum age of 0.7 ± 0.04 ka (SL-R21); in the south wall, two charcoal samples from C1 yield minimum constraints of 0.7 ± 0.04 ka (SL-R15) and 2.4 ± 0.1 ka (SL-R16). However, we dismiss the 2.4-ka minimum age (SL-R17), which is for charcoal likely derived from ~2.3-ka soil sediment in the faulted C2 wedge (thus, predating unit C1 deposition). Maximum times of unit C1 deposition are 1.1 ± 0.1 ka based on north-wall sample SL-R22 and 2.3 ± 0.1 ka based on south-wall sample SL-R17. Based on these ages, unit C1 deposition likely occurred between ~0.7 and 1.1 ka.

Colluvial wedges CF1–CF3 were deposited following movement on faults F1 (CF1 and CF2) and F3 (CF3). Unit CF1 is only present in the north wall where it overlies sheared sediment near the top of the complex fault F1, and is east of the buried free face adjacent to colluvial wedge C1 (h-25 m, v-8m, plate 1). CF1 has a maximum thickness of 0.6 m; however, this is a poor estimate on account of its limited exposure (~0.6-m lateral extent). We also exposed a colluvial wedge, unit CF2, in the north wall and footwall of the faults within the F1 fault zone that underlie and are adjacent to colluvial wedges C1–C6. CF2 has a lateral extent of 3.0 m and a maximum thickness of 0.6 m. Unit CF3 is exposed on the down-thrown (west) side of fault F3 in both the north and south walls. The colluvial wedge has a lateral extent of ~2.6–3.3 m and a maximum thickness of ~0.3 m. Unit CF3 was deposited after a 6.1 ± 0.1 -ka age (SL-R24) for soil S2cA1 (beneath unit CF3) and before a 3.6 ± 0.1 -ka age (SL-R25) for the basal part of the unit. Units CF1 and CF2 do not have numerical ages constraining their deposition times.

Wasatch Fault Zone

The WFZ at the Spring Lake site is characterized by 1) a main and westernmost shear zone (F1), 2) a central zone of complex faulting primarily in Lake Bonneville lacustrine sediments (F2), and 3) an easternmost fault trace (F3) (plate 1).

Fault F1 comprises about 4–6 traces that juxtapose Lake Bonneville lacustrine and post-Bonneville alluvial-fan sediments in the footwall with alluvial-fan sediments and scarp-derived colluvium in the hanging wall (figure 7). These traces form a complex, upward-diverging fault zone about 0.3–1.2 m wide in the north wall and 0.4–2.1 m wide in the south wall. These fault

zones consist of sheared silt, sand, and gravel containing clasts rotated parallel to one of several fault planes. In the south wall, the dip of the fault traces ranges from about 50° west to near vertical, and locally as much as about 20° overturned (east dipping); however, the main shear zone dips about 65° west. In the north wall, the fault-trace dip ranges from about 60° west to near vertical (locally 10° overturned), and the main shear zone dips about 70–80° west (h-25 m, v-5 m, south wall, plate 1).

Fault F2 consists of an about 6.5–8.0-m wide zone of complex and diffuse faulting primarily within Lake Bonneville lacustrine sediments (units S1 and N1). In both walls, the faults primarily dip 55–75° west; however, locally the faults have shallow (~35–50°) west or moderate (~60–75°) east dips. In the north wall, several minor-displacement faults in F2 terminate near the top of well-bedded unit N1b1 (e.g., h-18 m, v-10 m, north wall, plate 1). We did not observe faulting in overlying units N1b2, N1c, or N1d. Although the mostly massive character of these could have obscured evidence of faulting, we also observed faults that clearly displace unit N1b1, but are truncated by post-Bonneville alluvial-fan unit N2b (h-15 m, v-11.4 m, north wall, plate 1). In the south wall, several faults clearly displace well-bedded unit S1b1, but not the overlying units S1c and S1d. These fault terminations indicate at least one earthquake postdating the time of the Bonneville highstand, but predating the post-Bonneville alluvial fan (units N1d/S1d and N2/S2).

At the eastern end of the exposure, fault F3 consists of a single, west-dipping strand that displaces alluvial fan units N2 (h-11.2 m, v-14 m, north wall, plate 1) and S2 (h-11 m, v-14 m, south wall, plate 1). Fault F3 dips about 55–70° and vertically offsets S2 subunit contacts about 0.2 m and N2 subunit contacts about 0.2–0.4 m. Based on the minor displacement and single colluvial wedge exposed (unit CF3), we infer that movement of fault F3 has only occurred in a single earthquake.

We observed only minor rotation (flattening) of unit contacts in the hanging wall of fault F1. For example, in the north and south walls, the bases of lowermost colluvial wedges C5 and C6 are sub horizontal, whereas the base of the uppermost colluvial wedge C1 dips about 15–20° west. We did not observe significant fault rotation or drag (steepening on the hanging-wall contacts) along faults F2 or F3.

There is considerable uncertainty in the total vertical displacement at the Spring Lake site because of the deposition of alluvial-fan deposits on the hanging-wall following several surface-faulting earthquakes. As a result, footwall and hanging-wall alluvial fan sediments and soils are non-contemporaneous, which complicates both the measurement of total site displacement and the period of time over which that displacement occurred. One possibility is that the lowermost soil (S3sA/N3bA) exposed in the fault hanging wall, which has ages of ~7.6–8.0 ka (R2 and L2), is approximately contemporaneous with the soils (N2bA/S2bA or N2cA/S2cA) exposed near the surface of the fan exposed in the fault footwall. The footwall soils are broadly dated to ~6.1 ka (S2cA) to ~13.7 ka (S2bA). However, we have more confidence in the younger (~6.1 ka) soil age, which corresponds well with several mid-Holocene surface ruptures at the site and is stratigraphically consistent with the early Holocene (~10-ka) age for post-Bonneville unit N1c. Furthermore, the footwall (e.g., N2bA) and hanging-wall (e.g., N3bA) soils both postdate a period of alluvial erosion and deposition (units N2/S2 in the footwall and N3/S3 in the hanging

wall) that occurred after deposition of massive (possibly eolian or slope-wash-derived) sand across the site (units N1c/S1c in the footwall and N1c?/S1c? in the hanging wall). If the footwall and hanging-wall soils are contemporaneous, then the total displacement at the site is 6.0–7.3 m, based on 6.0–7.1 m measured in the south wall and 7.0–7.3 m in the north wall. The range in these displacement values stems from the limited exposures of these soils and their projections into the main fault zone (F1).

We estimate the minimum site displacement by summing the individual colluvial wedge maximum thicknesses, which represent the minimum displacement in each earthquake (after DuRoss, 2008). The sum of the C6 to C1 colluvial wedges exposed along fault F1 is 3.4 m (using the preferred values in table 2); including the footwall colluvial wedges (CF1/CF2 and CF3), the minimum site displacement is 4.3 m. The total minimum displacement based on colluvial wedges C6–C1 (4.3 m) is several meters less than the stratigraphic offset of the soils (6.0–7.3 m). We have less confidence in the wedge-based value because of the alluvial-fan deposition on the hanging wall and adjacent to the fault zone that has occurred between several faulting events. Fan deposition along the fault occurred partly in response to surface faulting (the creation of accommodation space), which would have limited the amount of colluvial-wedge sedimentation.

Per-event vertical displacements for the Spring Lake site are based on the assumption that 1) each colluvial wedge along fault F1 represents a separate surface-faulting earthquake, 2) the maximum colluvial wedge height represents the minimum fault displacement, and 3) the maximum total displacement based on the stratigraphic offset of soils S3bA/N3bA represents a reasonable upper-bound displacement. To estimate the upper-bound displacement per event, we took the individual wedge thicknesses and increased them by 70%, so that their sum equaled the maximum stratigraphic offset at the site (7.3 m) (following DuRoss and others, in press). To account for the offset in footwall colluvial wedges CF1 (~0.6 m; north wall) and CF2 (~0.6 m; south wall), we allocated 0.6 m for these wedges (since they were exposed in opposite trench walls) equally to main-fault colluvial wedges C1–C6 prior to scaling. To account for colluvial wedge CF3, we added one-half of its 0.3-m height to colluvial wedges C4 and C3 (on the basis of their numerical constraints; discussed below) prior to the scaling. The revised heights for C1–C6 have a mean of 0.7 m, which we increased by 70%, yielding a scaled mean height of 1.2 m. Using the revised height as the lower bound and the scaled height as the upper bound, the midpoint and range displacements for C1–C6 have a mean of 1.0 ± 0.3 m and range from 0.8 ± 0.2 m (C2) to 1.1 ± 0.3 m (C1 and C6). These displacements are similar to a mean per-event vertical displacement of 1.0–1.2 m found by dividing the total site displacement (6.0–7.3 m) by six surface-faulting earthquakes (colluvial wedges C6–C1 that postdate soils S3bA and N3bA).

Because we did not expose lacustrine sediments on the hanging-wall of the fault, we were unable to constrain the total vertical displacement of the Lake Bonneville transgressive and highstand units.



Figure 1. Segments of the Wasatch fault zone (WFZ) in southern Idaho and northern Utah. The central WFZ, which has evidence of repeated Holocene surface-faulting earthquakes, is shown in red; less-active end segments of the WFZ are shown in black. Other Quaternary faults in northern Utah are shown in dark gray. Fault traces are from Black and others (2003); base map is true-color satellite image from the National Aeronautics & Space Administration (NASA, 2012; taken May 31, 2001).

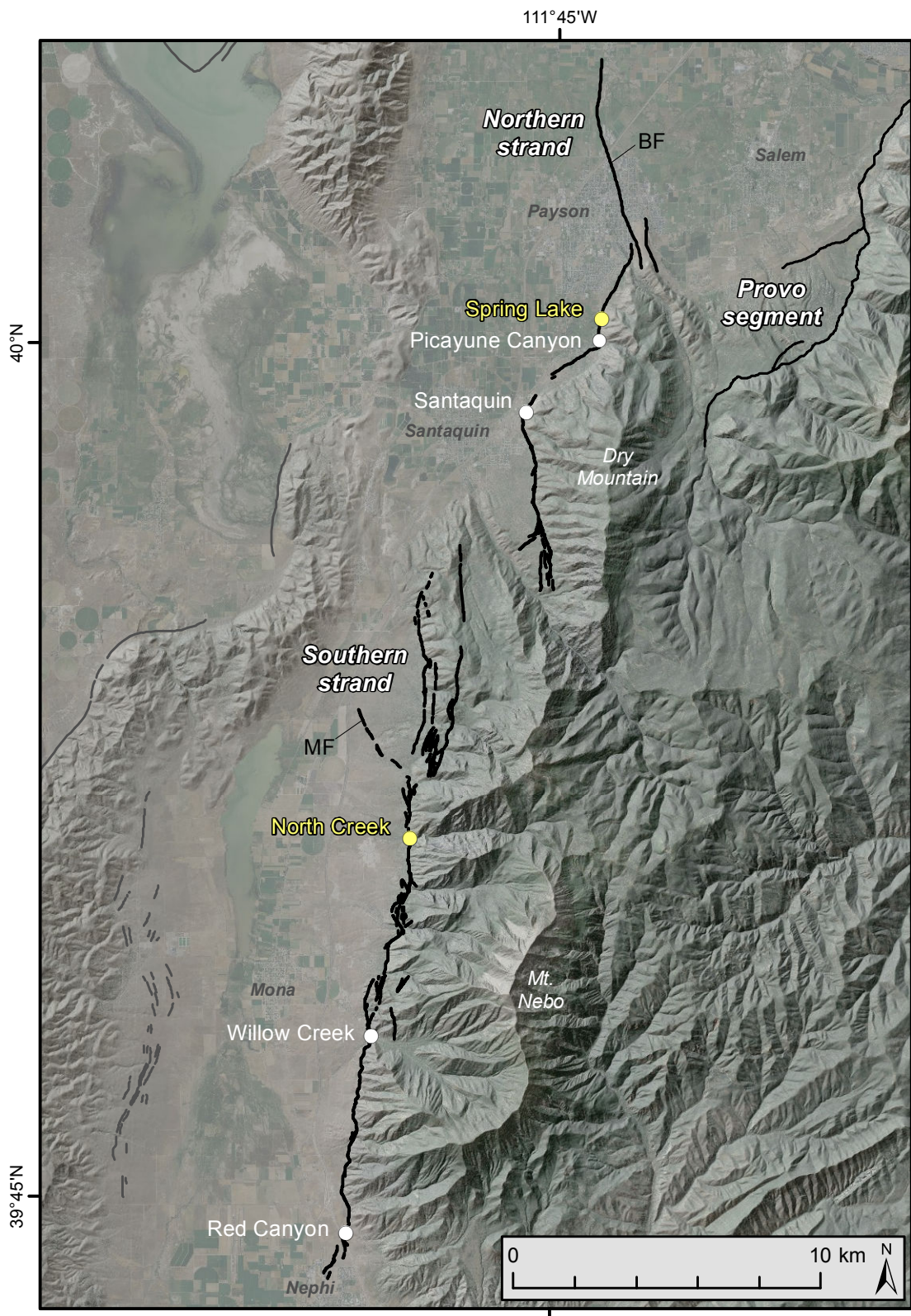


Figure 2. Nephi segment of the WFZ, showing the northern and southern fault strands and the southern extent of the Provo segment. Gray faults are other Quaternary faults in the area (all fault traces from Black and others, 2003). Circles indicate paleoseismic trench sites: white – previous investigations; yellow – this study. BF – Benjamin fault, MF – Mendenhall fault. Base maps are 2011 NAIP aerial photography (U.S. Department of Agriculture [USDA], 2013)

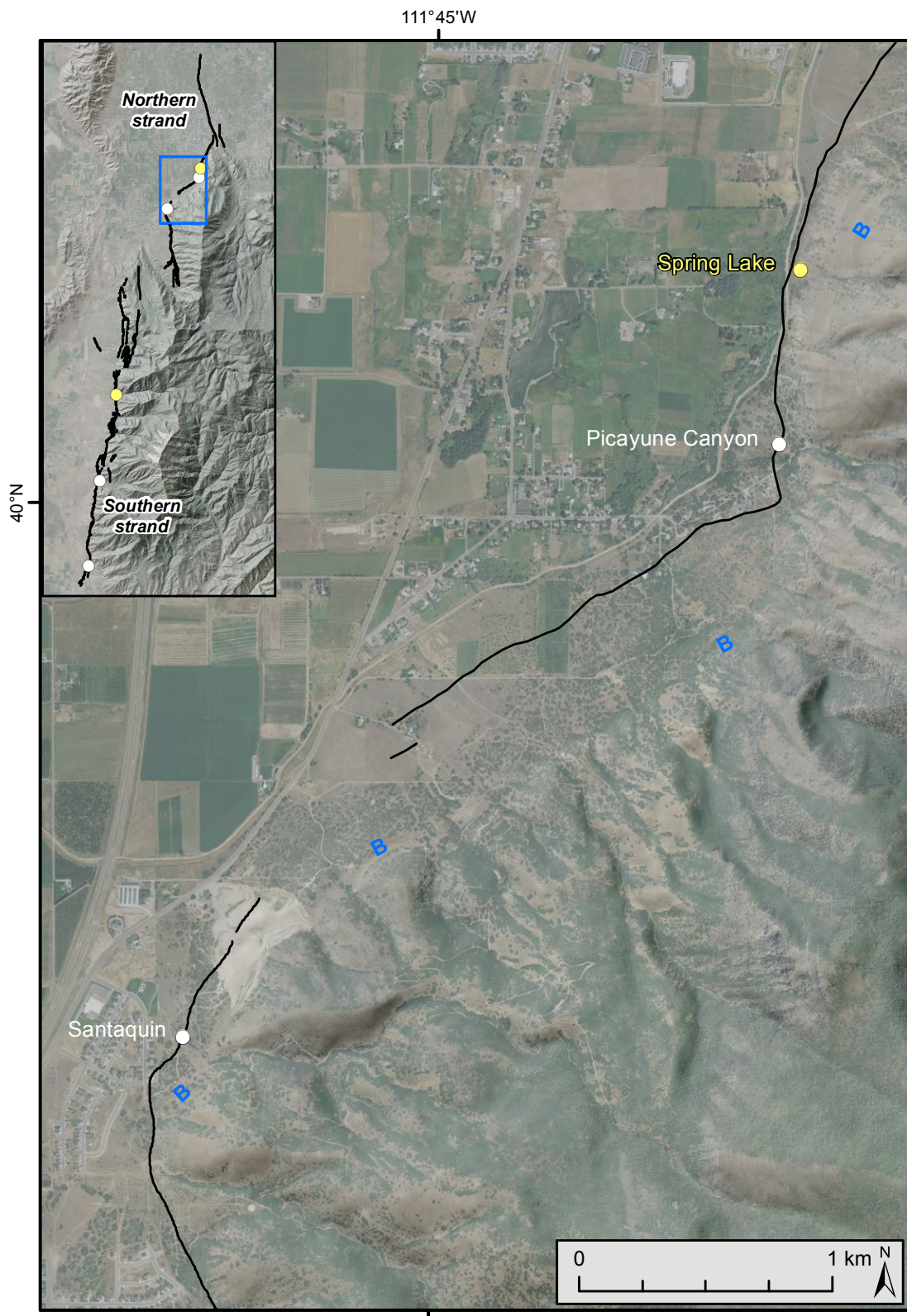


Figure 3. Northern strand of the Nephi segment showing the Spring Lake and adjacent trench sites. Fault traces from Black and others (2003) show the approximate location of the WFZ. B indicates highstand shoreline of Lake Bonneville. Base maps are 2011 NAIP aerial photography (USDA, 2013) overlain on a 10-m DEM with hillshade (AGRC, 2013).



Figure 4. Spring Lake site on the northern strand. A) View to the east of the alluvial fan (white dashed lines) incised into Lake Bonneville highstand sediments on the footwall of the WFZ (red line). The Spring Lake site is below the Lake Bonneville highstand shoreline and above the elevation of the Provo shoreline (not shown). B) Excavation of the Spring Lake site. The scarp shown is approximately 8 m high. View to the southeast.

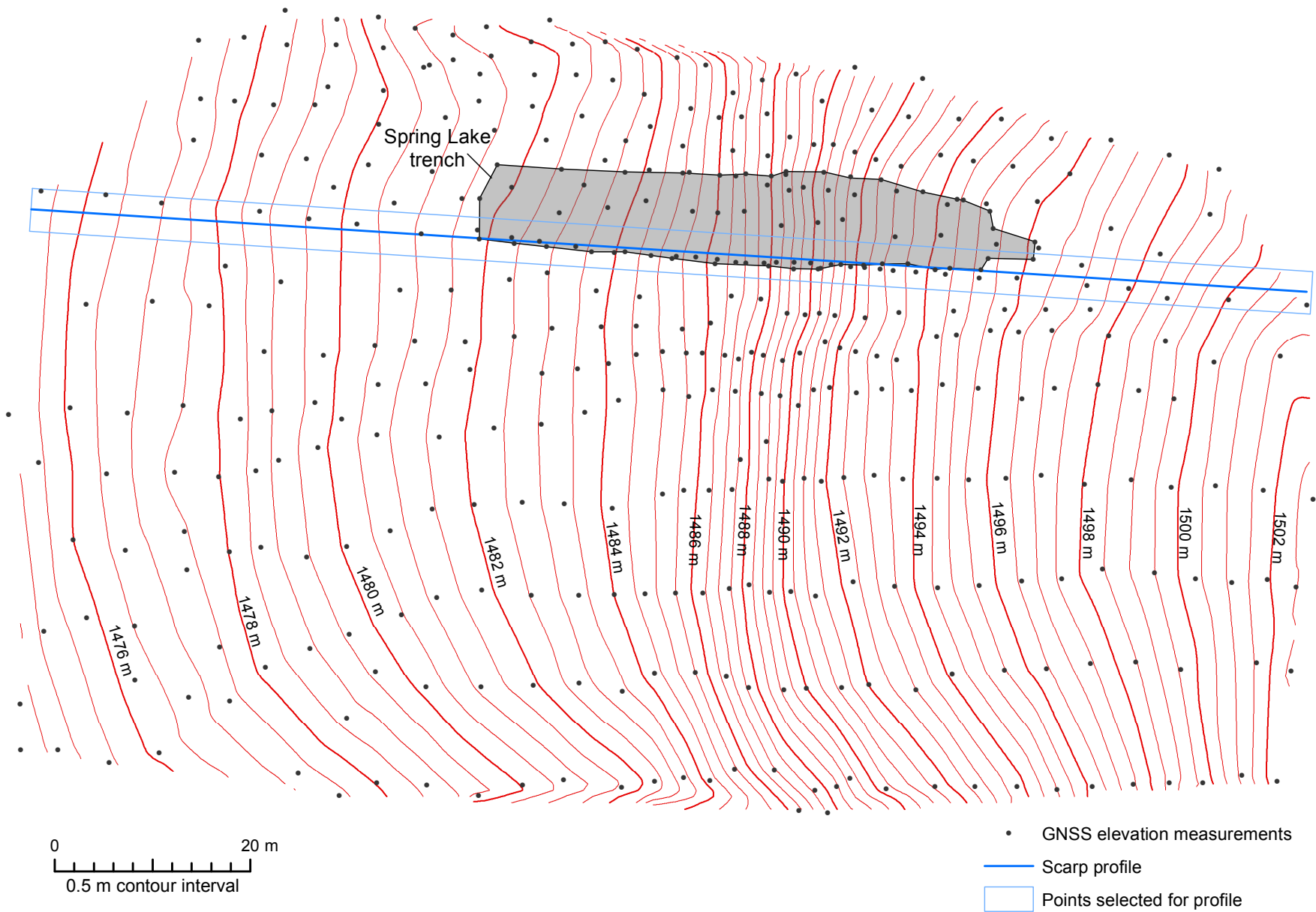


Figure 5. Topographic map of the Spring Lake site based on high-precision GNSS data measured prior to trench excavation. Gray-filled polygon indicates extent of the Spring Lake trench; blue line indicates scarp profile (figure 6). Contours interpolated from a triangulated irregular network (TIN) generated using the point elevation data.

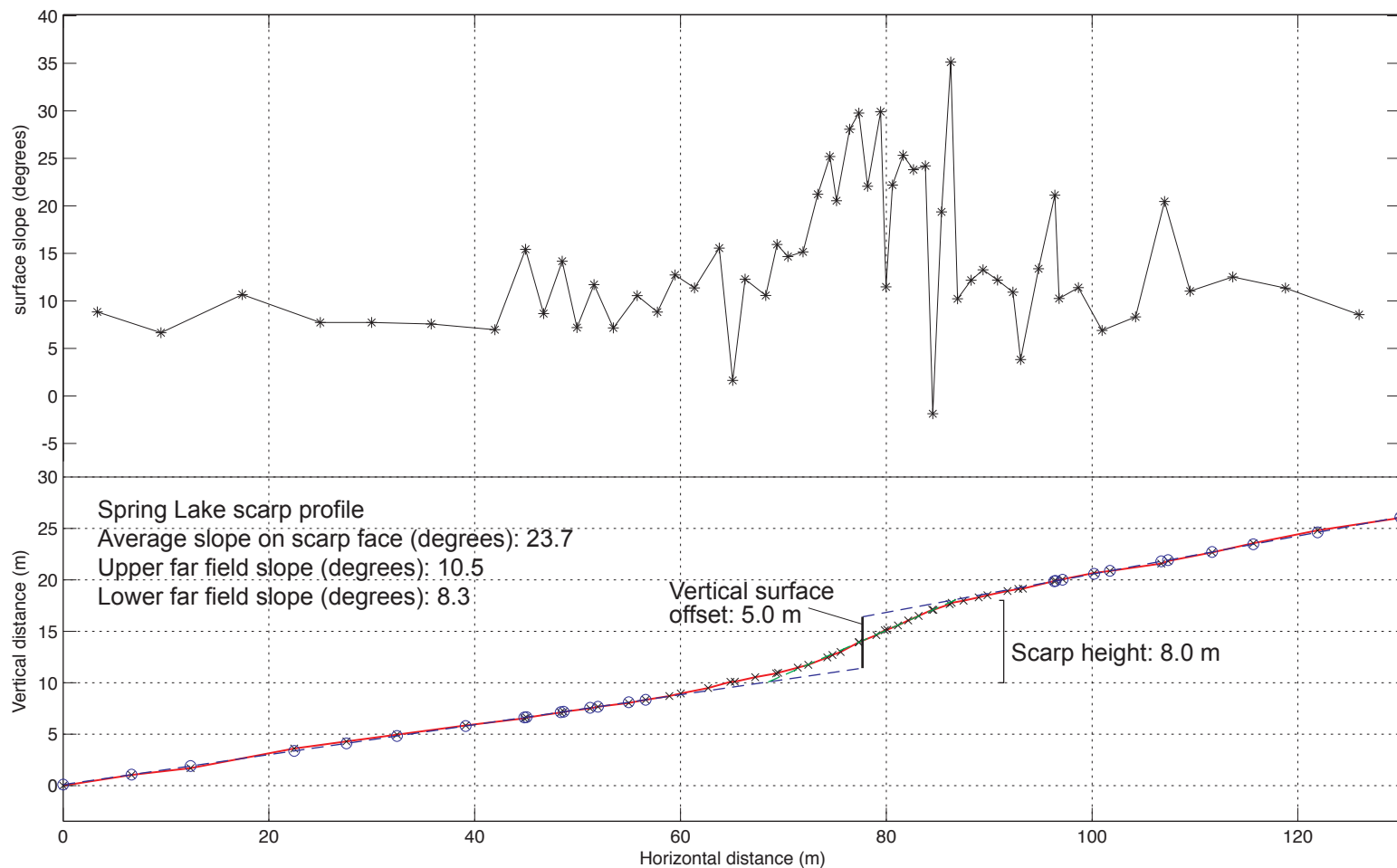


Figure 6. Scarp profile measured across the Spring Lake site. Profile points (X's) measured using high-precision GNSS; vertical distance is relative to the minimum surface elevation at the site (1475 m above mean sea level). Black asterisks show surface slope at midpoint distances between profile points. Blue circles indicate profile points selected for upper and lower surface-slope measurements. Vertical surface offset is the vertical separation of the projected upper and lower surface slopes measured at the horizontal midpoint of the maximum scarp slope (green dashed line). Scarp height is the vertical distance between the intersections of the maximum scarp slope with the upper and lower surface-slope projections.

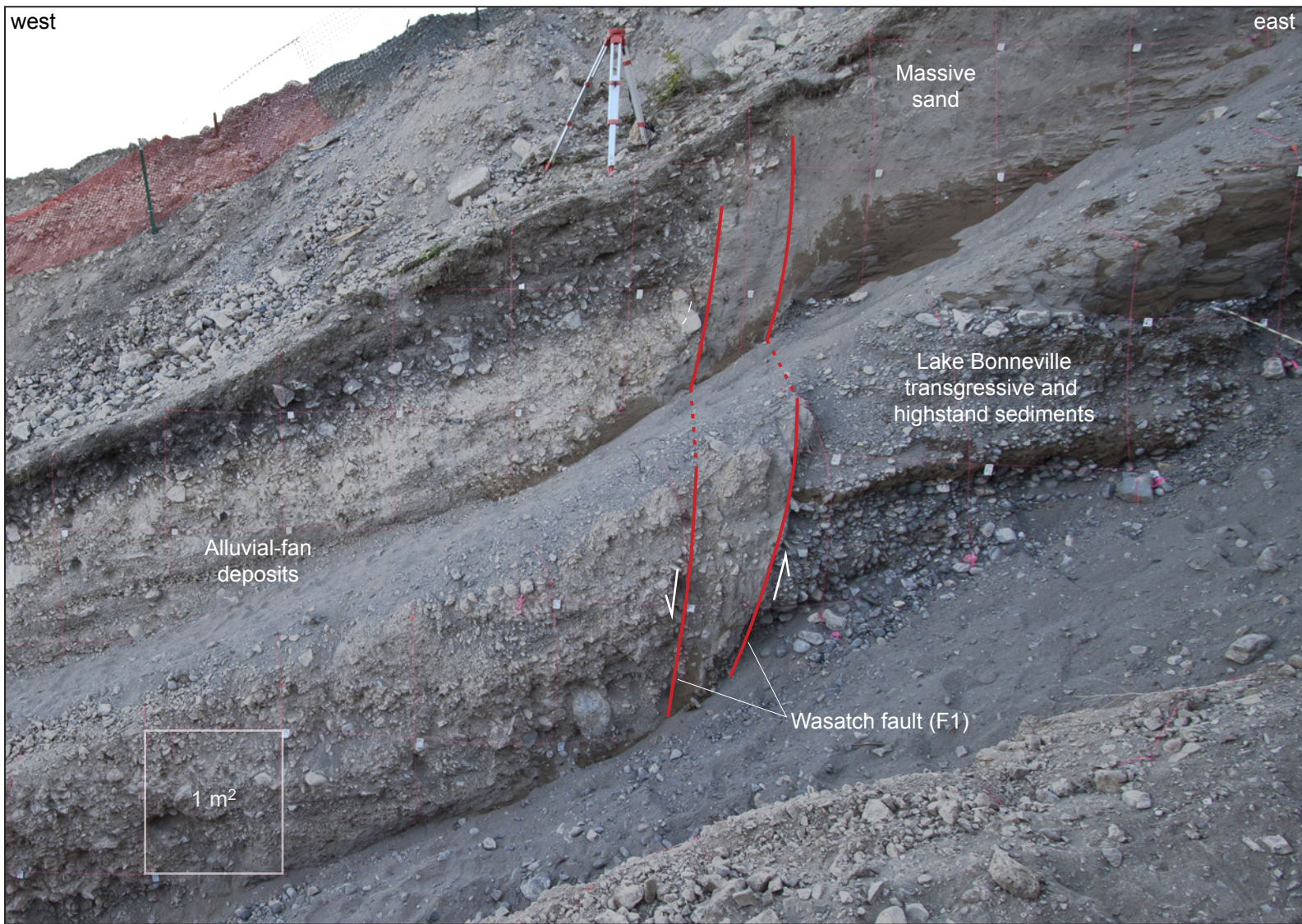


Figure 7. North wall of the Spring Lake trench, showing the main traces of the Wasatch fault (fault F1) that juxtapose Lake Bonneville lacustrine sediments in the footwall with post-Bonneville alluvial-fan deposits in the hanging wall. Pink string lines show a 1-m square grid.

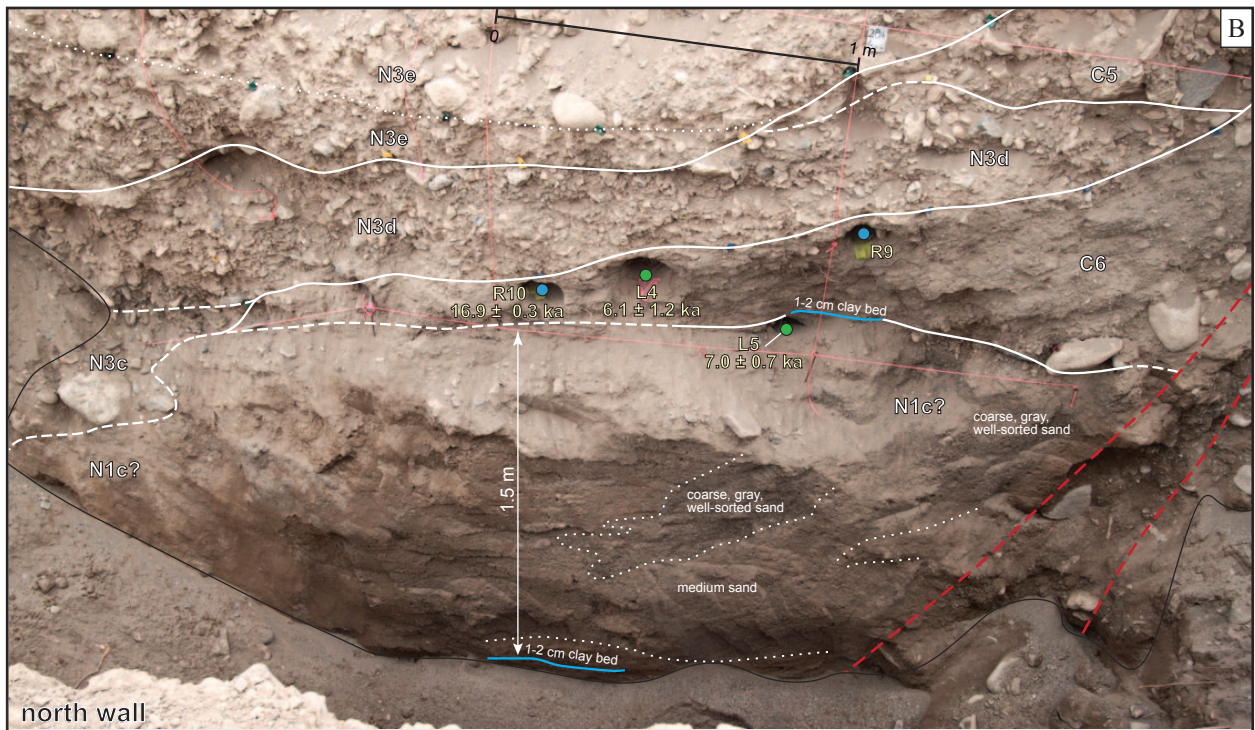


Figure 8. Colluvial-wedge unit C6 exposed adjacent to the Wasatch fault (red dashed lines). A) South-wall exposure, showing unit C6, which overlies massive sand in unit S1c?, and is overlain by several alluvial-fan deposits. Unit C6 likely postdates the ~7.8 ka OSL age for unit S1c? (sample SL-L3), which is interfingered with soils S3aA and S3bA (dated to ~7.6–8.0-ka based on OSL samples SL-L1 and -R2). B) North-wall exposure, showing unit C6 unconformably overlying the subhorizontal sand and fine silt and clay bed (upper blue line) in the uppermost part of unit N1c?. A lower clay bed in unit N1c? is the basis for a ~1.5-m minimum thickness of the unit. Unit C6 deposition predates the age for SL-L4 (~6.1 ka) and postdates the age for SL-L5 (~7.0 ka).

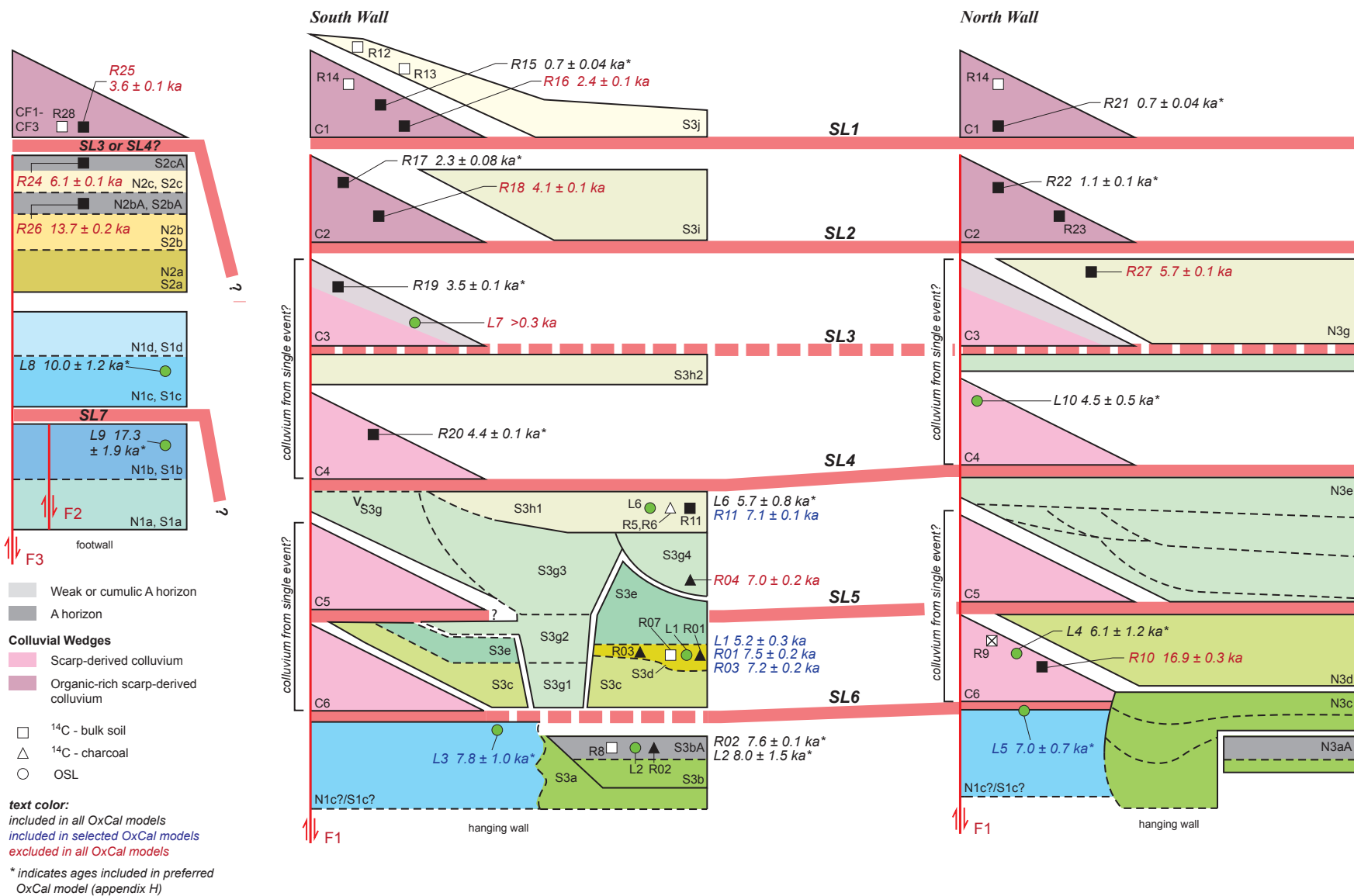
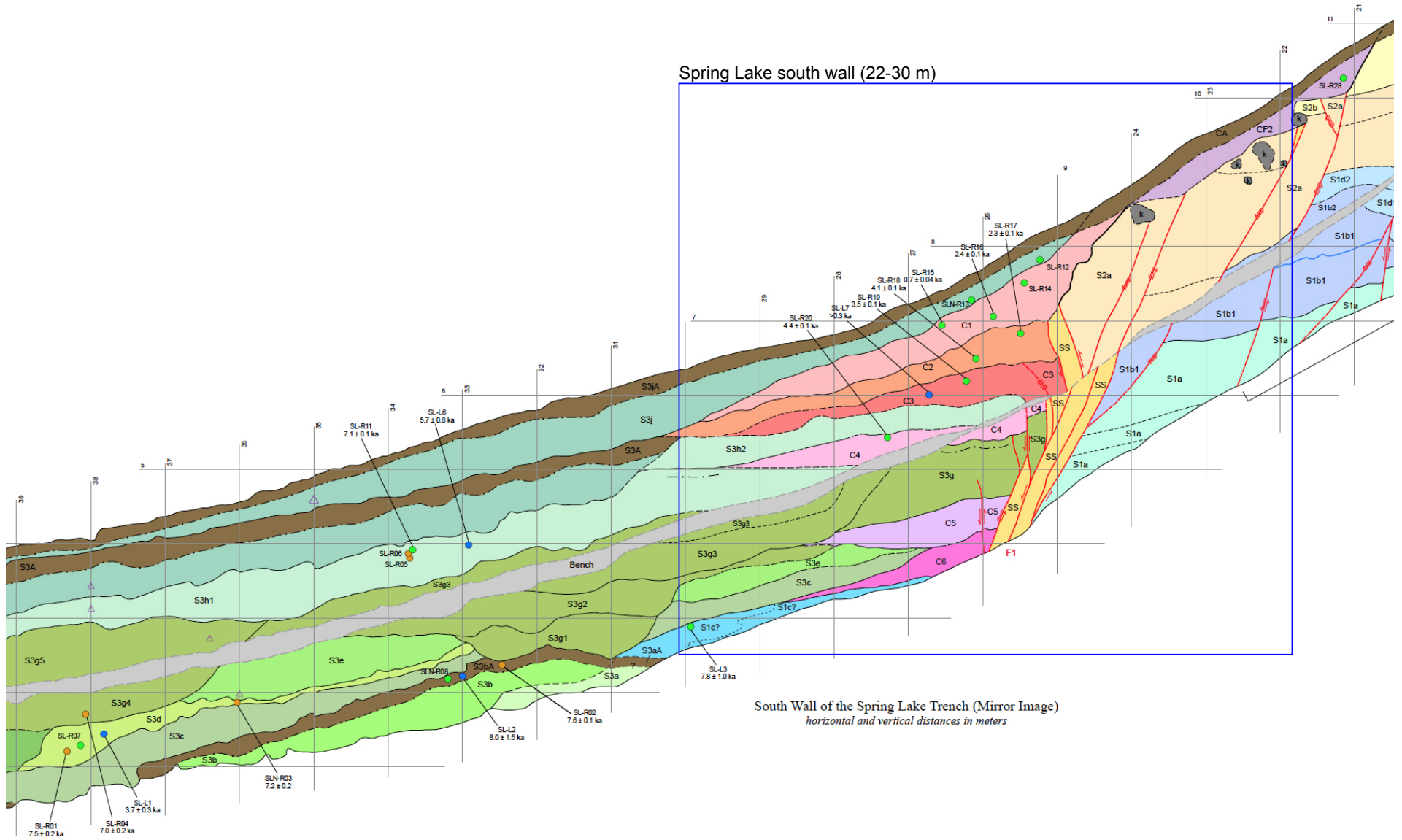


Figure 9. Summary of colluvial wedges exposed at the Spring Lake site and their relation to alluvial-fan and lacustrine sediments and ^{14}C and OSL ages. Text color for numerical ages indicates placement in several OxCal models constructed for the site (appendix H). Horizontal red bars indicate surface-faulting earthquakes in the context of the sedimentary deposits and numerical ages.



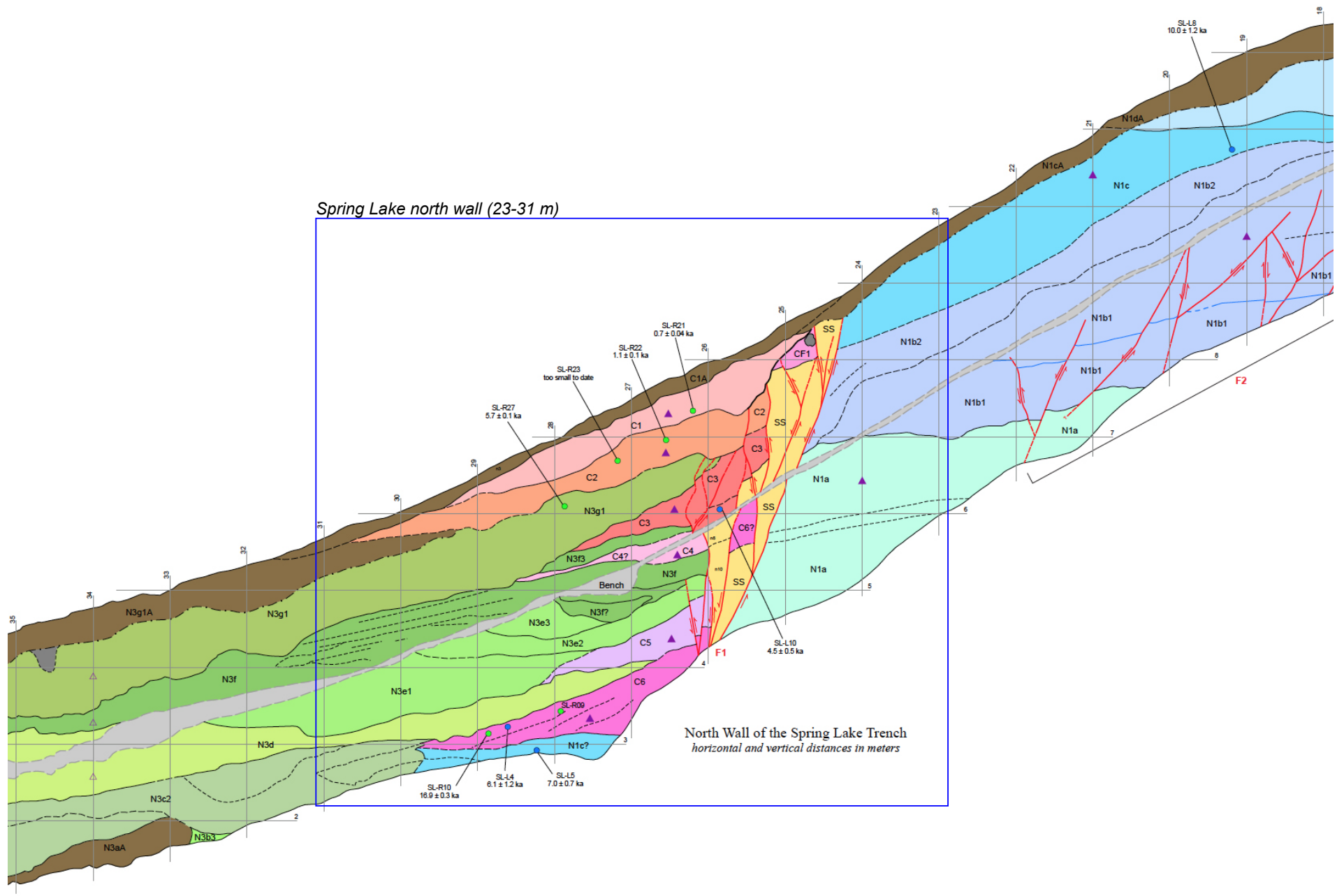
Spring Lake south wall (22-30 m)

South Wall of the Spring Lake Trench (Mirror Image)

horizontal and vertical distances in meters



Spring Lake south wall (22-30 m horiz.)





Spring Lake north wall (23-31 m horiz.)

EXAMINATION OF CHARCOAL AND BULK SOIL SAMPLES FOR
RADIOCARBON Datable MATERIAL FROM THE SPRING LAKE NORTH
AND NORTH CREEK TRENCH SITES ON THE NEPHI SEGMENT
OF THE WASATCH FAULT ZONE, UTAH

By

Kathryn Puseman

With assistance from
Peter Kováčik,
R. A. Varney,
and
Linda Scott Cummings

PaleoResearch Institute
Golden, Colorado

PaleoResearch Institute Technical Report 12-129

Prepared for

Utah Geological Survey, Salt Lake City, Utah
and
U.S. Geological Survey, Denver, Colorado

February 2013

vertically offset by the Wasatch fault. Local vegetation in these areas consists primarily of grasses and mountain brush, mostly oak (*Quercus*).

Spring Lake North Site

The Spring Lake North site is situated south of Payson, Utah, at an elevation of 1480–1490 meters. This elevation is below the highest shoreline of Lake Bonneville. The trench exposed Lake Bonneville lacustrine sediments, stream and debris flow (alluvial-fan) deposits, and fault scarp-derived colluvium. The drainage basin that is the source of the alluvial fan deposits ranges in elevation from 1510–1780 meters. A wildfire in 2001 burned both the trench site and the drainage basin. A total of 8 detrital charcoal samples and 15 bulk soil samples were examined from this site.

Unit C1A

Bulk samples SLN-R15 and SLN-R16 were recovered from an A horizon developed on or within (organic stringer) scarp colluvium in Unit C1A (Table 1). Sample SLN-R15 contained several fragments of charcoal too small for identification that weighed a total of 0.0011 g (Tables 2 and 3). Since the minimum weight of charred material needed for dating reported by Woods Hole Oceanographic Institution is 0.5 mg (0.0005 g), the 0.0011 g of charcoal recovered in sample SLN-R15 should be sufficient for AMS radiocarbon dating. The sample also contained an uncharred *Lactuca* seed, an uncharred Poaceae A floret, a few root fragments, and numerous rootlets from modern plants in the area. A few insect chitin fragments, two insect puparia, and several snail shells also were noted.

Several fragments of charcoal too small for identification and weighing 0.0019 g were present in sample SLN-R16, which should be a sufficient weight for dating. Two uncharred Poaceae stem fragments note modern grasses. In addition, the sample yielded a few root fragments, numerous rootlets, numerous snails with a depressed shape, and a few snails with an oblong shape.

Unit C1

Samples SLN-R13 and SLN-R21 were collected from scarp colluvium in Unit C1. Sample SLN-R13 yielded two fragments of Asteraceae charcoal weighing 0.0016 g, reflecting a woody member of the sunflower family that burned. Several fragments of charred monocot/herbaceous dicot stem fragments weighing 0.0026 g might reflect local grasses and other herbaceous plants that burned. A single insect puparium, a moderate amount of snail shells with a depressed shape, and seven snails with an oblong shape also were noted.

Detrital charcoal sample SLN-R21 was examined first. This sample consisted of several pieces of unidentified hardwood charcoal weighing 0.0006 g. A few rootlets and sclerotia were present. Because this charcoal is close to the minimum weight of 0.0005 g for dating, bulk sample SLN-R21 was floated to recover additional material. An additional 0.0003 g of unidentifiable charcoal fragments were recovered from the bulk sample, for a total charcoal weight of 0.0009 g. The sample also yielded root and rootlet fragments, a few insect chitin fragments, and a few depressed snail shells.

Unit C2

Bulk samples SLN-R23, SLN-R17, and SLN-R18 were taken from an A horizon developed on or within scarp colluvium in Unit C2A. The 15 fragments of charcoal in sample SLN-R23 were too small for identification and weighed only 0.0005 g. Extraction of microcharcoal is likely to result in additional charred material to supplement the charcoal for radiocarbon dating.

Several fragments of *Artemisia* charcoal in sample SLN-R17 yielded a total weight of 0.0074 g, which is sufficient for dating. Numerous snails with a depressed shape were noted in this sample, as well as fewer snails with an oblong shape. A few insect chitin fragments note insect activity in the area, while root fragments and rootlets represent modern plants.

Sample SLN-R18 yielded several pieces of charcoal too small for identification, although the total weight of 0.0014 g should be adequate for radiocarbon dating. Sub-surface disturbance indicators include a few insect chitin fragments, an insect puparium, a few depressed snails, several oblong snails, and a moderate amount of worm castings. The sample also yielded a few sclerotia. Sclerotia are commonly called "carbon balls." They are small, black, solid or hollow spheres that can be smooth or lightly sculpted. These forms range from 0.5 to 4 mm in size. Sclerotia are the resting structures of mycorrhizae fungi, such as *Cenococcum graniforme*, that have a mutualistic relationship with tree roots. Many trees are noted to depend heavily on mycorrhizae and might not be successful without them. "The mycelial strands of these fungi grow into the roots and take some of the sugary compounds produced by the tree during photosynthesis. However, mycorrhizal fungi benefit the tree because they take in minerals from the soil, which are then used by the tree" (Kricher and Morrison 1988:285). Sclerotia appear to be ubiquitous and are found with coniferous and deciduous trees including *Abies* (fir), *Juniperus communis* (common juniper), *Larix* (larch), *Picea* (spruce), *Pinus* (pine), *Pseudotsuga* (Douglas fir), *Alnus* (alder), *Betula* (birch), *Populus* (poplar, cottonwood, aspen), *Quercus* (oak), and *Salix* (willow). These forms originally were identified by Dr. Kristiina Vogt, Professor of Ecology in the School of Forestry and Environmental Studies at Yale University (McWeeney 1989:229-230; Trappe 1962).

Sample SLN-R22 was recovered in the north wall of Unit C2 from scarp-derived colluvial wedge. Charcoal in this sample includes a single vitrified piece of twig charcoal weighing 0.0008 g and several fragments of charcoal too small and vitrified for identification weighing 0.0002 g. The single piece of vitrified twig charcoal, either alone or combined with the unidentified charcoal fragments, can be submitted for radiocarbon dating. In addition, the sample contained a few uncharred rootlet fragments and numerous uncharred root fragments from modern plants, as well as a few depressed snail shells and a single oblong-shaped snail shell.

Unit C3A

Bulk sample SLN-R19 reflects an A horizon developed on or within scarp colluvium in Unit C3A. The sample contained four fragments of charred parenchymous tissue weighing 0.0008 g that can be submitted for dating, although it is possible that these fragments represent roots. Parenchyma is the botanical term for relatively undifferentiated tissue composed of many similar cells with thin primary walls. Parenchyma occurs in many different plant tissues in varying amounts, especially large fleshy organs such as roots and stems, but also in fruits,

seeds, cones, periderm (bark), leaves, needles, etc. (Hather 2000:1; Mauseth 1988). A sufficient amount (0.0010 g) of very small, unidentifiable charcoal fragments also were present. We recommend keeping these charcoal fragments separate from the charred parenchyma fragments, since the latter might represent roots. Non-floral remains include a few uncharred bone fragments and a moderate amount of snail shells.

Unit N3g

Bulk sample SLN-R27 represents alluvial fan sediments in Unit N3g. This sample yielded several fragments of charcoal too small for identification and weighing a total of 0.0010 g, which should be sufficient for radiocarbon dating. Numerous uncharred rootlets from modern plants and a few snail shells were the only other remains to be recovered.

Unit C4

Bulk sample SLN-R20 was recovered from scarp colluvium in Unit C4. This sample also contained several fragments of charcoal too small for identification that weighed 0.0008 g. This weight should be adequate for radiocarbon dating. Root and rootlet fragments, a moderate amount of depressed snail shells, and a few oblong snail shells also were noted.

Units S3g/h/N3e

Detrital charcoal samples SLN-R05 and SLN-R06 were taken from alluvial-fan sediments in Unit S3g/h/N3e. Two tiny pieces of unidentifiable charred tissue weighing less than 0.0001 g were noted in sample SLN-R06, while the six fragments of charcoal in sample SLN-R05 also were too small for identification and too small for dating, weighing less than 0.0001 g. An additional bulk sample SLN-R11 from Unit S3h1 was recovered adjacent to samples SLN-R05 and SLN-R06. This sample also yielded several fragments of charcoal too small for identification; however, a total weight of 0.0022 g for these charcoal fragments should be adequate for radiocarbon dating. A few uncharred roots and rootlets from modern plants also were present.

Unit S3bA

Sample SLN-R02 consists of charcoal from the A horizon developed on or within alluvial-fan sediments in Unit S3bA. The several fragments of charcoal present in this sample were too small and vitrified for identification; however, the fragments weighed a total of 0.0012 g, which should be sufficient for radiocarbon dating. Vitrified charcoal has a shiny, glassy appearance that can range from still recognizable in structure "to a dense mass, completely 'molten' and non-determinable" (Marguerie and Hunot 2007; McParland et al. 2010). Although vitrification of charcoal has been attributed to burning at high temperature and/or burning green wood, it currently is not clear what conditions produce vitrified charcoal. It likely is a combination of factors (McParland, et al. 2010). We have noted that vitrified charcoal often loses more mass during chemical pre-treatment than charcoal that is not vitrified.

Unit S3d

Detrital charcoal samples SLN-R01, SLN-R03, and SLN-R04 were collected from alluvial-fan sediments in Unit S3d. Sample SLN-R01 yielded a single piece of charred

parenchymous tissue weighing 0.0018 g that can be submitted for radiocarbon dating. A single piece of unidentified hardwood twig charcoal in sample SLN-R03 weighs 0.0012 g and also can be submitted for dating. The small pieces of unidentified hardwood charcoal in sample SLN-R04 yielded a weight of 0.0009 g. Single pieces of charcoal, when compared to multiple pieces with the same weight, usually lose less mass during chemical pre-treatment.

Unit C6

Samples SLN-R09 and SLN-R10 were recovered from scarp colluvium in Unit C6. Detrital charcoal sample SLN-R09 contained only a few small rocks; therefore, bulk sample SLN-R09 was processed. The bulk sample yielded five fragments of charcoal too small for identification and weighing less than 0.0001 g. The probability of obtaining sufficient microscopic charcoal from this bulk sample is small because the visible charcoal recovered from this bulk sample weighed so little.

Bulk sample SLN-R10 yielded five fragments of charred parenchymous tissue weighing less than 0.0001 g and five pieces of charred, vitrified tissue weighing 0.0007 g. This amount of charred material should be sufficient for radiocarbon dating.

Unit CF3

Bulk sample SLN-R25, collected from scarp colluvium in Unit CF3, yielded only three pieces of charcoal too small for identification and weighing less than 0.0001 g. Numerous uncharred rootlets and a few rocks were the only other remains to be recovered. A very minute quantity of visible charcoal was noted in this sample; however, it was selected for microcharcoal extraction. This sample yielded 0.0345 g of microscopic charcoal that can be submitted for dating.

Unit S2bA

Bulk sample SLN-R26 was taken from an A horizon developed on or within alluvial-fan sediments in Unit S2bA. Five fragments of charred, vitrified tissue were noted in this sample, weighing total of 0.0005 g. No other charred remains were recovered. The sample did contain root fragments and rootlets from modern plants, as well as a few oblong snail shells. It is likely that microscopic charcoal can be extracted from this bulk sample to boost the weight for dating.

Unit S2cA

The nine pieces of charcoal in sample SLN-R24, collected from an A horizon developed on or within alluvial-fan sediments in Unit S2cA, were too small and vitrified for identification. These charcoal fragments yielded a total weight of 0.0012 g, which should be sufficient for AMS radiocarbon dating. Numerous uncharred rootlets, an insect puparium fragment, and a few depressed and oblong snail shells also were noted.

North Creek Trench Site

The North Creek Trench site is located northeast of Mona, Utah, at an elevation of 1730–1740 meters. This elevation is above the highest shoreline of Lake Bonneville. Stream

TABLE 3
 INDEX OF MACROFLORAL REMAINS RECOVERED FROM
 THE SPRING LAKE NORTH TRENCH SITE AND THE NORTH CREEK TRENCH SITE
 ON THE NEPHI SEGMENT OF THE WASATCH FAULT ZONE, UTAH

Scientific Name	Common Name
FLORAL REMAINS:	
<i>Lactuca</i>	Lettuce
Monocot/Herbaceous dicot	A member of the Monocotyledonae class of Angiosperms, which include grasses, sedges, members of the agave family, lilies, and palms/ A non-woody member of the Dicotyledonae class of Angiosperms
Periderm	Technical term for bark; Consists of the cork (phellum) which is produced by the cork cambium, as well as any epidermis, cortex, and primary or secondary phloem exterior to the cork cambium
Poaceae	Grass family
Poaceae A	Members of the grass family with larger-sized caryopses, such as <i>Agropyron</i> (wheatgrass), <i>Elymus</i> (ryegrass), <i>Bromus</i> (brome grass), etc.
Poaceae B	Members of the grass family with medium-sized caryopses, such as <i>Festuca</i> (fescue), <i>Hordeum</i> (wild barley), <i>Stipa</i> (needlegrass), etc.
Parenchymous tissue	Relatively undifferentiated tissue composed of many similar cells with thin primary walls—occurs in different plant organs in varying amounts, especially large fleshy organs such as roots and stems, but also fruits, seeds, cones, periderm (bark), leaves, needles, etc.
Vitrified tissue	Charred material with a shiny, glassy appearance due to fusion by heat
Sclerotia	Resting structures of mycorrhizae fungi
CHARCOAL/WOOD:	
Asteraceae	Sunflower family
<i>Artemisia</i>	Sagebrush
Conifer	Cone-bearing, gymnospermous trees and shrubs, mostly evergreens, including the pine, spruce, fir, juniper, cedar, yew, hemlock, redwood, and cypress
<i>Juniperus</i>	Juniper
<i>Pseudotsuga menziesii</i>	Douglas-fir

TABLE 3 (Continued)

Scientific Name	Common Name
<i>Quercus</i>	Oak
<i>Quercus - Leucobalanus</i> group	White oak group - Species in the white oak group exhibit earlywood vessels occluded with tyloses, thin-walled and angular latewood vessels, and longer rays than species in the red oak group
Salicaceae	Willow family
Unidentified hardwood	Wood from a broad-leaved flowering tree or shrub
Unidentified hardwood - small	Wood from a broad-leaved flowering tree or shrub, fragments too small for further identification
Unidentified hardwood - vitrified	Wood from a broad-leaved flowering tree or shrub, exhibiting a shiny, glassy appearance due to fusion by heat
Unidentifiable - small	Charcoal fragments too small for further identification
Unidentifiable - vitrified	Charcoal exhibiting a shiny, glassy appearance due to fusion by heat
NON-FLORAL REMAINS:	
Chitin	A natural polymer found in insect and crustacean exoskeleton
Insect puparium	A rigid outer shell made from tough material that includes chitin (a natural polymer found in insect exoskeleton and crab shells) and hardens from a larva's skin to protect the pupa as it develops into an adult insect
Snail shell - depressed	Snail shell with a depressed (flat) shape where the width is much bigger than the height
Snail shell - oblong	Snail shell with an oblong shape where the height is much bigger than the width

APPENDIX D
SUMMARY OF ¹⁴C DATED CHARCOAL FOR THE SPRING LAKE SITE

Sample Name	NOSAMS ¹ Accession No.	Trench Wall			Sample	Unit Sampled	Notes	Macrofloral remains (total weight in mg) ²	Pre-treatment ³	Laboratory age (¹⁴ Cyr) ⁴			Calibrated age (cal yr BP) ⁵		Calibrated age (rounded) (ka)	
		Horiz. (m)	Vert. (m)	Wall						Age	Age error	Δ ¹³ C	Mean	1σ	Mean	2σ
SLN-R01	OS-105419	38.32	1.21	S	charcoal	S3d	Charcoal in massive silt/loess	1-PT (1.8)	ABA	6,620	110	-25.18	7507	90	7.5	0.2
SLN-R02	OS-104798	32.47	2.43	S	charcoal	S3bA	Charcoal from A horizon on AF sediments	31-UVC (1.2)	A	6680	40	-24.55	7547	36	7.6	0.1
SLN-R03	OS-105243	36.03	1.94	S	charcoal	S3d	Charcoal in massive silt/loess	1-UHT (1.2)	A	6260	80	-23.41	7164	105	7.2	0.2
SLN-R04	OS-105241	38.07	1.71	S	charcoal	S3g4	Charcoal in alluvial-fan sediments	UC (0.9)	A	6110	40	-26.18	7006	79	7.0	0.2
SLN-R05	-	33.71	3.81	S	charcoal	S3h1	Charcoal in alluvial-fan sediments	6-UC (<0.1)	-	-	-	-	-	-	-	-
SLN-R06	-	33.73	3.87	S	charcoal	S3h1	Charcoal in alluvial-fan sediments	2-UT (<0.1)	-	-	-	-	-	-	-	-
SLN-R07	-	38.14	1.29	S	bulk	S3d	Massive silt/loess	-	-	-	-	-	-	-	-	-
SLN-R08	-	33.20	2.23	S	bulk	S3bA	A horizon on AF sediments	-	-	-	-	-	-	-	-	-
SLN-R09	-	27.92	3.43	N	bulk + char.	C6	Top of C6	5-UC (<0.1)	-	-	-	-	-	-	-	-
SLN-R10	OS-104444	28.86	3.14	N	bulk	C6	Top of C6 (slightly more distal)	5-VT(0.7) , 5-PT(<0.1)	NP	13800	130	25	16920	144	16.9	0.3
SLN-R11	OS-104738	33.67	3.92	S	bulk	S3h1	Alluvial-fan sediments (charcoal fragments)	UC(2.2)	ABA	6170	35	-24.66	7074	57	7.1	0.1
SLN-R12	-	25.23	7.82	S	bulk	S3j	Slopewash above C1	-	-	-	-	-	-	-	-	-
SLN-R13	-	26.15	7.28	S	bulk	S3j	Slopewash above C1 (slightly more distal)	2-A(1.6) , 23-MHD(2.6)	ABA	-	-	-	-	-	-	-
SLN-R14	-	25.44	7.51	S	bulk	C1	Soil organics in uppermost C1	-	-	-	-	-	-	-	-	-
SLN-R15	OS-104825	26.55	6.94	S	bulk	C1	Soil organics in uppermost C1	UC (1.1)	A	790	25	-25.28	708	18	0.7	0.04
SLN-R16	OS-104739	25.86	7.06	S	bulk	C1A	Soil organics in C1	UC (1.9)	ABA	2390	25	-25.57	2420	65	2.4	0.1
SLN-R17	OS-104449	25.49	6.83	S	bulk	C2	Soil organics in uppermost C2	36-S (7.4)	ABA	2320	30	-17.6	2333	41	2.3	0.1
SLN-R18	OS-104824	26.09	6.49	S	bulk	C2	Soil organics in C2	UC(1.4)	A	3740	25	-23.05	4089	55	4.1	0.1
SLN-R19	OS-104829	26.22	6.19	S	bulk	C3	Soil organics in uppermost C3	UC(1.0) , 4-PT(0.8)	A	3280	40	-21.3	3509	50	3.5	0.1
SLN-R20	OS-105242	27.28	5.43	S	bulk	C4	C4 colluvial sediment	UC(0.8)	A	3930	35	-21.7	4365	62	4.4	0.1
SLN-R21	OS-104831	26.2	7.34	N	bulk + char.	C1	Base of C1 colluvial wedge	14-UC (0.9) ***	A	770	30	-25.76	700	19	0.7	0.04
SLN-R22	OS-104826	26.55	6.96	N	bulk	C2	Top of C2 colluvial wedge	10-UC(0.2), 1-UVT(0.8)	A	1150	30	-24.68	1060	53	1.1	0.1
SLN-R23	-	27.18	6.69	N	bulk + char.	C2	Top of C2 colluvial wedge	15-UC(0.5)	NP	sample lost during processing			-	-	-	-
SLN-R24	OS-104823	12.28	13.84	S	bulk	S2cA	A horizon on alluvial-fan sediments	9-UC (1.2)	A	5280	40	-21.11	6067	70	6.1	0.1
SLN-R25	OS-104740	11.34	14.08	S	bulk	CF3	Basal CF3	3-UC (<0.1), MC(34.5)	ABA	3380	30	-26.91	3624	43	3.6	0.1
SLN-R26	OS-104445	10.24	13.94	S	bulk	S2bA	A horizon within alluvial-fan sediments	5-VT(0.5)	NP	11850	95	-22.91	13684	120	13.7	0.2
SLN-R27	OS-104832	27.85	6.05	N	bulk	N3g	A horizon on AF deposits below C2 wedge	UC(1.0)	A	4960	45	-23.76	5697	65	5.7	0.1
SLN-R28	-	21.1	10.1	S	bulk	CF1	CF1 colluvial sediment	-	-	-	-	-	-	-	-	-

¹ National Ocean Sciences Accelerator Mass Spectrometry Facility, Woods Hole Oceanographic Institution (Woods Hole, Massachusetts).

² Number of fragments of charcoal and their weight (in parentheses) following sample sorting by PaleoResearch Institute (Golden, Colorado). Unidentified charcoal: MC - microcharcoal, MHD - monocot/Herbaceous dicot, PT - Parenchymous tissue (charred), UC - unidentified charcoal, UHT - unidentified hardwood twig (charred), UVT - unidentified twig (vitrified), UVC - unidentified charcoal (vitrified), UT - unidentified tissue (charred), VT - vitrified tissue. Identified charcoal: A - Asteraceae (sunflower family), S - Sagebrush (Artemisia). Bold text indicates subset of charcoal dated.

³ Pretreatment methods: A - acid wash only, ABA - acid-base-acid washes, NP - no pretreatment.

⁴ Delta ¹³C for SLN-R10 is assumed; all other values were measured.

⁵ Calibrated using OxCal version 4.2 (Bronk Ramsey, 1995, 2001) and the terrestrial calibration curve of Reimer and others (2009).

APPENDIX F
OPTICALLY STIMULATED LUMINESCENCE AGES FOR THE SPRING LAKE SITE

Sample ¹	% Water content ²	K (%) ³	U (ppm) ³	Th (ppm) ³	Cosmic dose ⁴ additions (Gy/ka)	Total Dose Rate (Gy/ka)	Equivalent Dose (Gy)	n ⁵	Age (yr) ⁶		Age (rounded) (ka)	
									mean	1σ	mean	2σ
SL-L1	6 (13)	1.60 ± 0.03	3.53 ± 0.11	9.40 ± 0.33	0.19 ± 0.01	3.28 ± 0.07	17.2 ± 0.43	21 (34)	5240	170	5.2	0.3
SL-L2	5 (14)	0.88 ± 0.06	1.78 ± 0.19	4.29 ± 0.45	0.18 ± 0.01	1.77 ± 0.11	14.1 ± 0.97	21 (28)	7980	740	8.0	1.5
SL-L3	6 (21)	1.26 ± 0.06	2.35 ± 0.20	3.75 ± 0.47	0.18 ± 0.01	2.19 ± 0.12	17.1 ± 0.52	30 (42)	7810	490	7.8	1.0
SL-L4	7 (27)	2.14 ± 0.06	2.57 ± 0.18	10.4 ± 0.48	0.18 ± 0.01	3.49 ± 0.11	21.3 ± 2.044	21 (32)	6100	610	6.1	1.2
SL-L5	4 (18)	2.24 ± 0.06	2.34 ± 0.16	10.0 ± 0.75	0.17 ± 0.01	3.58 ± 0.16	24.9 ± 0.62	12 (20)	6970	360	7.0	0.7
SL-L6	7 (44)	1.50 ± 0.04	2.88 ± 0.16	6.67 ± 0.57	0.23 ± 0.02	2.64 ± 0.13	15.1 ± 0.73	19 (24)	5720	390	5.7	0.8
SL-L7	3 (25)	2.08 ± 0.06	2.93 ± 0.20	8.77 ± 0.76	0.24 ± 0.02	3.48 ± 0.17	>1	2 (20)	>300	-	>0.3	-
SL-L8	2 (26)	2.33 ± 0.06	3.51 ± 0.19	12.4 ± 0.85	0.23 ± 0.02	3.66 ± 0.17	36.5 ± 1.44	25 (48)	9970	580	10.0	1.2
SL-L9	4 (29)	1.94 ± 0.05	2.33 ± 0.15	10.9 ± 0.75	0.19 ± 0.01	3.04 ± 0.15	52.6 ± 1.95	28 (30)	17,300	970	17.3	1.9
SL-L10	9 (25)	1.83 ± 0.04	3.00 ± 0.15	10.7 ± 0.69	0.22 ± 0.02	3.38 ± 0.14	15.2 ± 0.56	26 (30)	4500	240	4.5	0.5

¹ Analyses by the U.S. Geological Survey Luminescence Dating Laboratory (Denver, Colorado).

² Field moisture, with figures in parentheses indicating the complete sample saturation percent. Ages calculated using approximately 25% of total saturation value, except SL-8 and -9, at 50%.

³ Analyses obtained using in-situ gamma spectrometry (NaI detector) and lab gamma spectrometry (Ge detector).

⁴ Cosmic doses and attenuation with depth were calculated using the methods of Prescott and Hutton (1994).

⁵ Number of replicated equivalent dose (De) estimates used to calculate the equivalent dose. Figures in parentheses indicate total number of measurements included in calculating the represented equivalent dose and age using radial plots (weighed mean). Not all samples had adequate sand-sized grains for analyses; dispersion varied between 10-40%.

⁶ Dose rate and age for fine-grained 125-90 microns or 150-125 microns sized quartz. Exponential + linear fit used on equivalent dose, errors to one sigma.

APPENDIX H

OXCAL MODELS FOR THE SPRING LAKE AND NORTH CREEK SITES

OxCal models for the Spring Lake and North Creek sites were created using OxCal calibration and analysis software (version 4.2; Bronk Ramsey, 1995, 2001; using the IntCal09 calibration curve of Reimer and others, 2009). The models include *C_Date* for luminescence ages, *R_Date* for radiocarbon ages, and *Boundary* for undated events (paleoearthquakes). These components are arranged into ordered sequences based on the relative stratigraphic positions of the samples. The sequences may contain *phases*, or groups where the relative stratigraphic ordering information for the individual radiocarbon ages is unknown. Ages following two forward slashes (//) are not considered during model analysis. The models are presented here in reverse stratigraphic order, following the order in which the ages and events are evaluated in OxCal.

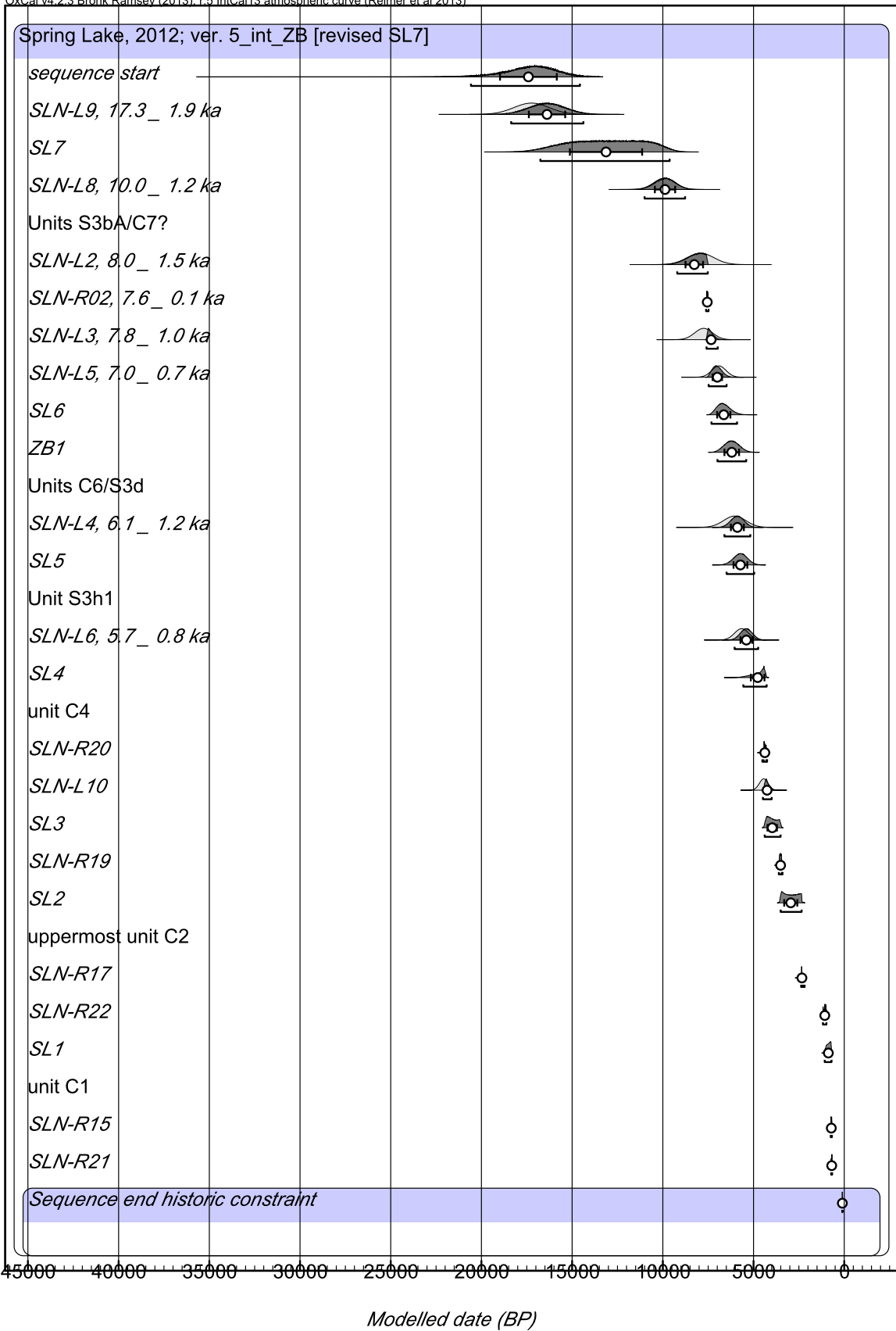
Spring Lake Site

```
Plot()
{
Sequence("Spring Lake, 2012; ver. 5_int_ZB")
{
Boundary("sequence start");
C_Date("SLN-L9, 17.3 ± 1.9 ka", -15288, 970);
Date("SL7");
C_Date("SLN-L8, 10.0 ± 1.2 ka", -7958, 580);
Phase("Units S3bA/C7?");
{
C_Date("SLN-L2, 8.0 ± 1.5 ka", -5968, 740);
R_Date("SLN-R02, 7.6 ± 0.1 ka", 6680, 40);
C_Date("SLN-L3, 7.8 ± 1.0 ka", -5798, 490);
C_Date("SLN-L5, 7.0 ± 0.7 ka", -4958, 390);
};
Boundary("SL6");
Zero_Boundary("ZB1");
Phase("Units C6/S3d");
{
C_Date("SLN-L4, 6.1 ± 1.2 ka", -4088, 610);
//R_Date("SLN-R01, 7.5 ± 0.1 ka", 6620, 110); [detrital?]
//R_Date("SLN-R03, 7.2 ± 0.2 ka", 6260, 80); [detrital?]
//C_Date("SLN-L1, 5.2 ± 0.3 ka", -3228, 170); [stratigraphically inverted]
};
Boundary("SL5");
//R_Date("SLN-R04", 6110, 40); [relation to P5 unclear]
Phase("Unit S3h1");
```

```

{
//R_Date("SLN-R11, 7.1 ± 0.1 ka", 6170, 35); [detrital?]
C_Date("SLN-L6, 5.7 ± 0.8 ka", -3708, 390);
};
//R_Date("SLN-R24", 5280, 40); [unknown relation]
Boundary("SL4");
Phase("unit C4");
{
R_Date("SLN-R20", 3930, 35);
C_Date("SLN-L10", -2488, 240);
};
Boundary("SL3");
R_Date("SLN-R19", 3280, 40);
//R_Date("SLN-R25", 3380, 30); [unknown relation]
//R_Date("SLN-R27", 4960, 45); [detrital?]
Boundary("SL2");
//R_Date("SNL-R18", 3740, 25);
Phase("uppermost unit C2");
{
//R_Date("SLN-R18", 4089, 55); [likely sourced from C3A]
R_Date("SLN-R17", 2320, 30);
R_Date("SLN-R22", 1150, 30);
};
Boundary("SL1");
Phase("unit C1");
{
//R_Date("SLN-R16", 2390, 25); [likely sourced from C2A]
R_Date("SLN-R15", 790, 25);
R_Date("SLN-R21", 770, 30);
};
Boundary("Sequence end historic constraint", 1847);
};
Difference("SL7-SL6", "SL6", "SL7");
Difference("SL6-SL5", "SL5", "SL6");
Difference("SL5-SL4", "SL4", "SL5");
Difference("SL4-SL3", "SL3", "SL4");
Difference("SL3-SL2", "SL2", "SL3");
Difference("SL2-SL1", "SL1", "SL2");
Difference("SL7-SL1", "SL1", "SL7");
Difference("SL6-SL1", "SL1", "SL6");
Difference("SL5-SL1", "SL1", "SL5");
Difference("SL4-SL1", "SL1", "SL4");
Difference("SL3-SL1", "SL1", "SL3");
};

```



Spring Lake, 2012; ver. 5_int_ZB	Unmodelled (cal yr BP)				Modelled (cal yr BP)				Agreement
	central 95%	mean	sigma		central 95%	mean	sigma		
sequence start					20577	14569	17410	1565	
SLN-L9, 17.3 ± 1.9 ka	19174	15304	17239	970	18362	14379	16384	1001	81.6
SL7					16751	9623	13132	1992	
SLN-L8, 10.0 ± 1.2 ka	11067	8751	9909	580	11007	8771	9880	561	101.4
Units S3bA/C7?									
SLN-L2, 8.0 ± 1.5 ka	9395	6442	7919	740	9207	7522	8266	484	112.1
SLN-R02, 7.6 ± 0.1 ka	7615	7476	7547	36	7617	7479	7551	35	99.5
SLN-L3, 7.8 ± 1.0 ka	8727	6770	7749	490	7592	6971	7337	174	98.7
SLN-L5, 7.0 ± 0.7 ka	7688	6129	6909	390	7476	6485	6995	260	114.6
SL6					7320	5907	6640	364	
ZB1					6989	5403	6200	403	
Units C6/S3d									
SLN-L4, 6.1 ± 1.2 ka	7256	4821	6039	610	6605	5177	5890	358	119.2
SL5					6487	4966	5722	380	
Unit S3h1									
SLN-L6, 5.7 ± 0.8 ka	6438	4879	5659	390	6044	4743	5396	327	94.7
SL4					5563	4277	4773	377	
unit C4									
SLN-R20	4510	4248	4365	61	4515	4252	4377	60	100.2
SLN-L10	4919	3959	4439	240	4483	3998	4254	120	102.2
SL3					4385	3508	3971	260	
SLN-R19	3607	3402	3509	47	3606	3402	3510	47	99.8
SL2					3506	2348	2948	362	
uppermost unit C2									
SLN-R17	2378	2184	2334	37	2377	2184	2333	38	97.6
SLN-R22	1174	979	1066	57	1175	982	1073	57	97.6
SL1					1077	700	876	109	
unit C1									
SLN-R15	739	674	708	18	744	680	713	17	99.8
SLN-R21	734	668	700	19	722	667	690	14	110
Sequence end historic constraint	104	103	104	0	104	103	104	0	100

Intervals:	central 95%		mean	sigma
SL7-SL6	2867	10232	6492	2027
SL6-SL5	106	1758	918	438
SL5-SL4	1	1799	950	502
SL4-SL3	-2	1766	802	518
SL3-SL2	82	1860	1023	478
SL2-SL1	1413	2728	2072	380
SL7-SL1	8733	15904	12256	1995
SL6-SL1	4994	6479	5764	380
SL5-SL1	4057	5638	4846	395
SL4-SL1	3290	4731	3897	392
SL3-SL1	2569	3591	3095	281

All values are in calendar years before 1950 (cal yr BP)

Indices:

Amodel 106.8

Aoverall 106

Paleoseismology of the Spring Lake Site

Chronology of Surface-Faulting Earthquakes

OxCal models for the Spring Lake site constrain the timing of seven surface-faulting earthquakes that postdate the highstand of Lake Bonneville (~18 ka) (table 3). These earthquakes stem from the distinct colluvial-wedge units C1–C6 exposed along the main fault F1 (figure 9) and upward terminations of faults (F2) in the footwall of fault F1. We constructed several OxCal models for the Spring Lake site to account for 1) possibly erroneous ^{14}C and OSL ages (e.g., SL-L1 and SL-R11), 2) the possibility that the detrital-charcoal ages (for SL-R1, -R3, and -R11) do not reflect the time of fan deposition (are erroneously old), and 3) uncertainty in the context of samples SL-L3 and -L5. These models have agreement indices, or the overall agreement of the ages in the stratigraphic model, which varied from low (~30–40) to high (>100). We found the best agreement for models that excluded OSL sample SL-L1 and the detrital charcoal samples SL-R1, -R3, and -R11. Our preferred model (version 5; appendix H) excludes these ages, but includes the ages for SL-L3 and -L5, and has a model agreement of 107. Alternative models with high agreement exclude SL-L3 and (or) -L5, but we have less confidence in these results. After consideration of the SL-L3 and -L5 OSL-sample equivalent-dose populations as well as the context of the samples (using the photomosaics), we consider SL-L3 and -L5 to be good ages for units S1c? and C6, respectively.

Table 3. Earthquake timing and recurrence at the Spring Lake site.

Event ¹	Earthquake timing		Earthquake recurrence	
	Mean \pm $2\sigma^2$ (ka)	Central 95% ³ (ka)	Inter-event (kyr)	Mean (kyr)
SL7	13.1 \pm 4.0	9.6–16.8	SL7–SL6: 6.5	SL7–SL1: 2.0
SL6	6.6 \pm 0.7	5.9–7.3	SL6–SL5: 0.9	SL6–SL1: 1.2
SL5	5.7 \pm 0.8	5.0–6.5	SL5–SL4: 1.0	SL5–SL1: 1.2
SL4	4.8 \pm 0.8	4.3–5.6	SL4–SL3: 0.8	SL4–SL1: 1.3
SL3	4.0 \pm 0.5	3.5–4.4	SL3–SL2: 1.0	SL3–SL1: 1.5
SL2	2.9 \pm 0.7	2.3–3.5	SL2–SL1: 2.1	-
SL1	0.9 \pm 0.2	0.7–1.1	-	-

¹ Spring Lake earthquakes; color shading indicates events that could possibly be grouped (e.g., SL6 and SL5 could be related to single earthquake); see text for discussion.

² Mean \pm two sigma (2σ) based on OxCal model results (model v. 5; appendix H).

³ Earthquake time range including 95.4% of the total area of the time distribution with the highest probability density (Bronk Ramsey, 2013).

SL7 is the oldest earthquake at the site, which occurred at 13.1 ± 4.0 ka based on our preferred OxCal model (appendix H). Several faults (F2) that complexly displace the Lake Bonneville highstand lacustrine sediments (unit N1b/S1b) but not overlying loess (unit N1c/S1c), debris-flow (N1d/S1d), or alluvial-fan sediments (N2/S2) provide evidence of earthquake SL7. Thus, earthquake SL7 has a maximum constraint of ~17.3 ka (OSL sample SL-L9 for unit N1b) and a minimum of ~10.0 ka (OSL sample SL-L8 for unit N1c). Earthquake SL7 also likely predates the ~7.0-ka OSL age for uppermost unit N1c? as well as the ^{14}C and OSL ages for soil S3bA that range from 7.0 to 8.0 ka (SL-L5, -L3, -L2, and -R2).

Earthquake SL6 occurred at 6.6 ± 0.7 ka. SL6 postdates the 7.0–8.0 ka ages for N1c? and S3bA (samples SL-L5, L3, L2, and R2) and predates an OSL age for C6 colluvium of 6.1 ± 1.2 ka (SL-L4). Because we consider the sample of uppermost unit N1c?, where buried by unit C6, to be a better approximation of the earthquake SL6 time than the minimum age of 6.1 ka from the uppermost part of unit C6, we used a Zero_Boundary grouping in OxCal to implement this interpretation (see DuRoss and others, 2011 for discussion). As discussed above, we excluded detrital charcoal ages (~ 7.2 – 7.5 -ka for SL-R1 and -R3) for the overlying alluvial-fan unit S3d, which are stratigraphically inverted with samples L5 and L4 (~ 6.1 – 7.0 ka). If included, these ages result in an OxCal model with low agreement.

Earthquake SL5 occurred at 5.7 ± 0.8 ka. Although we did not sample sediment from the C5 colluvial wedge to date, earthquake SL5 is limited to a maximum by the 6.1-ka age (SL-L4) for uppermost unit C6, and to a minimum by an OSL age of ~ 5.7 -ka (SL-L6) for alluvial-fan unit S3h, which clearly postdates unit C5. We excluded the detrital charcoal ages for units S3d (~ 7.2 – 7.5 ka) and S3h (7.1 ka). While there is stratigraphic consistency in these ^{14}C ages for the alluvial-fan sediment, the ages are stratigraphically inverted with the OSL ages and yield low OxCal-model agreement if included. Thus, we consider OSL ages for samples SL-L4 (~ 6.1 ka) and -L6 (~ 5.7 ka) to best constrain the time of earthquake SL5. As discussed previously, there is uncertainty in whether colluvial wedges C6 (SL6) and C5 (SL5) represent one or two earthquakes. Earthquakes SL6 and SL5 have mean times that are ~ 0.9 -kyr apart and 95% ranges that have ~ 0.6 -kyr of overlap (between 5.9 and 6.5 ka). Although we prefer a model of separate earthquakes for SL6 and SL5, considering the overlap in the earthquake times and the limited extent of the C5 colluvial wedge, we cannot rule out the possibility that these events represent separate pulses of colluvium deposited following the same earthquake.

Earthquake SL4 occurred at 4.8 ± 0.8 ka. The timing of earthquake SL4 is constrained to a maximum by the 5.7-ka OSL age for the alluvial fan unit S3h, and to a minimum of ~ 4.4 – 4.5 ka by a ^{14}C age (SL-R20) and OSL age (SL-L10) for uppermost C4 colluvium. Based on the maximum limiting ages, colluvium related to earthquake SL4 (C4) could also correspond with the footwall colluvial wedge CF3 along fault F3. However, CF3 is broadly constrained to ~ 3.6 – 6.1 ka based on maximum and minimum limiting ^{14}C ages (SL-R24 and -R25). Displacement along fault F3 in earthquake SL3 would help explain why the C4 colluvial wedge is poorly expressed along the main fault (F1). However, we have low confidence in this interpretation because the CF3 colluvial wedge is broadly constrained and could also correspond with earthquake SL3.

Earthquake SL3 occurred at 4.0 ± 0.5 ka using the 4.4–4.5-ka ages for C4 colluvium as a maximum constraint and a 3.5-ka ^{14}C age for C3 colluvium as a minimum. Using its minimum limiting age (3.5 ka), SL3 (and C3 colluvium) could correspond with footwall colluvial wedge CF3, which has an approximate age range of 3.6–6.1 ka. The 0.8-kyr time difference in the mean times for SL4 (~ 4.8 ka) and SL3 (~ 4.0 ka) and the minimal (~ 0.1 -kyr) overlap in their 95% ranges supports our interpretation of two separate earthquakes. Although we prefer a model of separate earthquakes for SL4 and SL3, we cannot rule out a single-earthquake model.

Earthquake SL2 occurred at 2.9 ± 0.7 ka. The timing of earthquake SL2 is based on the 3.5-ka ^{14}C age for C3 colluvium (SL-R19) that provides a maximum constraint, and two ^{14}C ages

of 1.1–2.3 ka for C2 colluvium (SL-R22 and -R17) that provided a minimum constraint. We excluded an additional age for the C2 colluvium of 4.1 ka (SL-R18) because it is stratigraphically inconsistent with SL-R17, -R22, and -R19. Sample SL-R18 likely included charcoal derived from the soil developed in unit C3.

Earthquake SL1 occurred at 0.9 ± 0.2 ka, postdating the 1.1–2.3-ka ^{14}C ages for C2 colluvium and predating two 0.7-ka ^{14}C ages for C1 colluvium. An additional sample of C1 colluvium yielded an age of 2.4 ka (SL-R16), which is significantly older than the 0.7-ka minimum ages and stratigraphically inverted with the 2.3-ka age for C2. We chose to exclude the 2.4-ka age for SL-R16 from the OxCal model as the charcoal dated is likely derived from the faulted soil in the C2 colluvial wedge.

Earthquake Recurrence and Fault Slip Rate

We calculated inter-event and mean recurrence intervals between individual Spring Lake earthquakes SL7 and SL1 using the mean earthquake times (table 3; appendix I). Inter-event recurrence is the elapsed time between two successive earthquakes (e.g., SL7–SL6); mean recurrence is the mean over several seismic cycles based on the elapsed time between the oldest and youngest earthquakes (e.g., SL7–SL1) divided by the number of closed inter-event intervals.

Inter-event recurrence intervals between earthquakes SL7 and SL1 have a broad range, varying from ~0.8 kyr for SL4–SL3 to ~6.5 kyr for SL7–SL6 (table 3). The relatively long interval between SL7 and SL6 is related to the poorly resolved time of earthquake SL7 (~4 kyr timing uncertainty at 2σ). In addition, we consider the SL7–SL6 interval a maximum value because of the limited (and short duration) exposure of units N1c/S1c in the fault zone, uncertainty in the correlation these unit with footwall units N1c/S1c, and the well sorted and unstratified texture of units N1c/S1c that could mask evidence of individual surface-faulting earthquakes. We also report a long, ~2.1-kyr elapsed time occurred between earthquakes SL2 and SL1. However, as opposed to the SL7–SL6 interval, we do not consider the SL2–SL1 interval poorly constrained on account of limited stratigraphy or limiting ages. Excluding the SL7–SL6 interval, the inter-event intervals are less than 2.1 kyr, and yield a coefficient of variation (COV) on recurrence—the standard deviation of the inter-event recurrence values divided by their mean—of 0.45 (0.52 kyr divided by 1.15 kyr).

To account for the long (~6.5 kyr) elapsed time between earthquakes SL7 and SL6 we considered the possibility that slope-parallel sand lenses in units N1c and S1c are related to at least one earthquake contemporaneous with deposition of these units over about 10–7 ka. The earthquake(s) would predate formation of hanging-wall soil N3aA/S3bA (~7.6–8.0 ka) and deposition of colluvial wedge unit C6 (~6.1 ka). Although earthquakes in this period would help explain the long gap in surface faulting between SL7 and SL6, we have low confidence in this interpretation because of the thick, massive character of units N1c/N1c and S1c/S1c. That is, without local changes in sedimentary texture or the presence of buried soils, colluvial wedges derived primarily from sandy unit N1c/S1c in the fault footwall would be difficult to discern from units N1c/S1c in the hanging wall. Reconstruction of the vertical displacement on fault F1 may help resolve the possibility for additional earthquakes between SL7 and SL6.

APPENDIX I
SUMMARY OF EARTHQUAKE-TIMING, RECURRENCE, AND FAULT-SLIP-RATE ESTIMATES FOR THE SPRING LAKE SITE

Earthquake timing (cal yr B.P.)

Event	mean	1 σ	2 σ	central 95%	
SL7	13,132	1992	3984	9623	16,751
SL6	6643	364	728	5911	7321
SL5	5722	380	760	4966	6488
SL4	4779	387	774	4279	5562
SL3	3971	260	520	3509	4386
SL2	2948	362	724	2348	3506
SL1	876	109	218	700	1077

OxCal model: Spring_Lake_N/SpringLake_ver_5_int_ZB.

central 95% range is based on the OxCal time distribution with the highest probability density.

Inter-event recurrence

Events	Mean	1 σ	2 σ	central 95%	
SL7-SL6	6492	2027	4054	2867	10232
SL6-SL5	920	438	876	109	1759
SL5-SL4	950	502	1004	1	1799
SL4-SL3	802	517	1034	0	1766
SL3-SL2	1023	478	956	82	1859
SL2-SL1	2072	380	760	1414	2728

Coefficient of variation (COV)

events	mean	stdev	COV
SL7-SL1	2043	2228	1.09
SL6-SL1	1153	520	0.45

COV is the standard deviation (stdev) of inter-event recurrence times divided by their mean.

Inter-event intervals (e.g., between SL7 and SL6) calculated using the "Difference" command in OxCal.

Mean recurrence

Events	Total time interval					Intervals	Mean recurrence				
	mean	1 σ	2 σ	central 95%			mean	1 σ	2 σ	central 95%	
SL7-SL1	12,256	1995	3990	8733	15,904	6	2043	333	665	1456	2651
SL6-SL1	5766	380	760	4995	6480	5	1153	76	152	999	1296
SL5-SL1	4846	396	792	4058	5639	4	1212	99	198	1015	1410
SL4-SL1	3897	392	784	3293	4734	3	1299	131	261	1098	1578
SL3-SL1	3095	281	562	2569	3592	2	1548	141	281	1285	1796

Total time intervals between events (eg., SL7 and SL1) calculated using the "Difference" command in OxCal.

Mean recurrence is elapsed time divided by the number of intervals.

Slip rate

Event	Mean time	Ind. displacement			Total displacement				Total time interval				Slip rate		
		midpt	min	max	events	midpt	min	max	events	mean	95th range	mean	min	max	
SL7	13,132	-	-	-	-	-	-	-	-	-	-	-	-	-	-
SL6	6643	1.1	0.8	1.4	SL6-SL1	5.9	4.4	7.4	SL7-SL1	12,256	8733	15904	0.48	0.28	0.85
SL5	5722	0.95	0.7	1.2	SL5-SL1	4.8	3.6	6.0	SL6-SL1	5766	4995	6480	0.83	0.56	1.20
SL4	4779	0.9	0.7	1.1	SL4-SL1	3.85	2.9	4.8	SL5-SL1	4846	4058	5639	0.79	0.51	1.18
SL3	3971	1.05	0.8	1.3	SL3-SL1	2.95	2.2	3.7	SL4-SL1	3897	3293	4734	0.76	0.46	1.12
SL2	2948	0.8	0.6	1.0	SL2-SL1	1.9	1.4	2.4	SL3-SL1	3095	2569	3592	0.61	0.39	0.93
SL1	876	1.1	0.8	1.4	SL1	1.1	0.8	1.4	SL2-SL1	2072	1414	2728	0.53	0.29	0.99

Slip rate is total displacement (e.g., for earthquakes SL6 to SL1) divided by the total time interval (e.g., SL7 to SL1).

REFERENCES

- Biasi, G.P., and R. J. Weldon (2006). Estimating surface rupture length and magnitude of paleoearthquakes from point measurements of rupture displacement, *Bull. Seismol. Soc. Am.*, **96**, no. 5, 1612–1623.
- Biasi, G. P., and R. J. Weldon (2009). San Andreas fault rupture scenarios from multiple paleoseismic records: stringing pearls, *Bull. Seismol. Soc. Am.* **99**, no. 2A, 471–498.
- Black, B. D., W. R. Lund, D. P. Schwartz, H. E. Gill, and B. H. Mayes (1996). Paleoseismic investigation on the Salt Lake City segment of the Wasatch fault zone at the South Fork Dry Creek and Dry Gulch sites, Salt Lake County, Utah, in *Paleoseismology of Utah*, W. R. Lund (Editor), Utah Geol. Surv. Spec. Stud. 92, Vol. 7, 22 pp.
- Bronk Ramsey, C. (1995). Radiocarbon calibration and analysis of stratigraphy—the OxCal program, *Radiocarbon*, **37**, no. 2, 425–430.
- Bronk Ramsey, C. (2001). Development of the radiocarbon program OxCal, *Radiocarbon*, **43**, no. 2a, 355–363.
- Bronk Ramsey, C. (2008). Depositional models for chronological records, *Quaternary Sci. Rev.*, **27**, no. 1–2, 42–60.
- Burbank, D.W., and R. S. Anderson (2001). Tectonic Geomorphology, *Blackwell Scientific*, Oxford, UK, 274 p.
- Burbank, D.W., and R. S. Anderson (2011). Tectonic Geomorphology; 2nd edition, *John Wiley & Sons, Ltd.*, Chichester, UK, 454 p.
- Chang, W. L., and R. B. Smith (2002). Integrated seismic-hazard analysis of the Wasatch Front, Utah, *Bull. Seismol. Soc. Am.*, **92**, no. 5, 1904–1922.
- Crone, A. J., M. N. Machette, M. G. Bonilla, M.G., J. J. Lienkaemper, K. L. Pierce, W. E. Scott, and R. C. Bucknam (1987). Surface faulting accompanying the Borah Peak earthquake and segmentation of the Lost River fault, central Idaho, *Bull. Seismol. Soc. Am.*, **77**, 739–770.
- Crone, A. J., S. F. Personius, C. B. DuRoss, M. N. Machette, and S. A. Mahan (2014). History of late Holocene earthquakes at the Willow Creek site on the Nephi segment, Wasatch fault zone, Utah, in *Paleoseismology of Utah*, W. R. Lund (Editor), Utah Geol. Surv. Spec. Stud. 151, Vol. 25, 55 pp.
- Duller, G. A. T. (2008). Luminescence dating—Guidelines on using luminescence dating in archaeology: Swindon, United Kingdom, English Heritage Publishing, 45 p., available online at http://www.aber.ac.uk/en/media/departmental/iges/pdf/english_heritage_luminescence_dating.pdf, accessed December, 2014.
- DuRoss, C. B. (2008). Holocene vertical displacement on the central segments of the Wasatch fault zone, Utah, *Bull. Seismol. Soc. Am.* **98**, no. 6, 2918–2933.
- DuRoss, C. B. (2014). Paleoseismic investigation to determine the mid-Holocene chronology of surface-faulting earthquakes on the Nephi segment of the Wasatch

- fault zone, Utah and Juab Counties, Utah, *Final Tech. Rept. to the U.S. Geol. Surv.*, award no. G12AP20076, 48 pp.
- DuRoss, C. B., and M. D. Hylland (2014). Synchronous ruptures along a major graben-forming fault system—Wasatch and West Valley fault zones, Utah, USA, *Bull. Seismol. Soc. Am.*, **105**, no. 1, manuscript no. 2014064.
- DuRoss, C. B., M. D. Hylland, G. N. McDonald, A. J. Crone, S. F. Personius, R. D. Gold, and S. A. Mahan (2014). Holocene and latest Pleistocene paleoseismology of the Salt Lake City segment of the Wasatch fault zone, Utah, at the Penrose Drive trench site, in *Evaluating surface faulting chronologies of graben-bounding faults in Salt Lake Valley, Utah—new paleoseismic data from the Salt Lake City segment of the Wasatch fault zone and the West Valley fault zone—Paleoseismology of Utah*, C. B. DuRoss and M. D. Hylland, Utah Geol. Surv. Spec. Stud. 149, Vol. 24, 1–35.
- DuRoss, C. B., G. N. McDonald, and W. R. Lund (2008). Paleoseismic investigation of the northern strand of the Nephi segment of the Wasatch fault zone at Santaquin, Utah, in *Paleoseismology of Utah*, W. R. Lund (Editor), Utah Geol. Surv. Special Study 124, Vol. 17, 33 pp.
- DuRoss, C. B., S. F. Personius, A. J. Crone, G. N. McDonald, and R. Briggs (2012). Late Holocene earthquake history of the Brigham City segment of the Wasatch fault zone at the Hansen Canyon, Kotter Canyon, and Pearsons Canyon trench sites, Box Elder County, Utah, in *Paleoseismology of Utah*, W. R. Lund (Editor), Utah Geol. Surv. Spec. Stud. 142, Vol. 22, 28 pp.
- DuRoss, C. B., S. F. Personius, A. J. Crone, G. N. McDonald, and D. J. Lidke (2009). Paleoseismic investigation of the northern Weber segment of the Wasatch fault zone at the Rice Creek trench site, North Ogden, Utah, in *Paleoseismology of Utah*, W. R. Lund (Editor), Utah Geol. Surv. Special Study 130, Vol. 18, 37 pp.
- DuRoss, C. B., S. F. Personius, A. J. Crone, S. S. Olig, and W. R. Lund (2011). Integration of paleoseismic data from multiple sites to develop an objective earthquake chronology: Application to the Weber segment of the Wasatch fault zone, Utah, *Bull. Seismol. Soc. Am.* **101**, no. 6, 2765–2781.
- DuRoss, C. B., S. F. Personius, S. S. Olig, A. J. Crone, M. D. Hylland, W. R. Lund, and D. P. Schwartz (in review). Surface-faulting earthquake history of the central Wasatch fault zone—implications for earthquake recurrence, fault slip rate, and fault segmentation, *Bull. Seismol. Soc. Amer.*, manuscript no. BSSA-D-14-00357.
- Friedrich, A. M., B. P. Wernicke, N. A. Niemi, R. A. Bennett, and J. L. Davis (2003). Comparison of geodetic and geologic data from the Wasatch region, Utah, and implications for the spectral character of Earth deformation at periods of 10 to 10 million years, *J. Geophys. Res.*, **108**, no. B4, p. 2199, doi:10.1029/2001JB000682.
- Gilbert, G. K. (1890). Lake Bonneville, *U.S. Geol. Surv. Mon. 1*, 438 pp.
- Hanks, T. C., and H. Kanamori (1979), A moment magnitude scale, *J. Geophys. Res.*, **84**, 2348–2350.

- Hylland, M. D., C. B. DuRoss, G. N. McDonald, S. S. Olig, C. G. Oviatt, S. A. Mahan, A. J. Crone, and S. F. Personius (2014). Late Quaternary paleoseismology of the West Valley fault zone, Utah: Insights from the Baileys Lake trench site, in *Evaluating surface faulting chronologies of graben-bounding faults in Salt Lake Valley, Utah—new paleoseismic data from the Salt Lake City segment of the Wasatch fault zone and the West Valley fault zone—Paleoseismology of Utah, Volume 24* C. B. DuRoss and M. D. Hylland, Utah Geol. Surv. Spec. Stud. 149, 41–71.
- Hylland, M. D., and M. N. Machette (2008). Surficial geologic map of the Levan and Fayette segments of the Wasatch fault zone, Juab and Sanpete Counties, Utah, *Utah Geol. Surv. Map 229*, 37 pp., 1 plate, scale 1:50,000.
- Lienkaemper, J. J., and C. Bronk Ramsey (2009). OxCal – versatile tool for developing paleoearthquake chronologies – A primer, *Seismol. Res. Lett.*, **80**, no. 3, 431–434.
- Lund, W. R. (2005). Consensus preferred recurrence-interval and vertical slip-rate estimates: review of Utah paleoseismic-trenching data by the Utah Quaternary Fault Parameters Working Group, *Utah Geol. Surv. Bull. 134*, 109 pp.
- Lund, W.R. (2013). Working Group on Utah Earthquake Probabilities preliminary fault characterization parameters for faults common to the Working Group study area and the U.S. National Seismic Hazard Maps, data provided to the U.S. Geological Survey for use in the 2014 update of the National Seismic Hazard Maps in Utah, *Utah Geol. Surv. Open-File Rept. 611*, 6 pp.
- Machette, M. N., S. F. Personius, and A. R. Nelson (1992). Paleoseismology of the Wasatch fault zone: a summary of recent investigations, interpretations, and conclusions, in *Assessment of regional earthquake hazards and risk along the Wasatch Front*, Utah P. L. Gori and W. W. Hays (Editors), U.S. Geol. Surv. Prof. Paper 1500, A1–A71.
- McCalpin, J. P., and S. P. Nishenko (1996). Holocene paleoseismicity, temporal clustering, and probabilities of future large ($M > 7$) earthquakes on the Wasatch fault zone, Utah, *J. Geophys. Res.*, **101**, No. B3, 6233–6253.
- Nelson, A. R. (1992). Lithofacies analysis of colluvial sediments —an aid in interpreting the recent history of Quaternary normal faults in the Basin and Range Province, western United States, *J. Sed. Pet.*, **62**, no. 4, 607–621.
- Nelson, A. R., M. Lowe, S. Personius, L. A. Bradley, S. L. Forman, R. Klauk, and J. Garr (2006). Holocene earthquake history of the northern Weber segment of the Wasatch fault zone, Utah, in *Paleoseismology of Utah*, W. R. Lund (Editor), Utah Geol. Surv. Misc. Pub. 05–8, Vol. 13, 39 pp.
- Nelson, A. R., S. F. Personius, B. L. Sherrod, H. M. Kelsey, S. V. Johnson, L. A. Bradley, and R. E. Wells (2014). Diverse rupture modes for surface-deforming upper plate earthquakes in the southern Puget Lowland of Washington State, *Geosphere*, **10**, no. 4, 769–796.
- Olig, S. S., G. N. McDonald, B. D. Black, C. B. DuRoss, W. R. Lund, M. D. Hylland, D. B. Simon, R. E. Giraud, and G. E. Christenson (2011). Extending the paleoseismic

- record of the Provo segment of the Wasatch fault zone, Utah, *Final Tech. Rep. to the U.S. Geol. Surv.*, 62 pp.
- Personius, S. F., and W. E. Scott (1992). Surficial geologic map of the Salt Lake City segment and parts of adjacent segments of the Wasatch fault zone, Davis, Salt Lake, and Utah Counties, Utah, *U.S. Geol. Surv. Misc. Invest. Series Map I-2106*, scale 1:50,000.
- Personius, S. F., C. B. DuRoss, and A. J. Crone (2012). Holocene behavior of the Brigham City segment: implications for forecasting the next large-magnitude earthquake on the Wasatch fault zone, Utah, *Bull. Seismol. Soc. Am.* **102**, no. 6, 2265–2281.
- Puseman, K., and L. S. Cummings, L. S. (2005). Separation and identification of charcoal and organics from bulk sediment samples for improved radiocarbon dating and stratigraphic correlations, in *Western States Seismic Policy Council, Proceedings Volume of the Basin and Range Province Seismic Hazards Summit II*, W. R. Lund (Editor), Utah Geol. Surv. Misc. Pub. 05-2, 10 pp.
- Reimer, P. J., M. G. L. Baillie, E. Bard, A. Bayliss, J. W. Beck, P. G. Blackwell, C. Bronk Ramsey, C. E. Buck, G. S. Burr, R. L. Edwards, M. Friedrich, P. M. Grootes, T. P. Guilderson, I. Hajdas, T. J. Heaton, A. G. Hogg, K. A. Hughen, K. F. Kaiser, B. Kromer, F. G. McCormac, S. W. Manning, R. W. Reimer, D. A. Richards, J. R. Southon, S. Talamo, C. S. M. Turney, J. van der Plicht, and C. E. Weyhenmeyer (2009). IntCal09 and Marine09 radiocarbon age calibration curves, 0–50,000 years cal B.P., *Radiocarbon* **51**, no. 4, 1111–1150.
- Scharer, K., R. Weldon, A. Streig, and T. Fumal (2014). Paleoearthquakes at Frazier Mountain, California delimit extent and frequency of past San Andreas Fault ruptures along 1857 trace, *Geophys. Res. Lett.*, **41**, 4527–4534.
- Schwartz, D. P., and K. J. Coppersmith (1984). Fault behavior and characteristic earthquakes: examples from the Wasatch and San Andreas fault zones, *J. Geophys. Res.* **89**, 5681–5698.
- Swan, F. H., III, D. P. Schwartz, and L. S. Cluff (1980). Recurrence of moderate to large magnitude earthquakes produced by surface faulting on the Wasatch fault zone, Utah, *Bull. Seismol. Soc. Am.* **70**, 1431–1462.
- Wallace, R. E. (1990). The San Andreas fault system, California, U.S. Geol. Surv. Prof. Paper: 1515, available online at <http://geologycafe.com/california/pp1515/>.
- Wells, D. L., and K. J. Coppersmith (1994). New empirical relationships among magnitude, rupture length, rupture width, rupture area, and surface displacement, *Bull. Seismol. Soc. Am.* **84**, no. 4, 974–1002.
- Wesnousky, S. G. (2008). Displacement and geometrical characteristics of earthquake surface ruptures—Issues and implications for seismic-hazard analysis and the process of earthquake rupture, *Bull. Seismol. Soc. Am.*, **98**, no. 4, 1609–1632.
- Working Group on Utah Earthquake Probabilities (in preparation). Earthquake probabilities for the Wasatch Front region—Utah Idaho, and Wyoming, *Utah Geol. Surv. Misc. Pub.*